Welcome / Bienvenidos

Prof. Dr. Steffen Härtel

www.scian.cl / www.cimt.cl / www.cens.cl / www.bni.cl / www.rsdue.cl

Laboratory for Scientific Image Analysis (SCIAN-Lab)
Centro de Informática Médica y Telemedicina (CIMT)
Centro Nacional en Sistemas de Información en Salud (CENS)
Biomedical Neuroscience Institute (BNI)
Red de Salud Digital de Universidades del Estado (RSDUE)
Institute of Biomedical Sciences (ICBM)
Núcleo Milenio de AutoOrganización y Mecánica de Tejidos (SELFO)
Facultad de Medicina, Universidad de Chile

https://scian.cl/scientific-image-analysis

Microscopy - Imaging - References

Day 1 | 7 January 2026

08:30 - 09:00	Registration
Opening of the course	
09:00 - 09:20	Welcome, presentation and general instructions
09:20 - 10:00	Self-presentation of students
Topic Lectures	
10:00 - 11:00	Principles of optics I
	Steffen Härtel
11:00 - 11:30	Coffee Break
11:30 - 12:30	Principles of optics II
	Ulrich Kubitscheck
12:30 - 14:00	Lunch Break
14:00 - 15:00	Microscopy tools
	Steffen Hartel / Ulrich Kubitscheck
Practical Session 1	
15:00 - 15:15	Briefing of practical activities and relevant safety measurements
15:15 - 18:45	Image acquisition: confocal / spinning disk / LSFM
	Self-service coffee and biscuits

https://meetings.embo.org/event/26-optics

Microscopy - Imaging - References

Links

- The Scale of the Universe https://htwins.net/scale2
- Global BioImaging https://globalbioimaging.org
- Latin American Bioimaging LABI https://labi.lat/es
- Sociedad Chilena de Imágenes Científicas SoChIC https://imagenescientificas.cl
- Red de Equipamiento Científico Avanzado REDECA UChile https://redeca.med.uchile.cl
- Microscopy Australia https://myscope.training
- Photomultipliers https://evidentscientific.com/en/microscope-resource/knowledge-hub/digitalimaging/concepts/photomultipliers
- Chrome Spectra Viewer www.chroma.com/spectra-viewer
- ThermoFisher Spectra www.thermofisher.com/order/fluorescence-spectraviewer

Software

- SVI Huygens Software, deconvolution https://svi.nl/tiki-login_scr.php
- FIJI, image processing package built upon ImageJ https://fiji.sc
- ilastik, interactive learning & segmentation toolkit https://www.ilastik.org/
- BioImage Model Zoo https://bioimage.io/#/models
- CellProfiler, pipelines http://cellprofiler.org
- Icy, open community platform for bioimage informatics http://icy.bioimageanalysis.org
- Napari, a Python imaging ecosystem https://napari.org

2025 LABI Meeting
UBA, Bs. Aires, Argentina

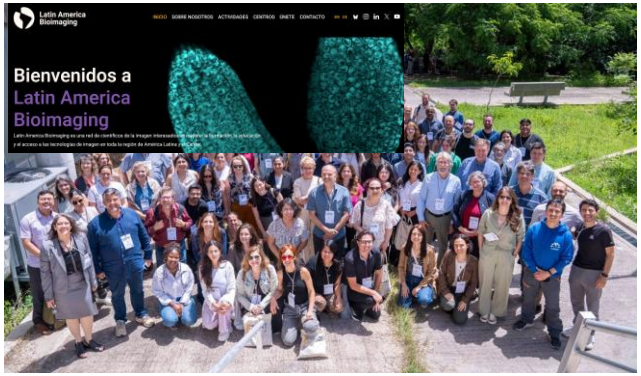

2025 SoChIC Meeting
UACh, Valdivia, Chile

Course material
https://scian.cl

Microscopy - Imaging - References

- The Good, the Bad and the Ugly. Helen Pearson. 2007. Nature 447: 138-140 https://dx.doi.org/10.1038/447138a
- Seeing is believing? A beginners' guide to practical pitfalls in image acquisition.
  Alison J. North. 2006. The Journal of Cell Biology, 172(1):9-18 https://doi.org/10.1083/jcb.200507103
- Computational methods for analysis of dynamic events in cell migration
  V Castañeda, M Cerda, F Santibáñez, J Jara, E Pulgar, K Palma, ... 2013. Current Molecular Medicine 14(2): 291-307
  https://doi.org/10.2174/1566524014666140128113952
- Fluorescence Microscopy, From Principles to Biological Applications.
  Ulrich Kubitscheck (Editor), 2nd Edition, June 2017, Hardcover, ISBN: 978-3-527-33837-5
- https://www.zeiss.com/microscopy/en/resources/insights-hub/life-sciences/basics-of-confocal-microscopy.html
- https://www.microscopyu.com/tutorials
- http://zeiss-campus.magnet.fsu.edu/tutorials/index.html
- https://www.leica-microsystems.com/science-lab/tag/basics-in-microscopy/
- Fluorescence Microscopes @LEO/SCIAN-Lab https://www.youtube.com/playlist?list=PLG8B8Uyfh7-Azddns5nv_kZU1YQGD4bBg
- Principles of Fluorescence Spectroscopy, Joseph R. Lakowicz. Chapter 4.1, Introduction to Fluorescence
- A Global View of Standards for Open Image Data Formats and Repositories
  JR Swedlow, P Kankaanpää, U Sarkans, W Goscinski, G Galloway, ... Nature Methods 18:1440-1446 https://doi.org/10.1038/s41592-021-01113-7
- Tutorial: guidance for quantitative confocal microscopy. Jonkman, J., Brown, C.M., Wright, G.D. *et al.* 2020. Nature Protocols 15: 1585-1611
  https://doi.org/10.1038/s41596-020-0313-9

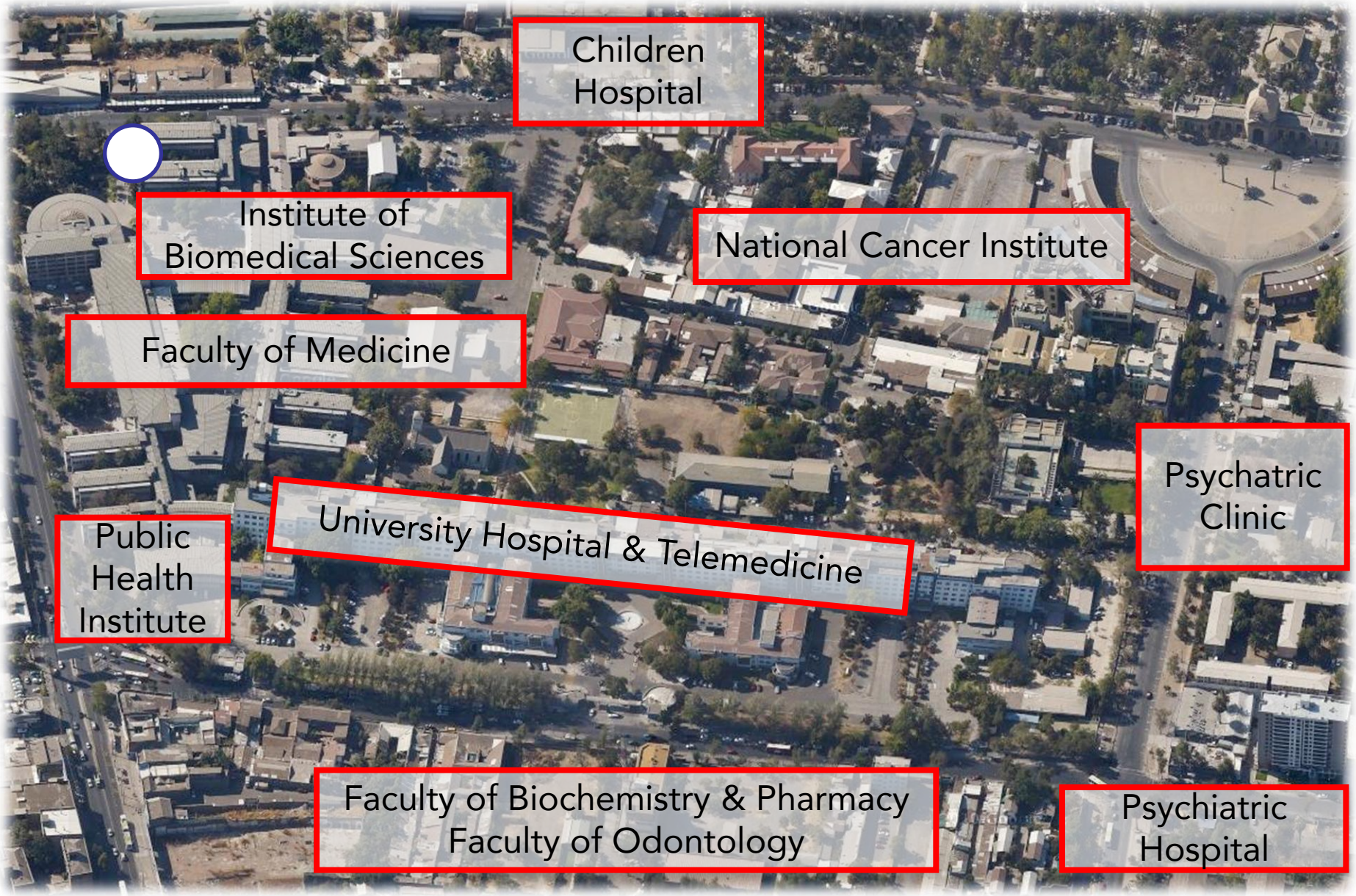
Children Hospital
Institute of Biomedical Sciences
National Cancer Institute
Faculty of Medicine
Psychatric Clinic
Public Health Institute
University Hospital & Telemedicine
Faculty of Biochemistry & Pharmacy
Faculty of Odontology
Psychiatric Hospital

Latin America Bioimaging

Existing bioimaging technologies in Chile …

FONDEQUIP …

~50 state-funded optical and electronic microscopes FONDEQUIP (2011 →)

https://servicios.conicyt.cl/buscadorequipos/#/search_result/microscopio
La Red de Equipamiento Científico Avanzado: https://redeca.med.uchile.cl

Santiago and public/private universities and institutes concentrate the largest quantity of equipment

- 10 microscopes @REDECA (F-Med, UChile)
- 7 in CEMC and other Faculties (UChile)
- 6 optical microscopes + 2 TEM 2 SEM @ PUC
- 9 microscopes @ CMA Bio Bio (U. Concepción)
- …

...the new Chilean Society of Scientific Imaging (SoChIC) holds its first meeting, 21-22.11.2025, Universidad Austral, Valdivia, Chile.

2022

2025

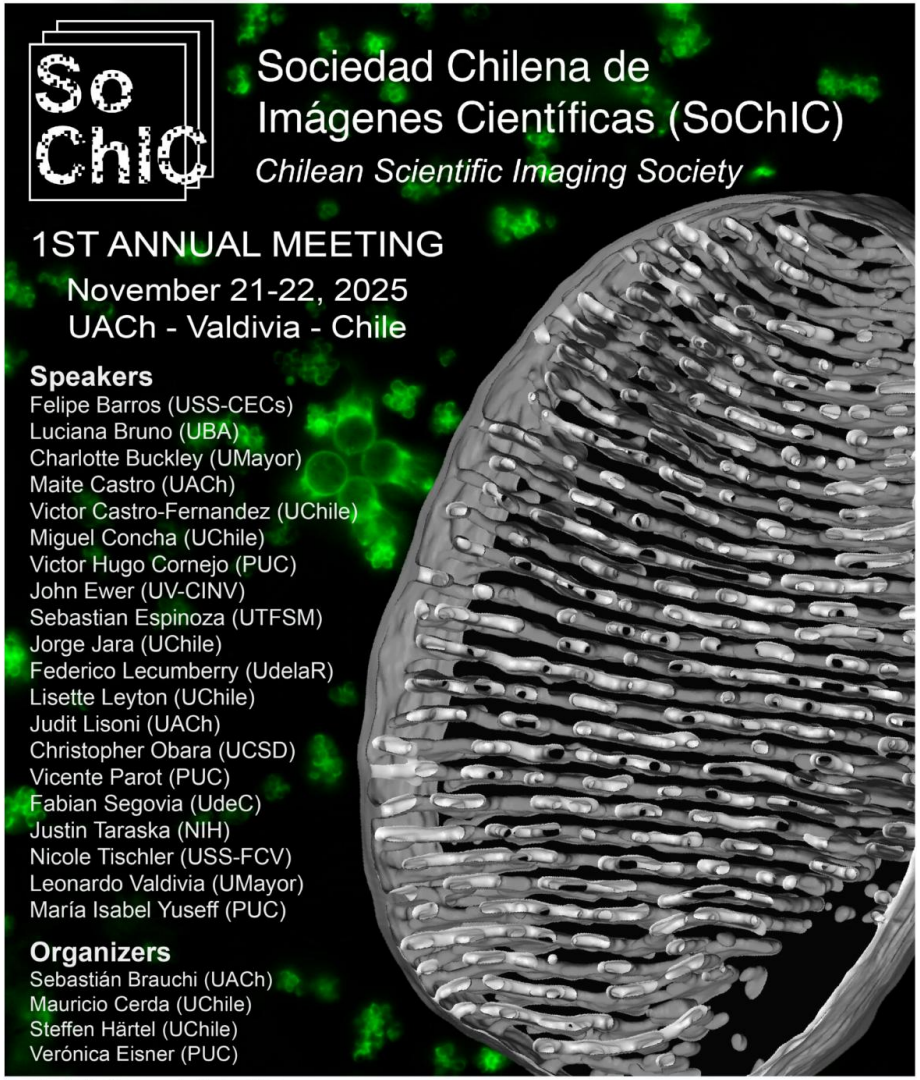

https://imagenescientificas.cl

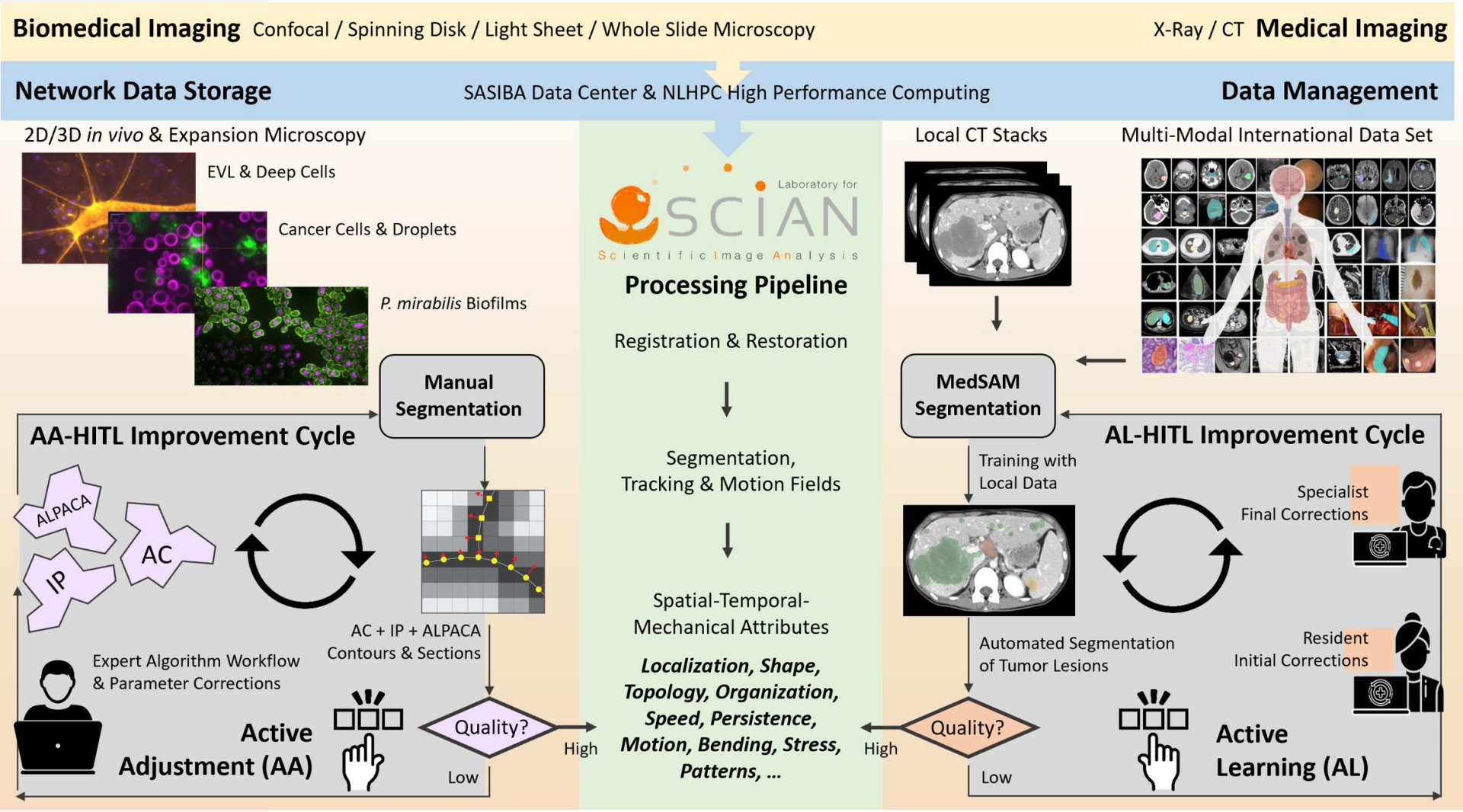
Biomedical Imaging
Confocal / Spinning Disk / Light Sheet / Whole Slide Microscopy
X-Ray / CT
Medical Imaging
Network Data Storage
SASIBA Data Center & NLHPC High Performance Computing
Data Management
2D/3D in vivo & Expansion Microscopy
EVL & Deep Cells
Cancer Cells & Droplets
P. mirabilis Biofilms
Manual Segmentation
AA-HITL Improvement Cycle
ALPACA
AC
IP
AC + IP + ALPACA
Contours & Sections
Expert Algorithm Workflow
& Parameter Corrections
Active
Adjustment (AA)
Quality?
High
Low
Laboratory for
SCIAN
Scientific Image Analysis
Processing Pipeline
Registration & Restoration
Segmentation,
Tracking & Motion Fields
Spatial-Temporal-
Mechanical Attributes
Localization, Shape,
Topology, Organization,
Speed, Persistence,
Motion, Bending, Stress,
Patterns, ...
Local CT Stacks
Multi-Modal International Data Set
MedSAM
Segmentation
AL-HITL Improvement Cycle
Training with
Local Data
Specialist
Final Corrections
Automated Segmentation
of Tumor Lesions
Resident
Initial Corrections
Quality?
High
Low
Active
Learning (AL)

Welcome

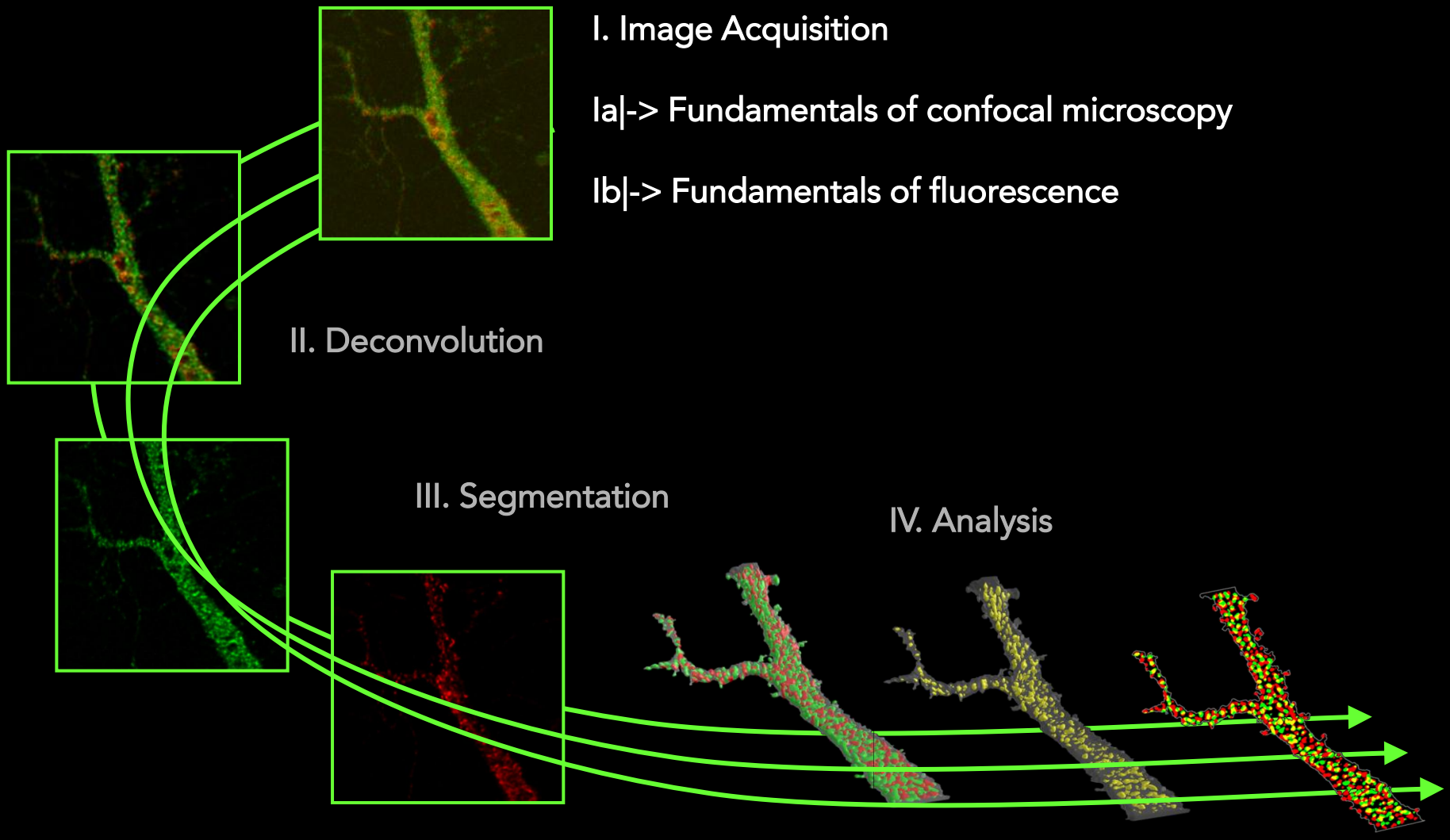
I. Image Acquisition
Ia|-> Fundamentals of confocal microscopy
Ib|-> Fundamentals of fluorescence
II. Deconvolution
III. Segmentation
IV. Analysis

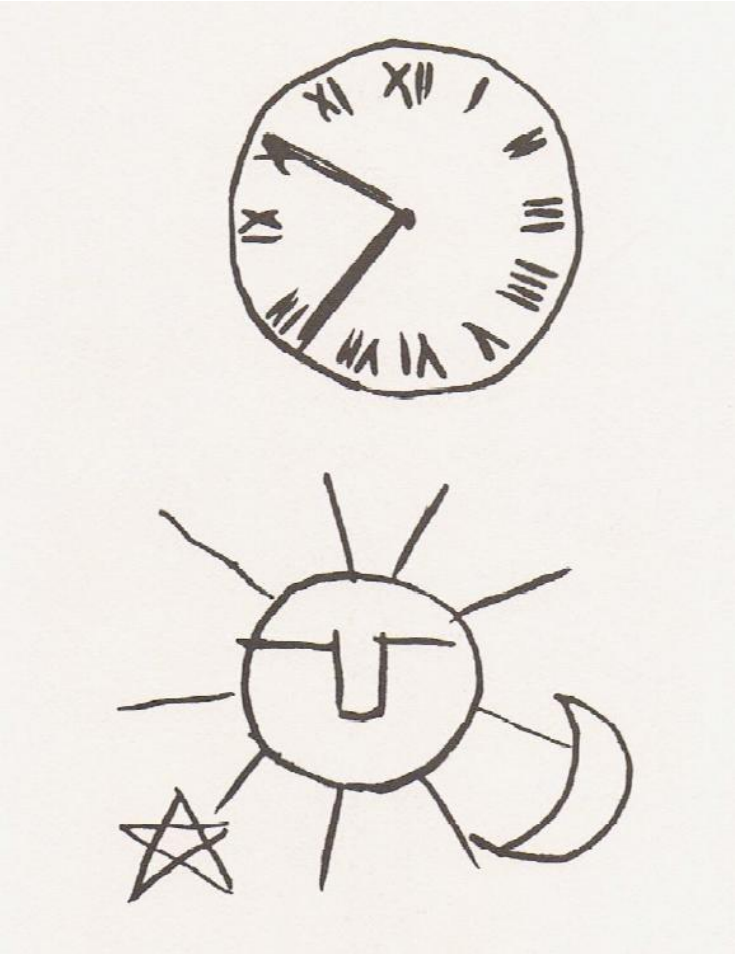

Joaquín Torres García

Uruguayan, painter and thinker,

Montevideo, Barcelona, París, NY …

TO THINK IS TO GEOMETRIZE

Geometry is like a keyboard of languages ...

... curves (regular or not), straight lines, angles, circles, arcs...

... are the few universal elements that can be used to express everything !!!!

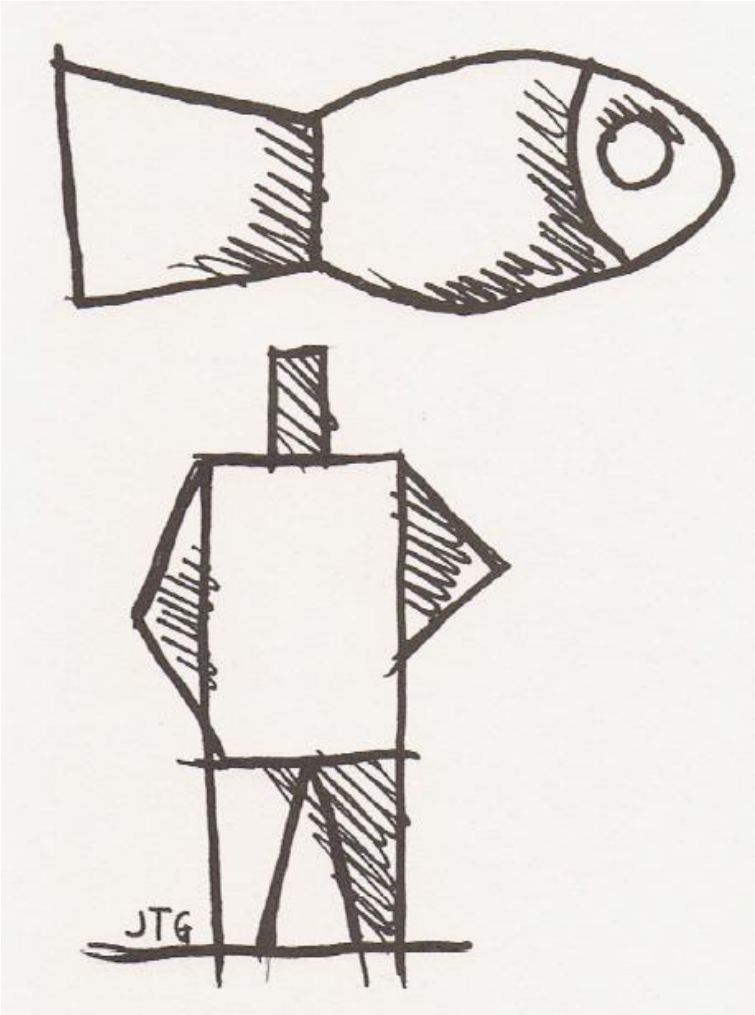

morphology

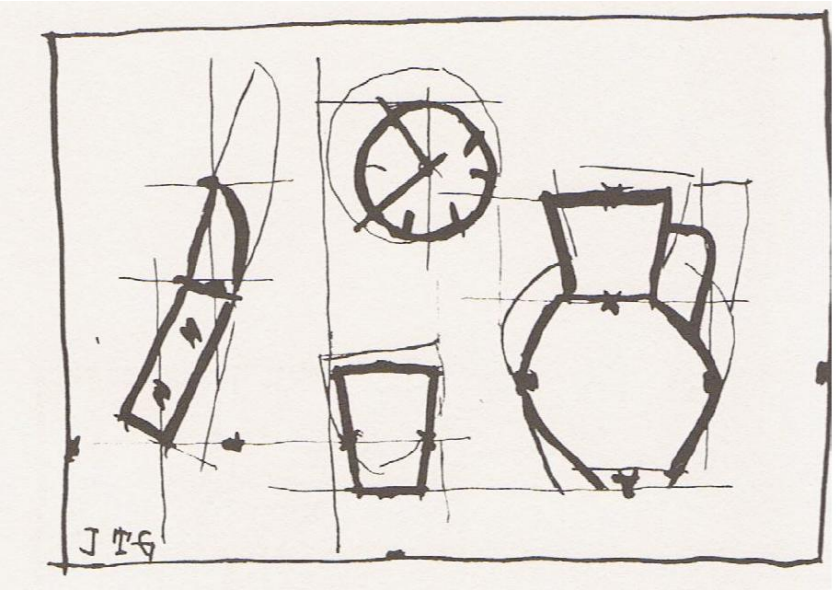

topology

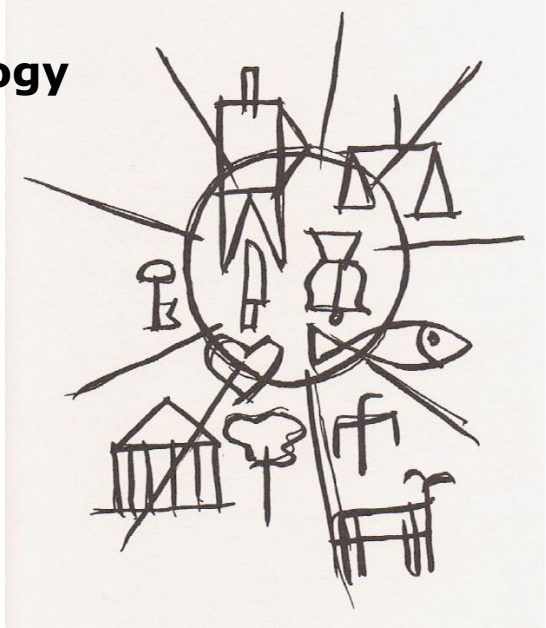

time

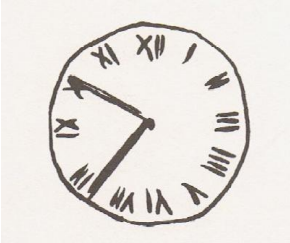

UNIVERSALISMO CONSTRUCTIVO

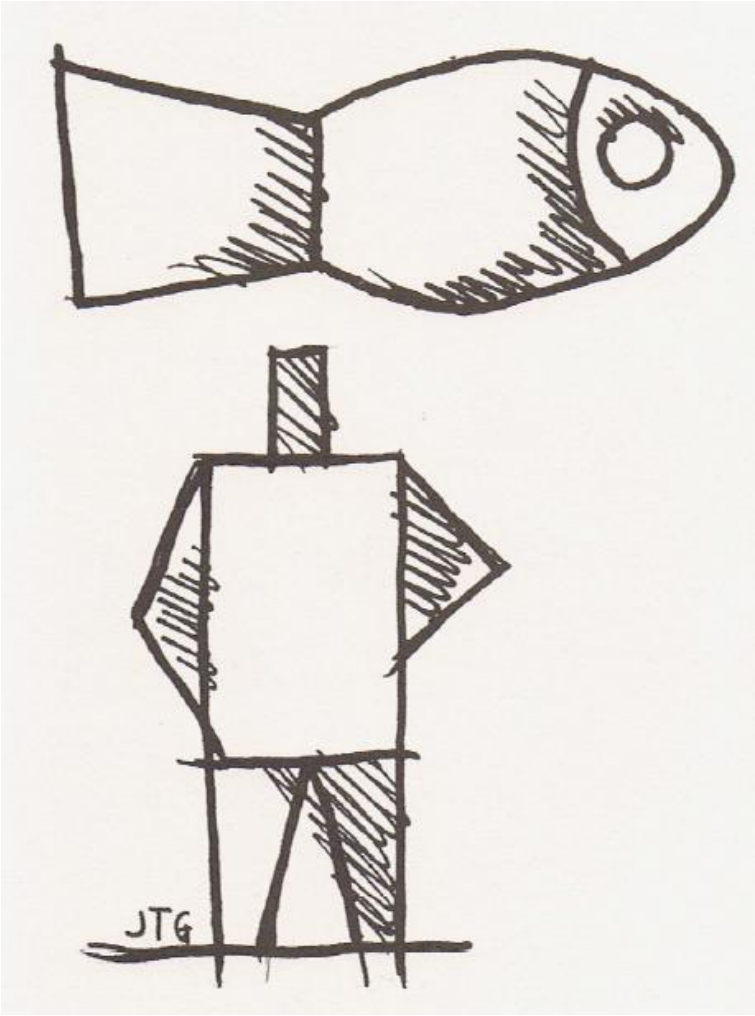

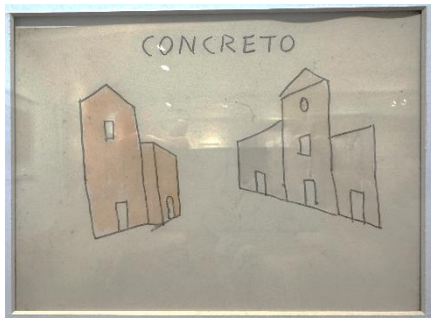

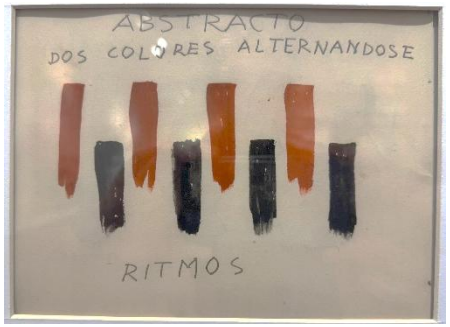

UNIVERSALISMO CONSTRUCTIVO

Shira Barzilay “KOTETIT”

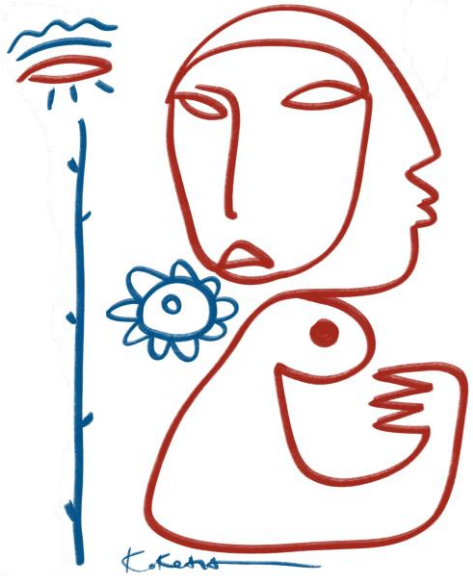

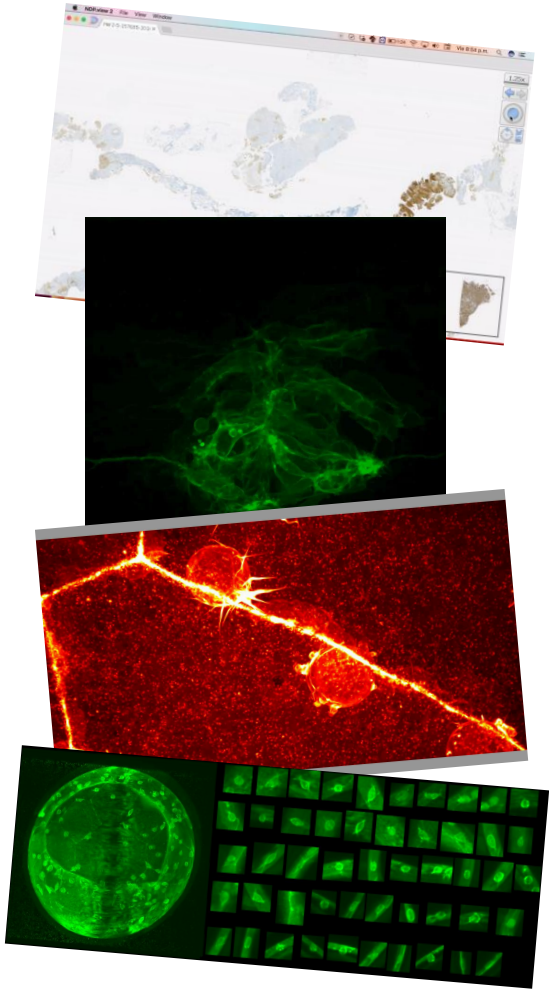

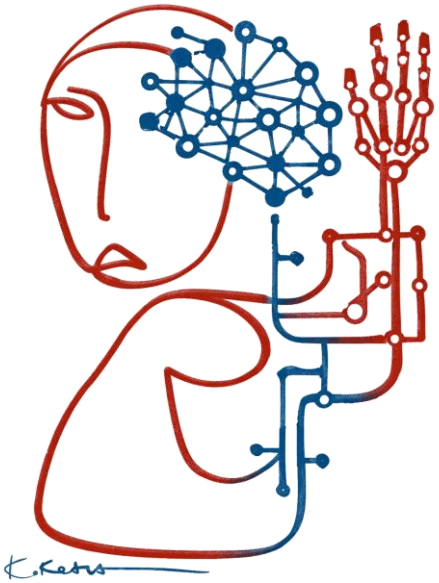

Human Observers

They interpret images **holistically, semantically, and contextually.**

...integrating prior experience, clinical knowledge, patient context, and complex visual cues, often implicitly.

Quantitative Computational Methods

They interpret images as **high-dimensional numerical data.**

... extracting explicit, reproducible, and measurable statistical and geometric patterns, without intrinsic semantic understanding.

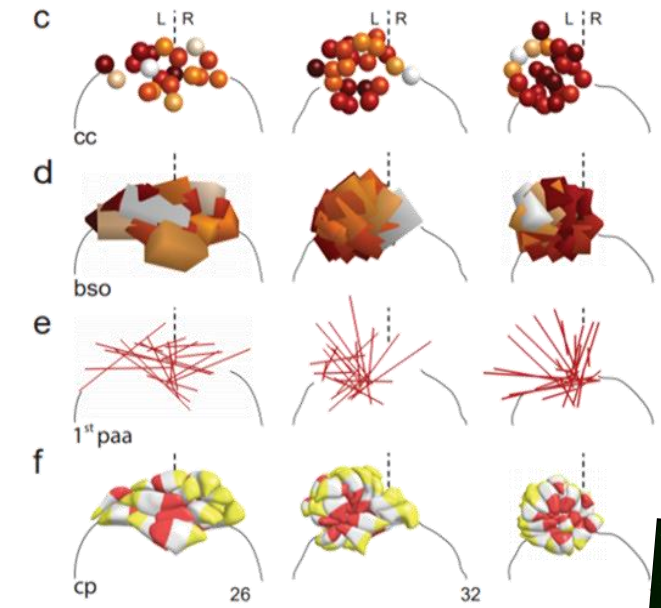

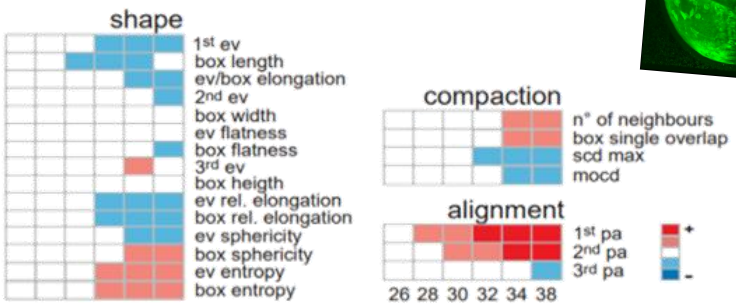

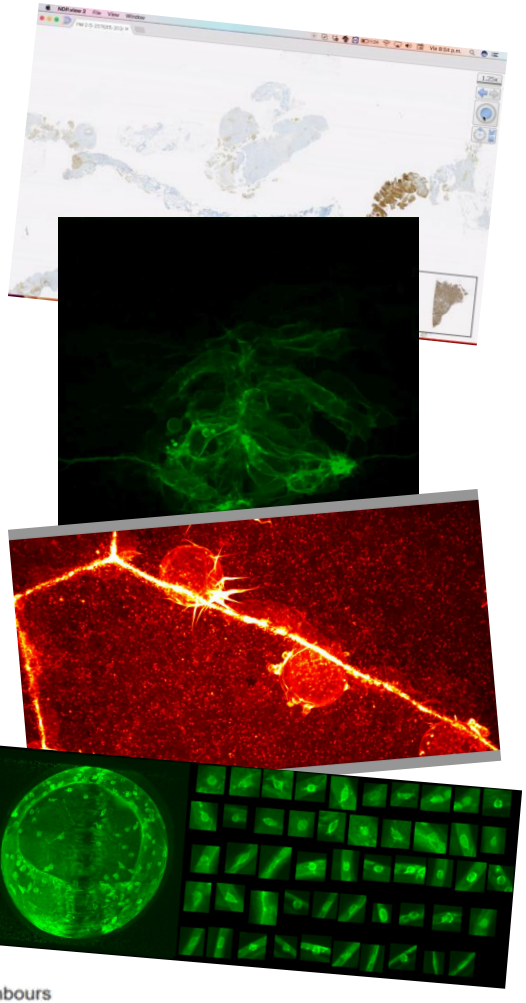

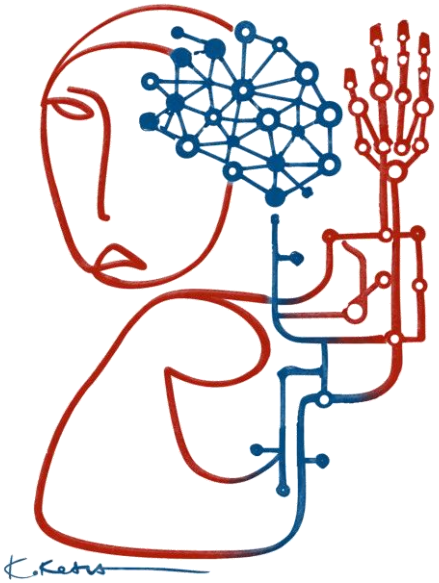

Quantitative Computational Methods

They interpret images as **high-dimensional numerical data**

... extracting explicit, reproducible, and measurable statistical and geometric patterns, without intrinsic semantic understanding.

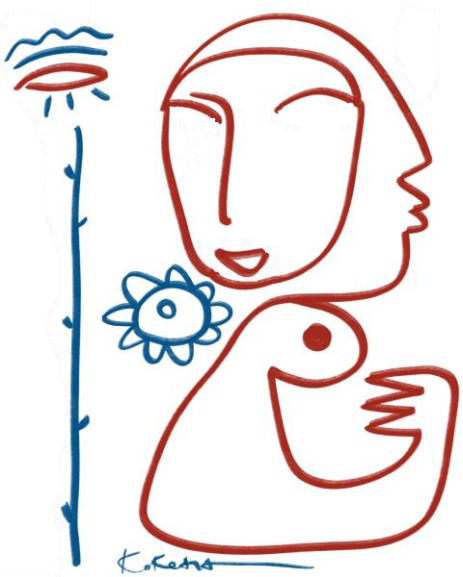

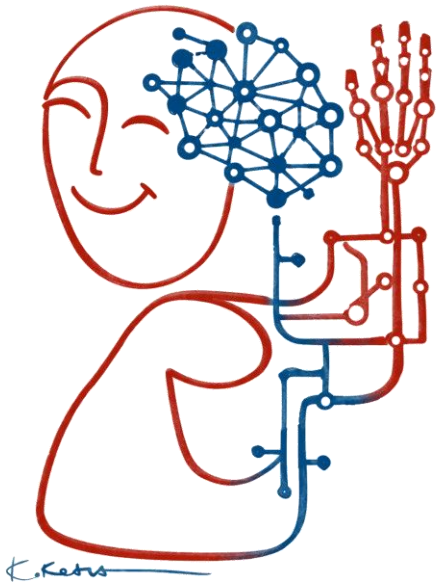

Métodos IA / Deep Learning

Interprets images as a hierarchy of automatically learned representations.
Early layers → edges, contrasts, simple textures
Intermediate layers → shapes, tissue patterns, structures
Deep layers → complex signatures associated with clinical outcomes
The interpretation is not semantic, but functional and statistical.

Human Observers

They interpret images **holistically, semantically, and contextually**.

Quantitative Computational Methods

They interpret images as **high-dimensional numerical data.**

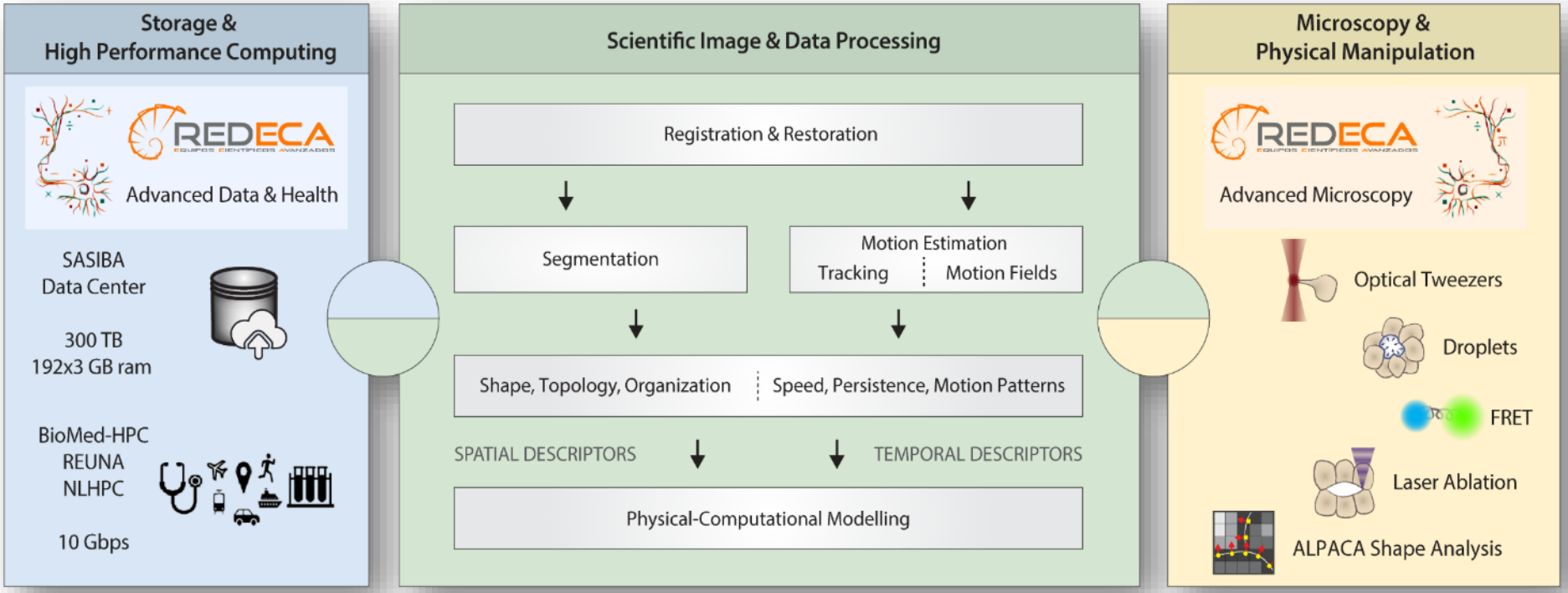

nature > nature methods > comment > article

Comment | Published: 04 May 2021

A global view of standards for open image data formats and repositories

Jason R. Swedlow, Pasi Kankaanpää, Ugis Sarkans, Wojtek Goscinski, Graham Galloway, Leonel Malacrida, Ryan P. Sullivan, Steffen Härtel, Claire M. Brown, Christopher Wood, Antje Keppler, Federica Paina, Ben Loos, Sara Zullino, Dario Livio Longo, Silvio Aime & Shuichi Onami

Miguel Concha
Developmental Biology

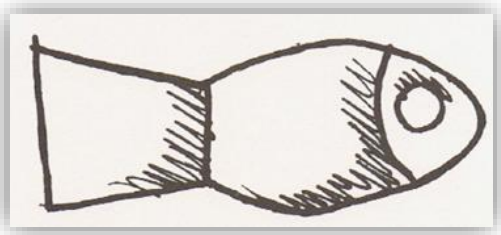

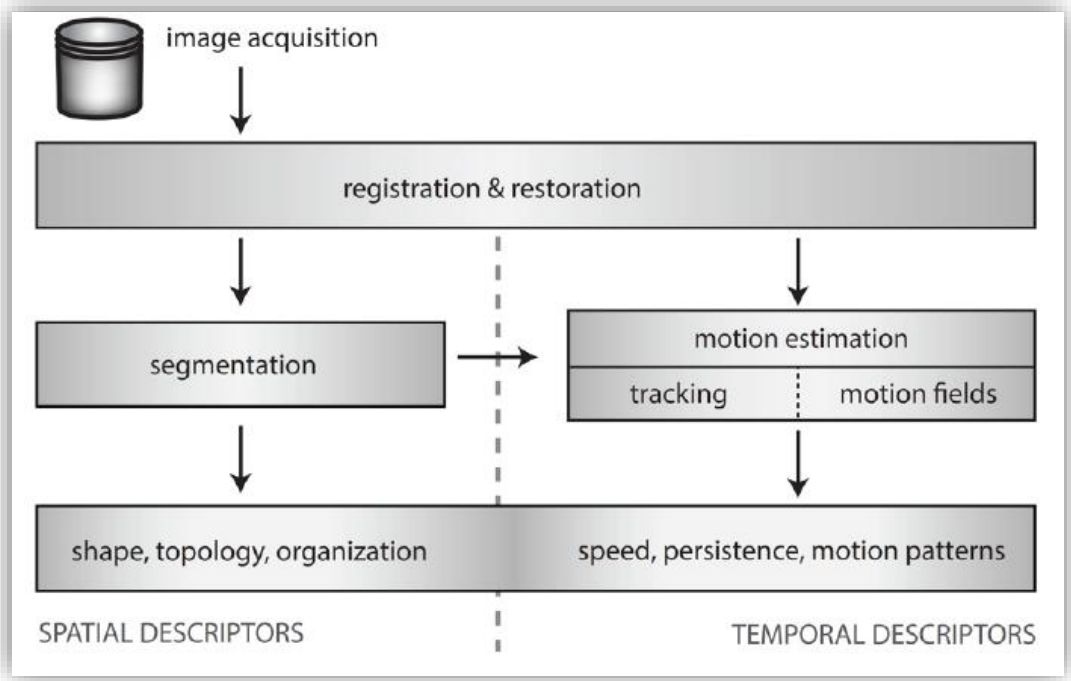

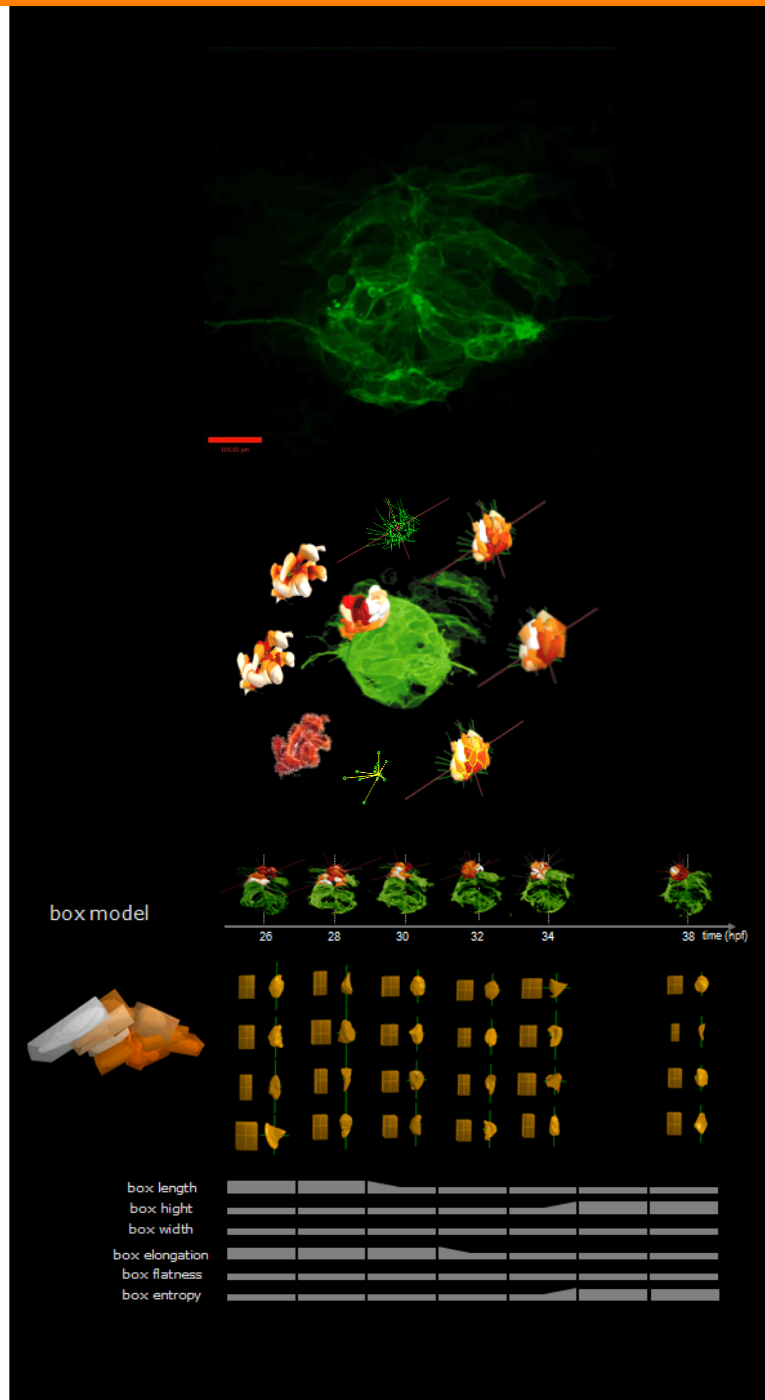

V Castañeda, M Cerda, F Santibáñez, J Jara, E Pulgar, K Palma, ...
Computational methods for analysis of dynamic events in cell migration,
Current molecular medicine 14 (2), 291-307

Laboratory for SCIAN Scientific Image Analysis

www.scian.cl

Biomedical Neuroscience Institute

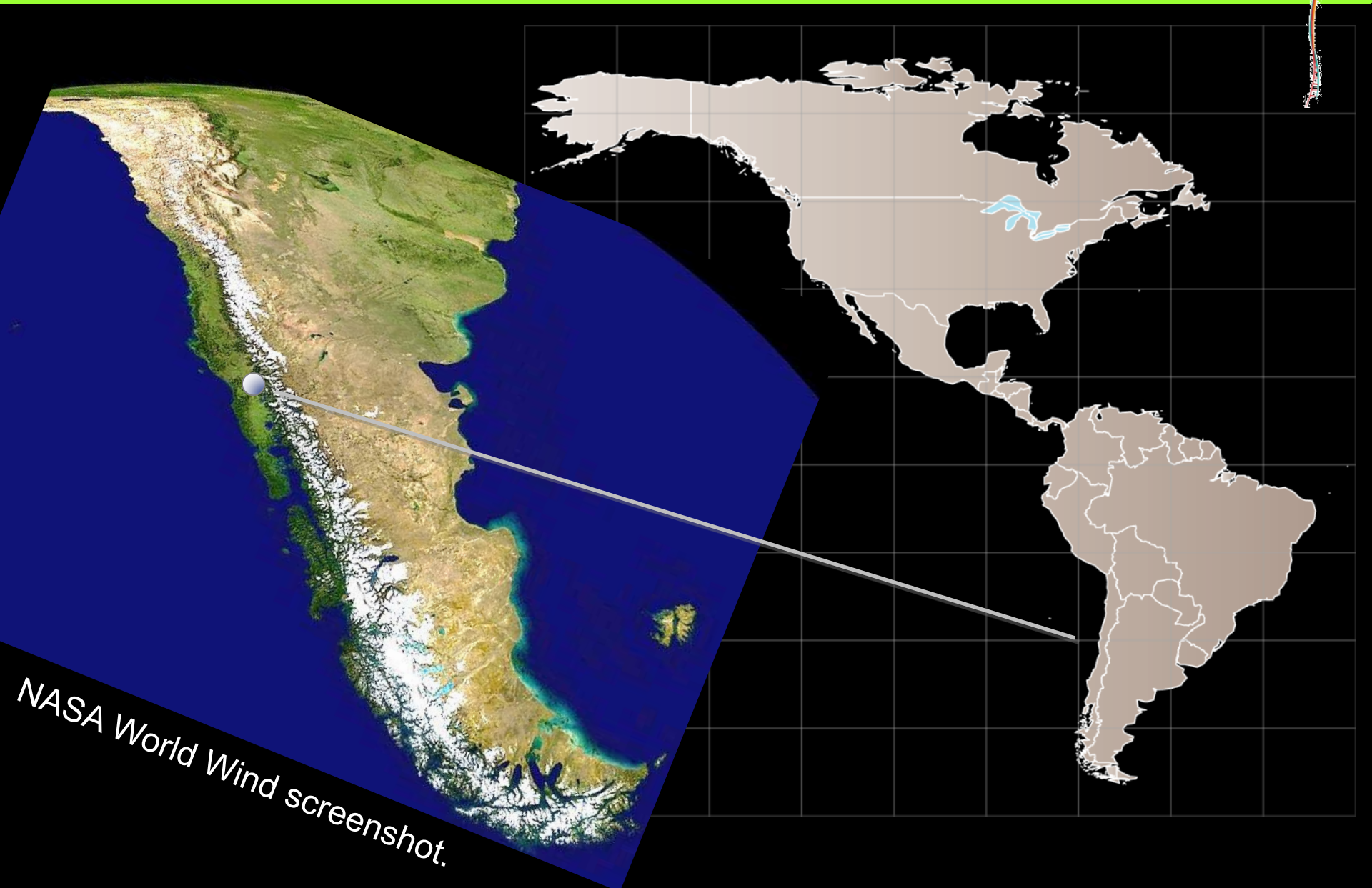

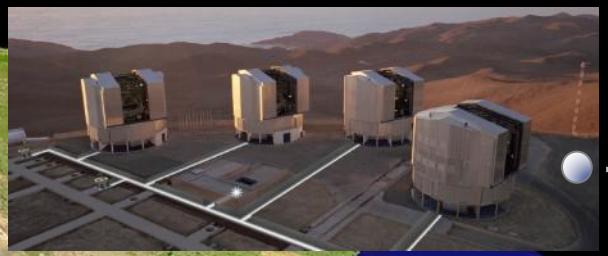

Very Large Telescope (VLT), 4 Telescopes, 8m, 2600 m

Atacama Large Millimeter/submillimeter Array (ALMA), 66 Antenna, 5000 m

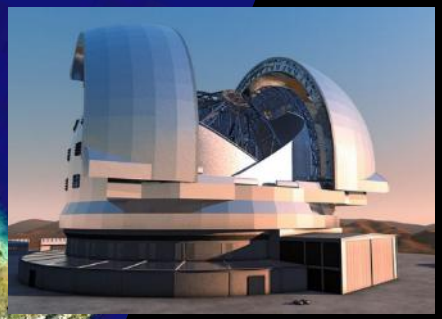

E-ELT European Extremely Large Telescope, 39 m, 3000 m

NASA World Wind screenshot

Extraterrestrial Monster Science produces:
TeraB, PetaB, ExaB, ZettaB, YottaB

… Tera is a unit prefix in the metric system denoting multiplication by 10E12 or 1.000.000.000.000 !

… Tera is derived from Greek τέρας (teras), meaning “monster”.

… Tera was confirmed for use in the SI in 1960…. Wiki !

Metric prefixes

Prefix	Symbol	1000^m	10^n	Decimal	English word[n 1]	Since[n 2]
yotta	Y	1000^8	10^{24}	1 000 000 000 000 000 000 000 000	septillion	1991
zetta	Z	1000^7	10^{21}	1 000 000 000 000 000 000 000	sextillion	1991
exa	E	1000^6	10^{18}	1 000 000 000 000 000 000	quintillion	1975
peta	P	1000^5	10^{15}	1 000 000 000 000 000	quadrillion	1975
tera	T	1000^4	10^{12}	1 000 000 000 000	trillion	1960
giga	G	1000^3	10^9	1 000 000 000	billion	1960
mega	M	1000^2	10^6	1 000 000	million	1960
kilo	k	1000^1	10^3	1 000	thousand	1795
hecto	h	$1000^{2/3}$	10^2	100	hundred	1795
deca	da	$1000^{1/3}$	10^1	10	ten	1795
		1000^0	10^0	1	one	–
deci	d	$1000^{-1/3}$	10^{-1}	0.1	tenth	1795
centi	c	$1000^{-2/3}$	10^{-2}	0.01	hundredth	1795
milli	m	1000^{-1}	10^{-3}	0.001	thousandth	1795
micro	µ	1000^{-2}	10^{-6}	0.000 001	millionth	1960
nano	n	1000^{-3}	10^{-9}	0.000 000 001	billionth	1960
pico	p	1000^{-4}	10^{-12}	0.000 000 000 001	trillionth	1960
femto	f	1000^{-5}	10^{-15}	0.000 000 000 000 001	quadrillionth	1964
atto	a	1000^{-6}	10^{-18}	0.000 000 000 000 000 001	quintillionth	1964
zepto	z	1000^{-7}	10^{-21}	0.000 000 000 000 000 000 001	sextillionth	1991
yocto	y	1000^{-8}	10^{-24}	0.000 000 000 000 000 000 000 001	septillionth	1991

The Scale of the Universe https://htwins.net/scale2

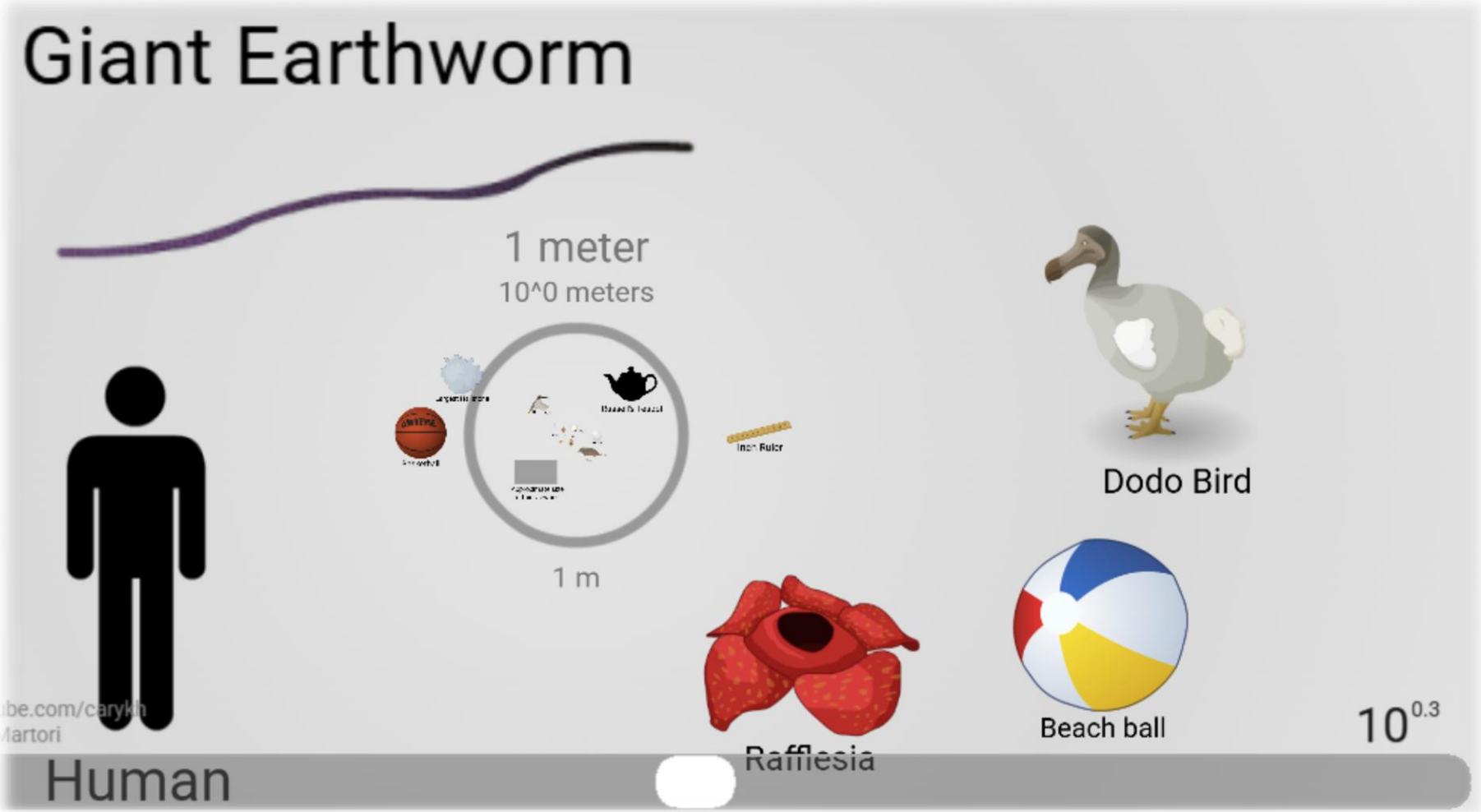

The Scale of the Universe https://htwins.net/scale2

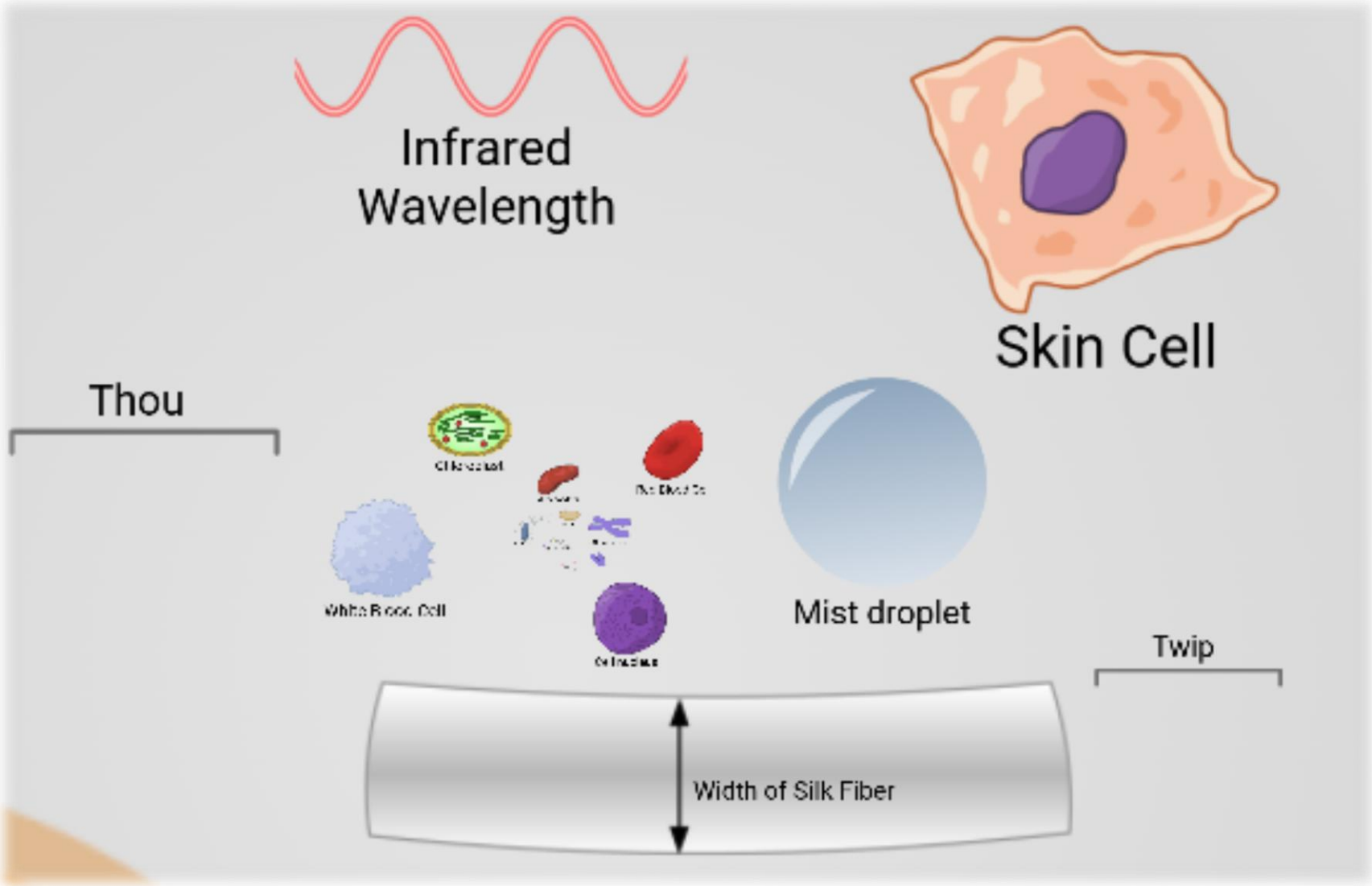

The Scale of the Universe https://htwins.net/scale2

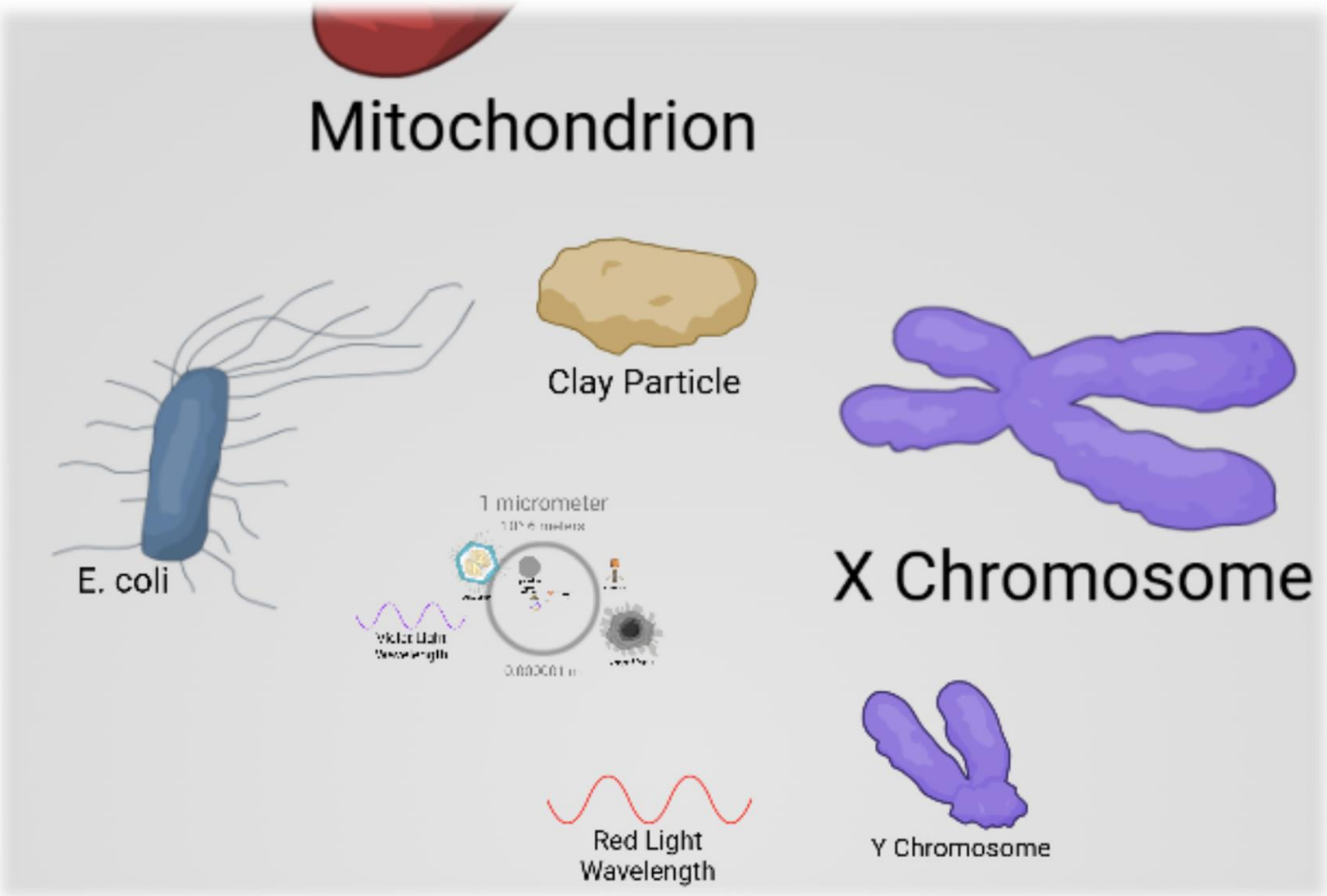

|-> Fluorescence

Luminescence :

- Fluorescence $\Delta t \sim 10^{-8}s$
- Phosphorescence $\Delta t \sim 10^{-3}\text{-}10^{0}s$

Interactions ...
- **intra- and intermolecular...**

produce changes ...
- **spectral**
- **lifetimes**
- **polarization**
- **intensity ...**

$\leftarrow \quad \Delta t \quad \rightarrow$

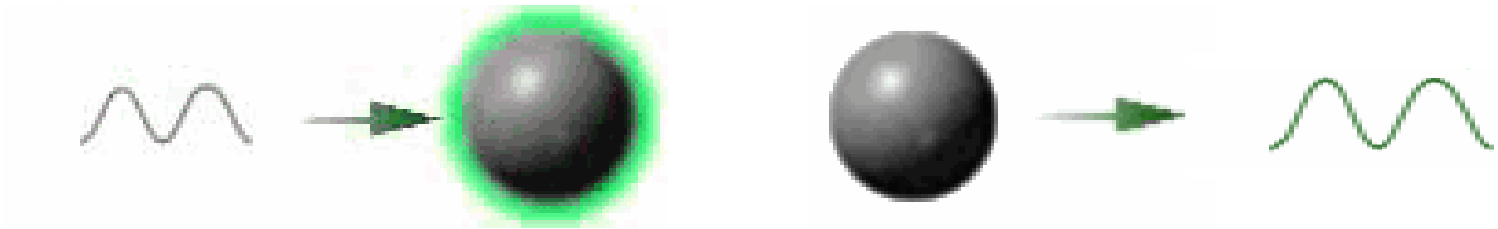

Absorption / Excitation ***Emission***

|-> Fluorescence

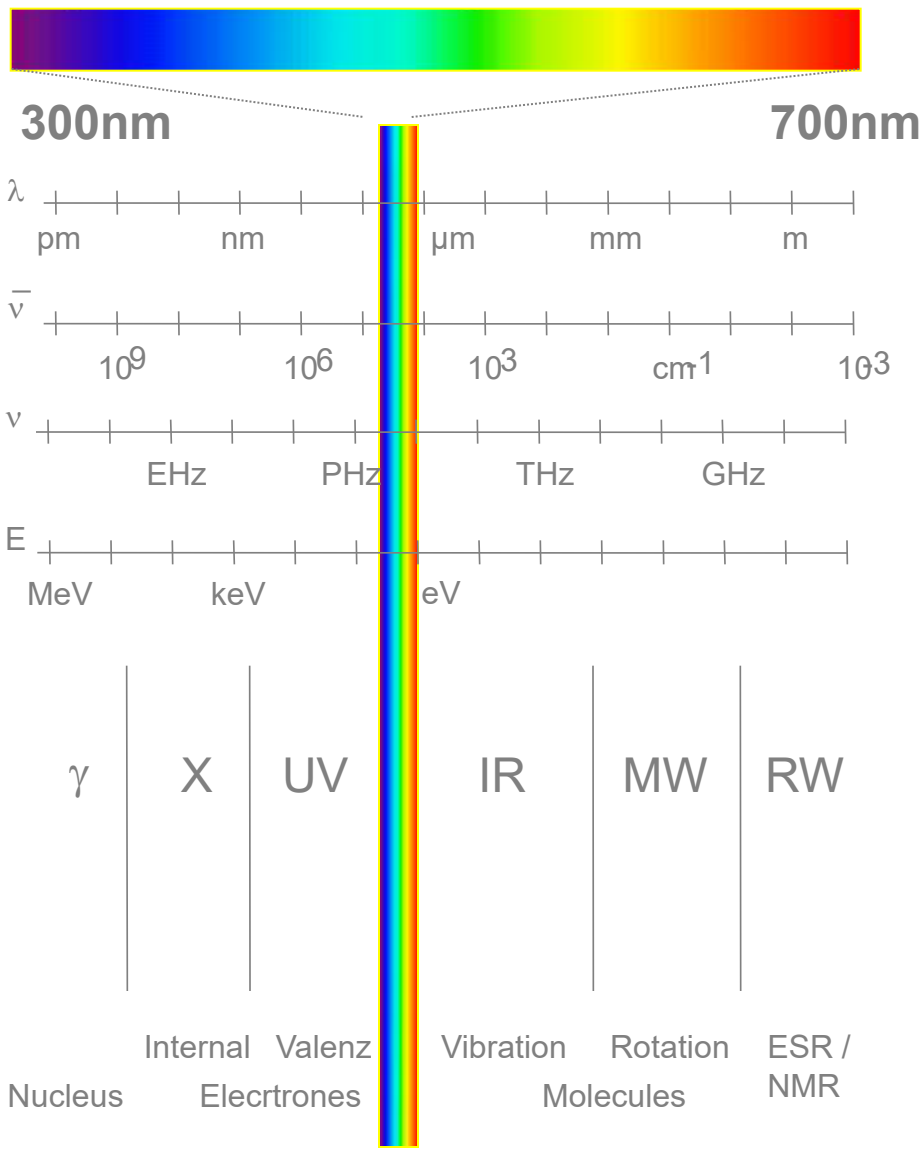

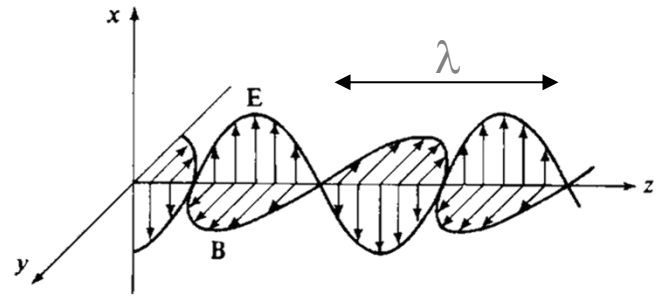

Energy of a photon : (~1-5eV)

$$E = h\nu = hc\lambda^{-1} \mid c = \nu\lambda$$

ν, frequency [s^{-1}]
h, Planck's constant [$6.626\ 10^{-34}\ Js^{-1}$]
λ, wavelength [m]
c, speed of light [$\sim 3\ 10^{8}\ ms^{-1}$]

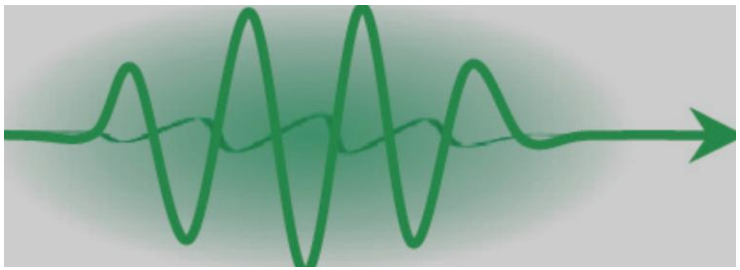

|-> Jablonski Diagram

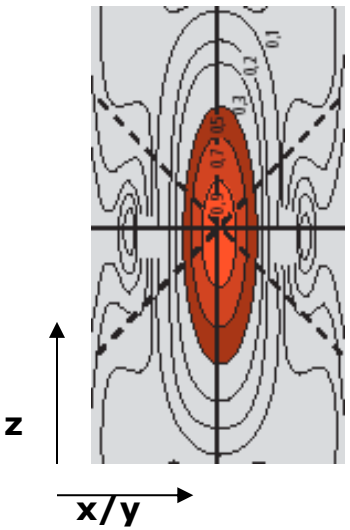

Transitions : → w radiación

w/o radiación

Levels: vibrational

electronicos

-> **heat**

-> **energy transfer (FRET)**

-> **radicales ... STED**

S_2

S_1

S_0

T_1

10^{-12}s

Internal conversio

$$\frac{N_{\Psi_{v''}}}{N_{\Psi_{v'}}} = \exp\left\{-\frac{\Delta E_{(\Psi_{v'},\Psi_{v''})}}{kT}\right\}$$

10^{-8}s

Intercombination

10^{-6} - 1s

10^{-15}s **Absorption**

10^{-9}-10^{-8}s **Fluorescence**

10^{-6} - 1s **Phosphorescence**

|-> Diffraction limited Microscopy

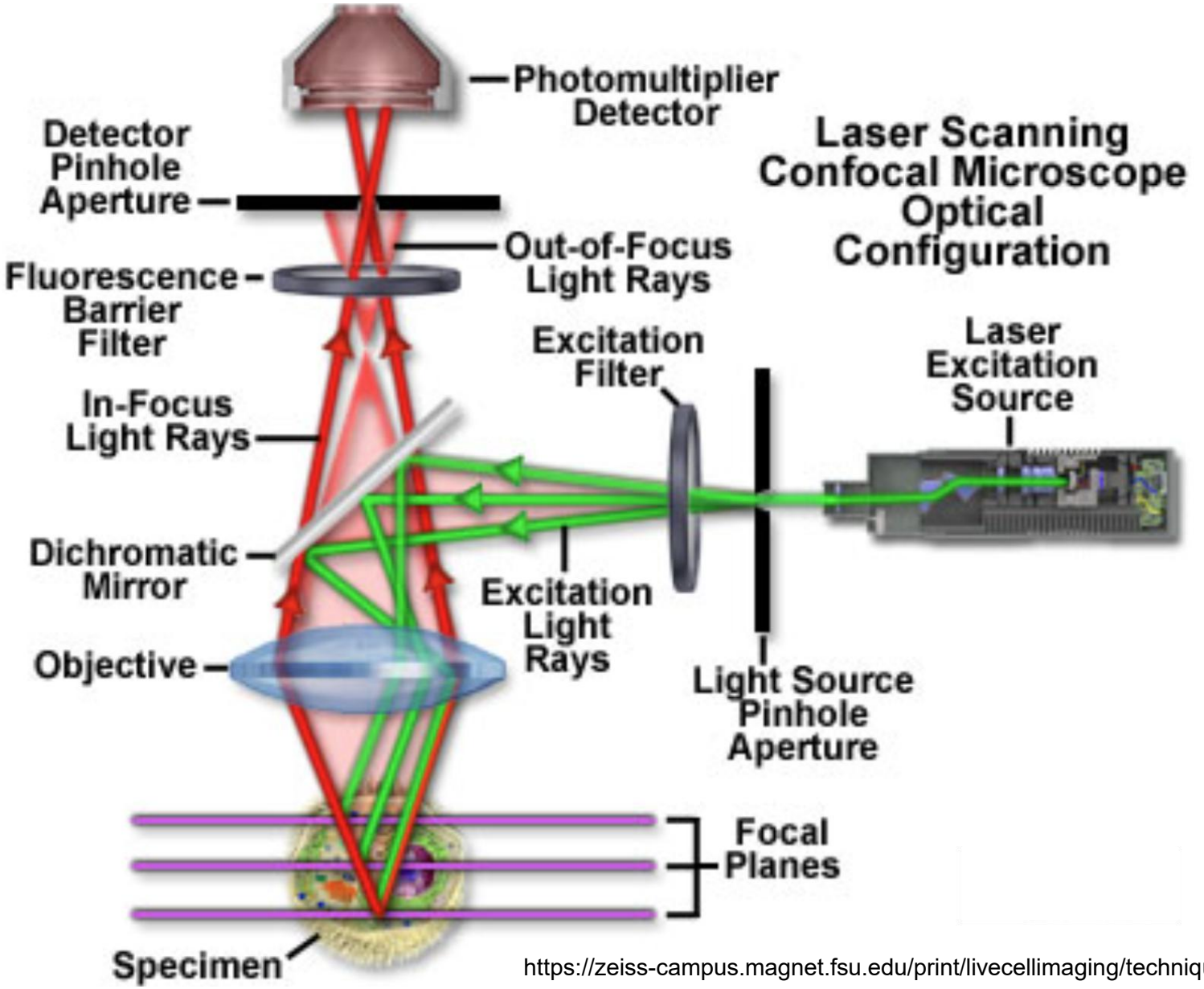

https://zeiss-campus.magnet.fsu.edu/print/livecellimaging/techniques-print.html

|-> Diffraction limited Microscopy

Non-geometric optics /

Diffraction theory

PSF = $|U|^2 = f(J_0)$

U, Kirhoff's Diffraction Integral

J_0, Bessel function series

(Born & Wolf, Priniples of Optics, 6th edition 1988, Pergamon Press)

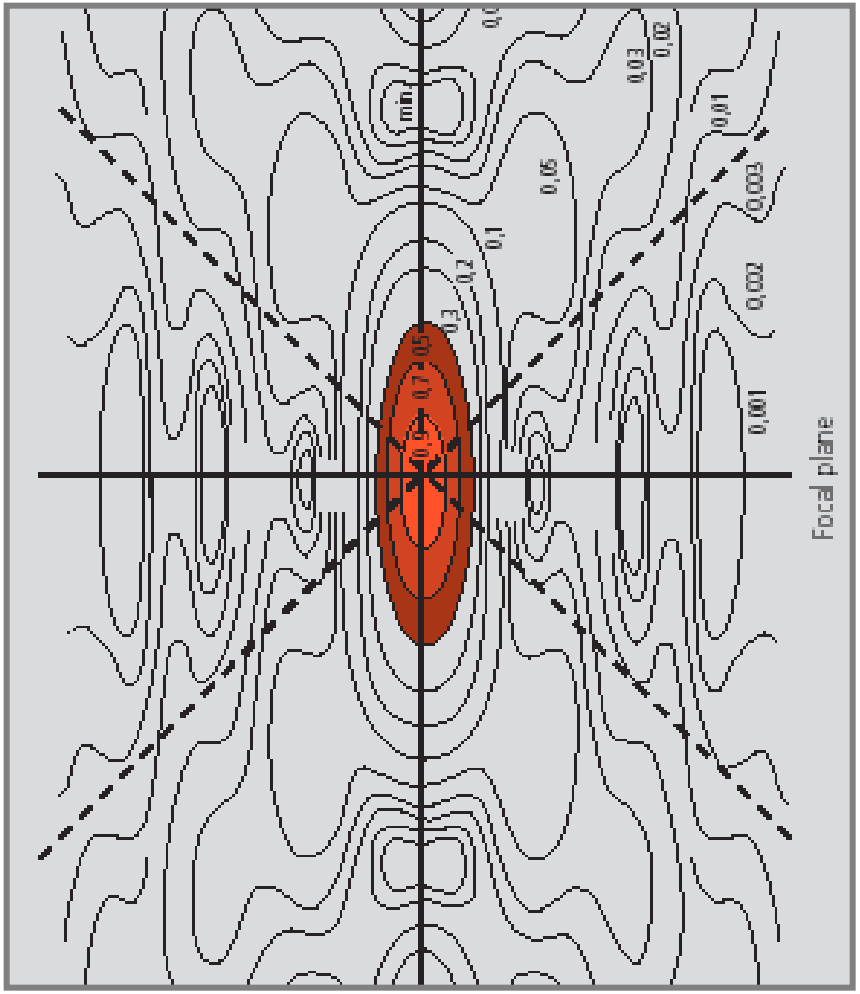

|-> Diffraction limited Microscopy

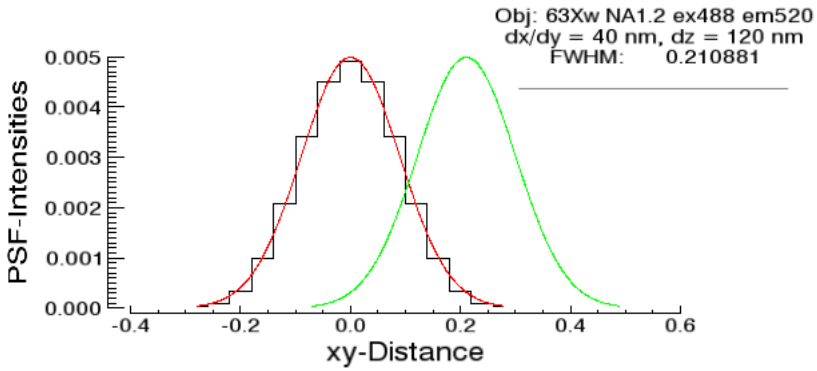

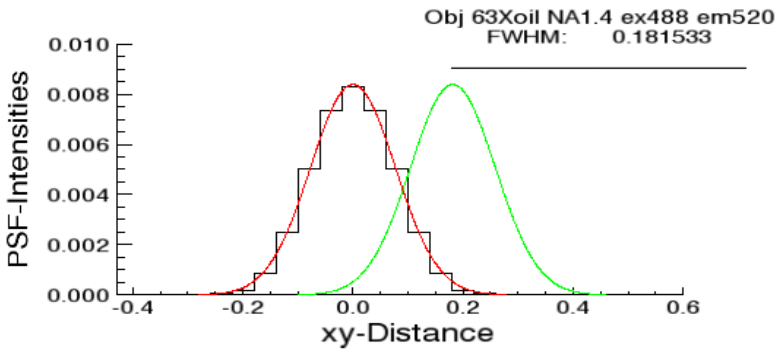

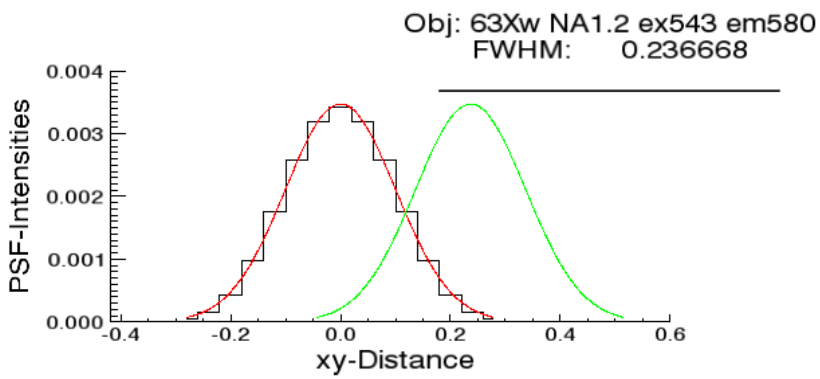

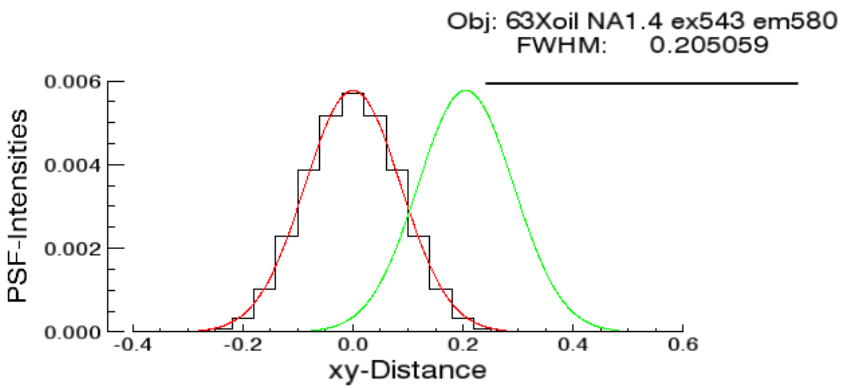

|-> Confocal, Spinning & Light Sheet Microscopy

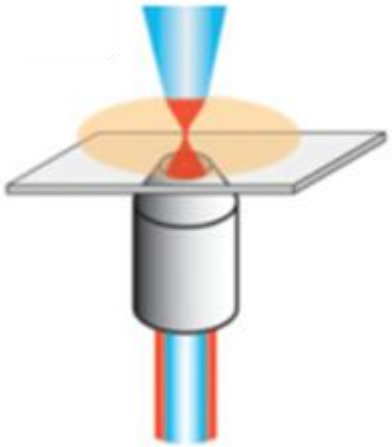

Laser scanning confocal

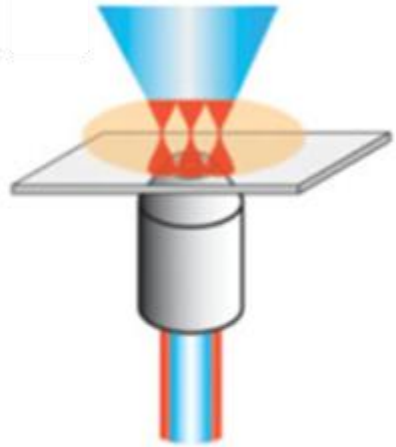

Spinning disk confocal

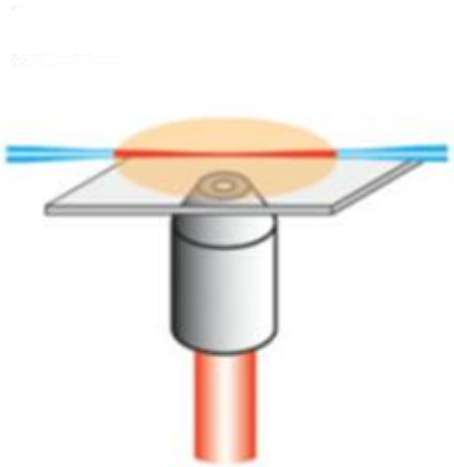

Light sheet

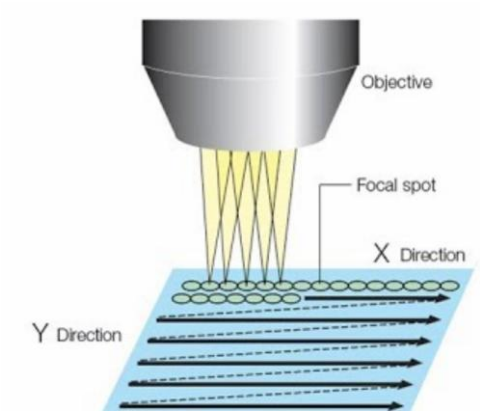

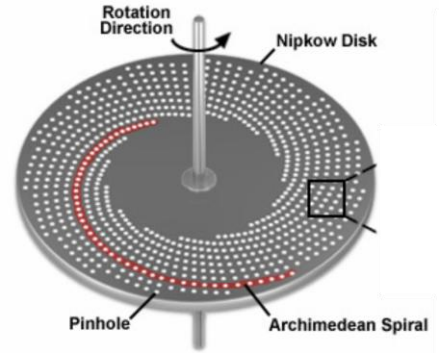

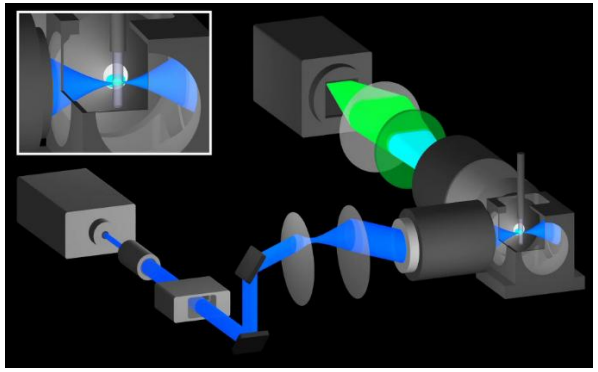

|-> Confocal, Spinning & Light Sheet Microscopy

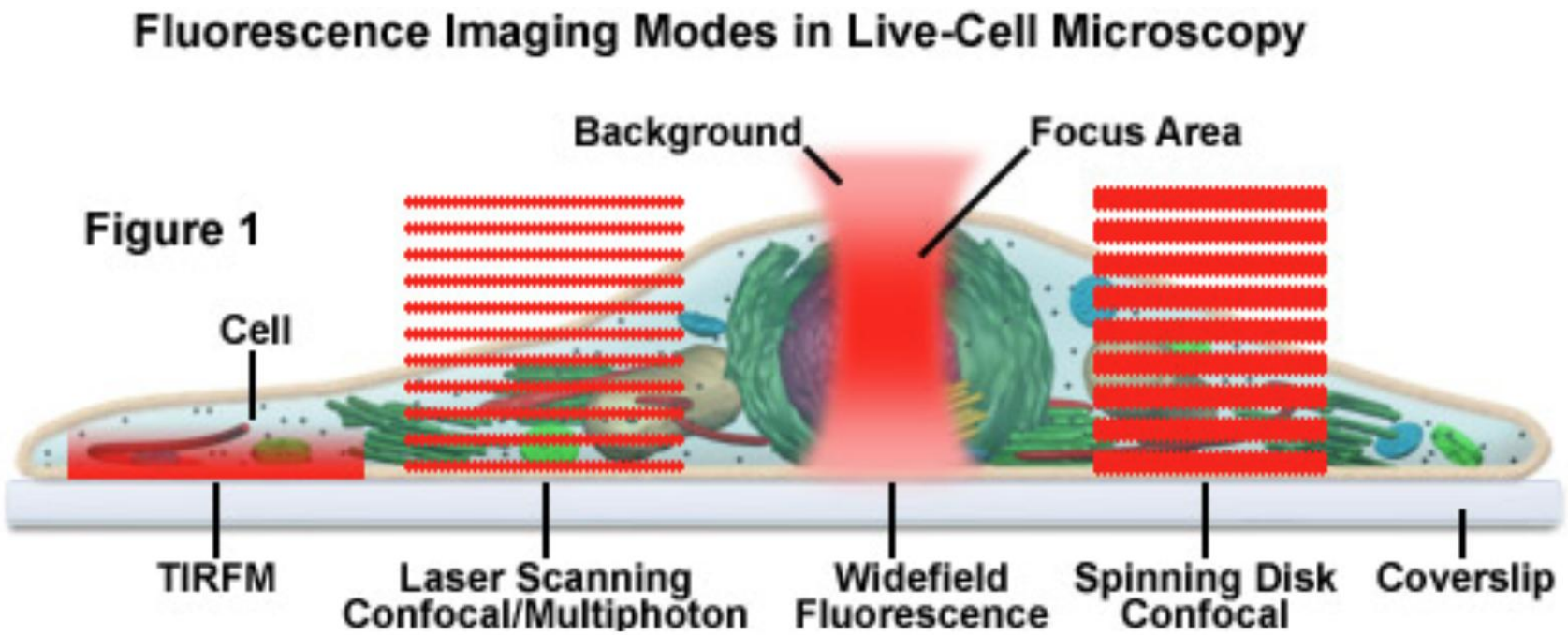

https://zeiss-campus.magnet.fsu.edu/print/livecellimaging/techniques-print.html

|-> Convoal vs Spinning Disk Microscopy

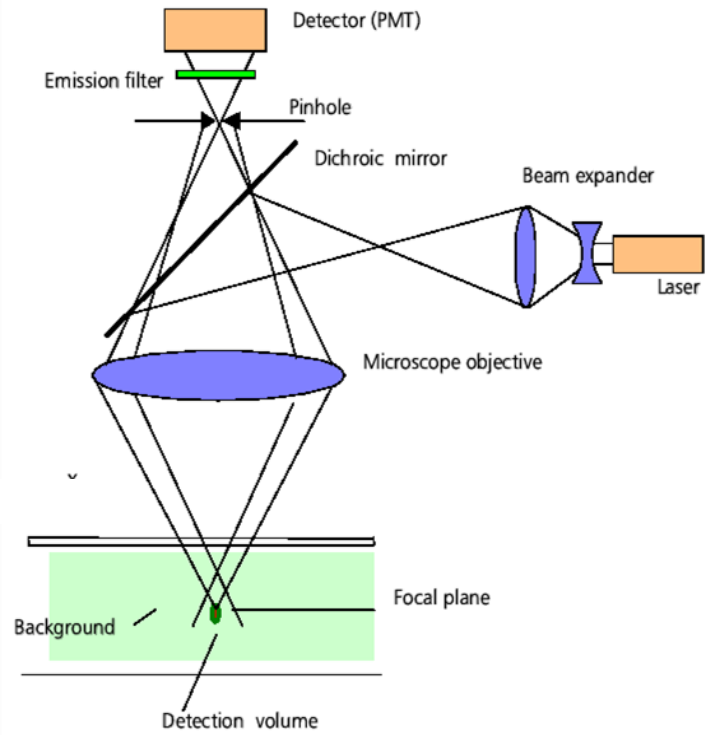

confocal

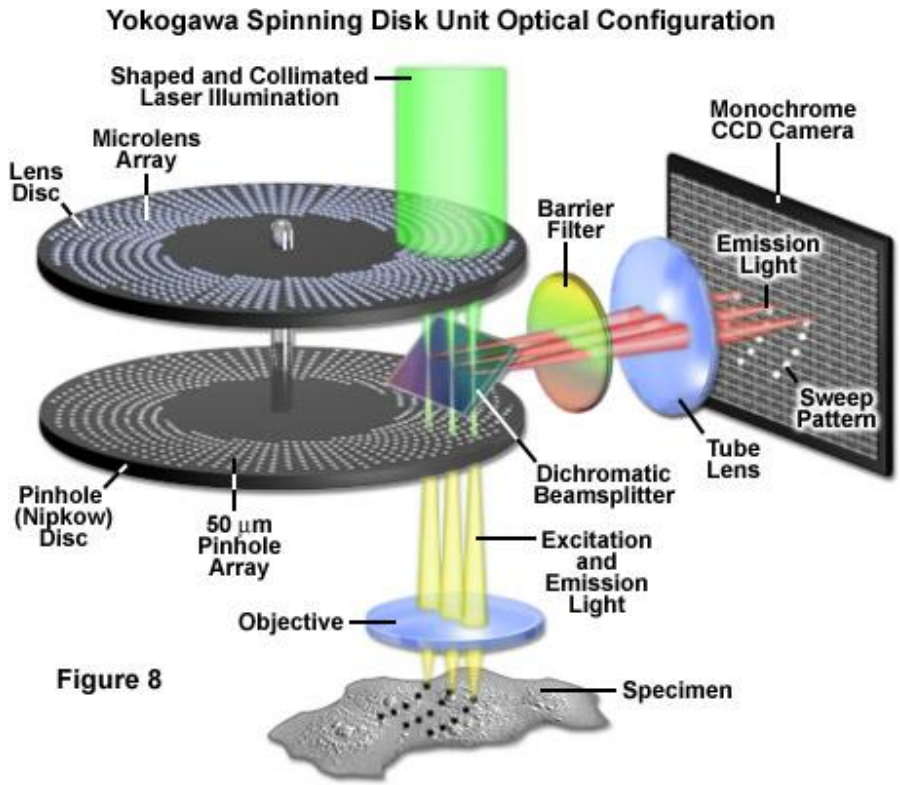

spinning disk

|-> Perkin Elmer Spinning Disk with laser ablation

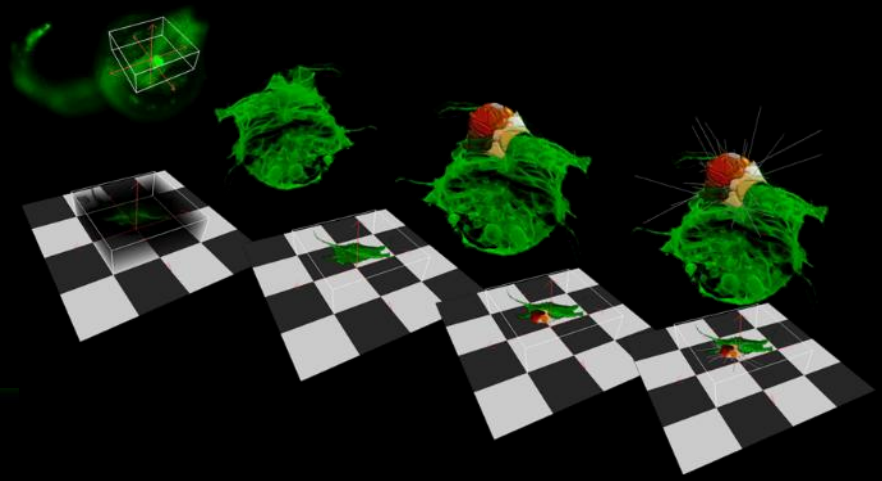

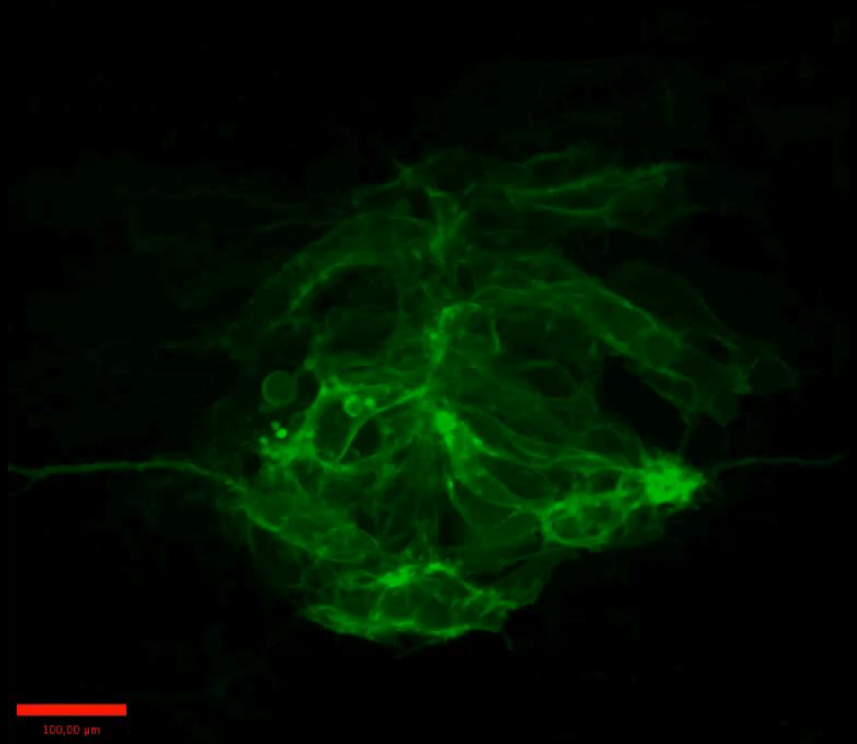

|-> Deconvolution

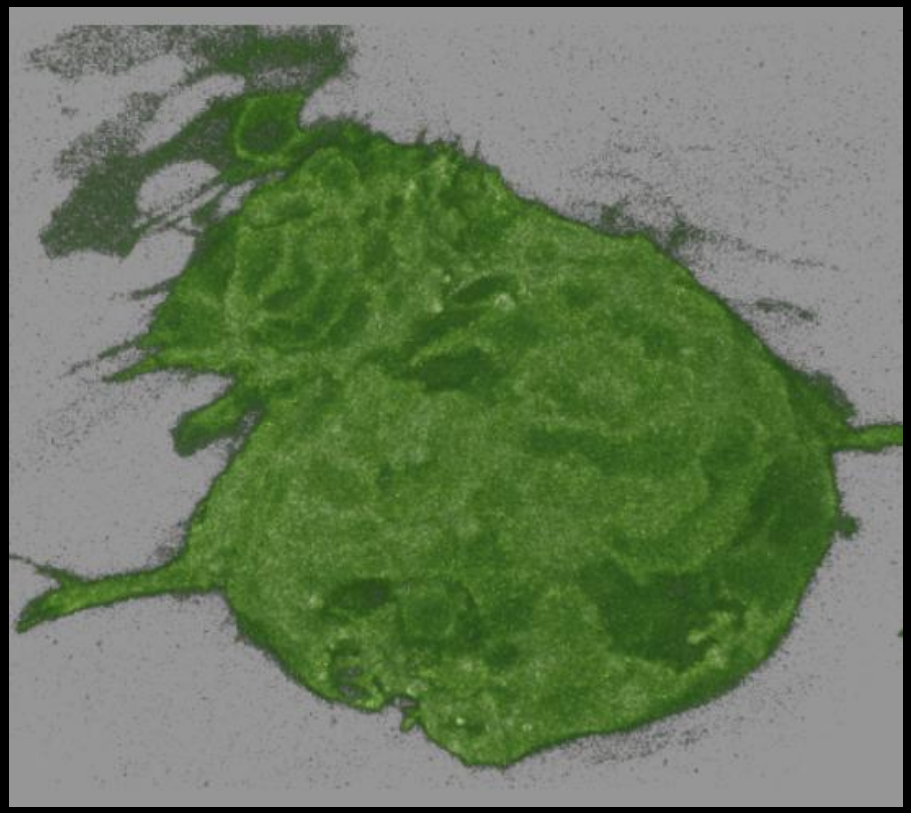

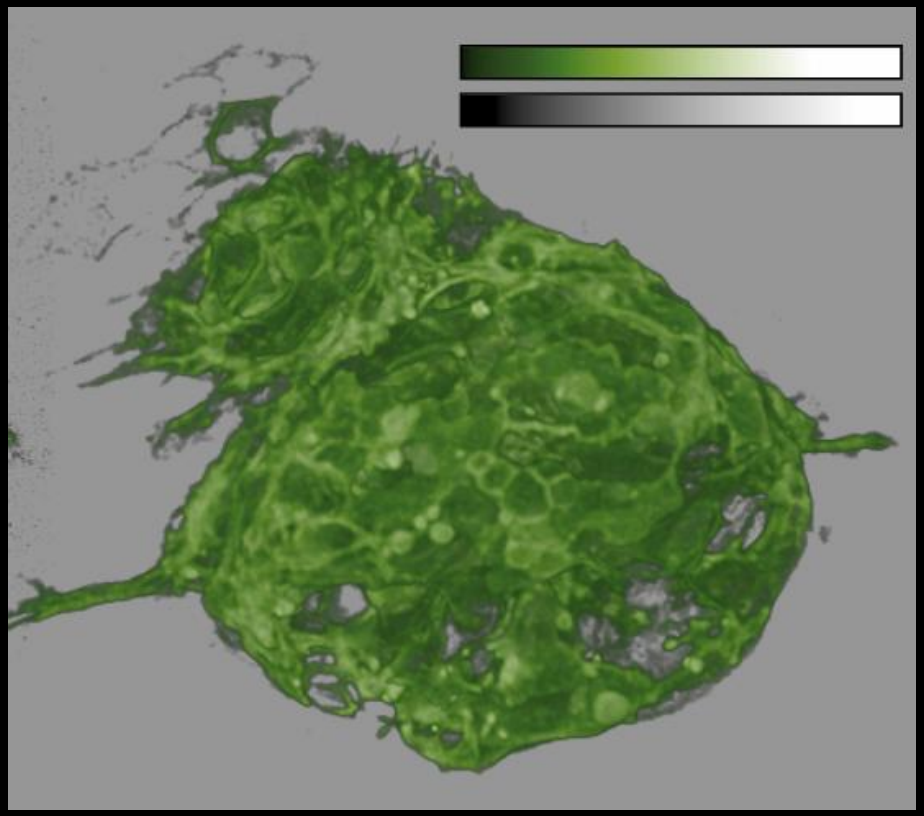

|-> Deconvolution

box model

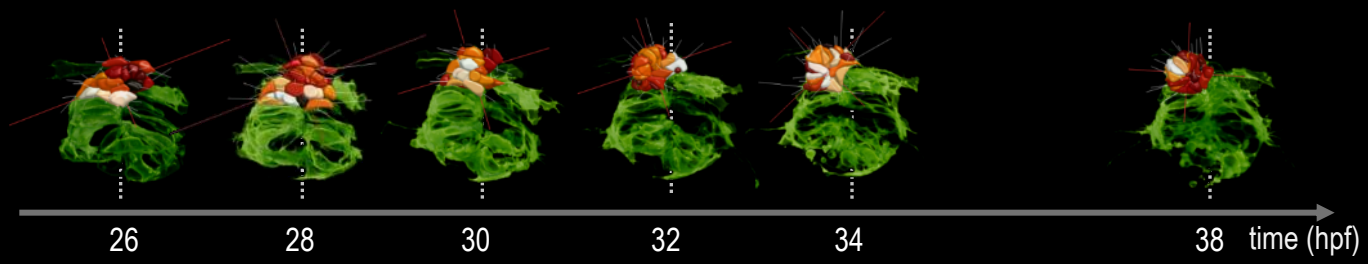

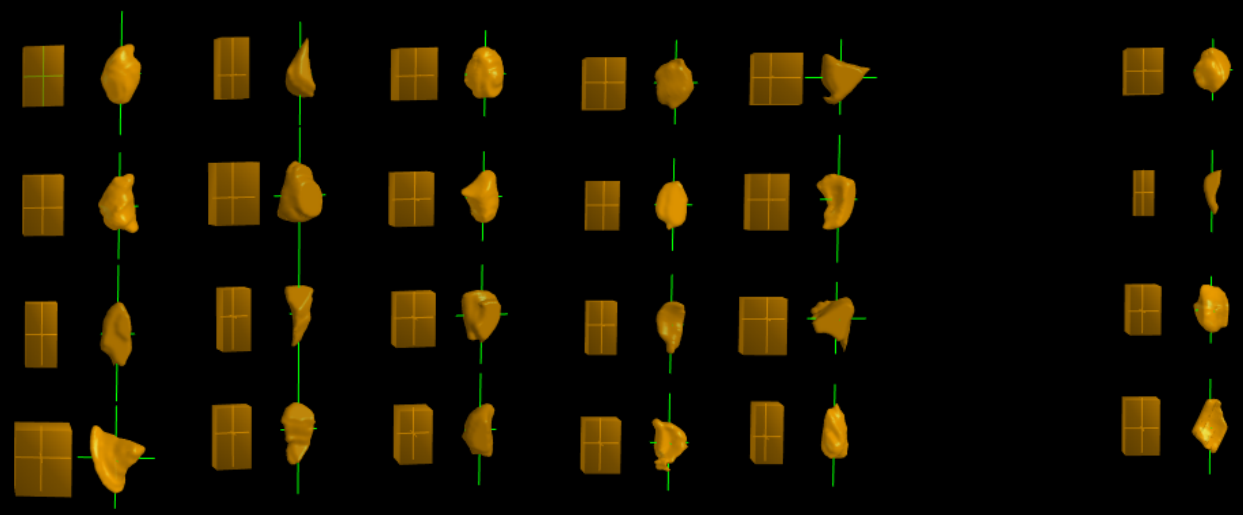

box length

box hight

box width

box elongation

box flatness

box entropy

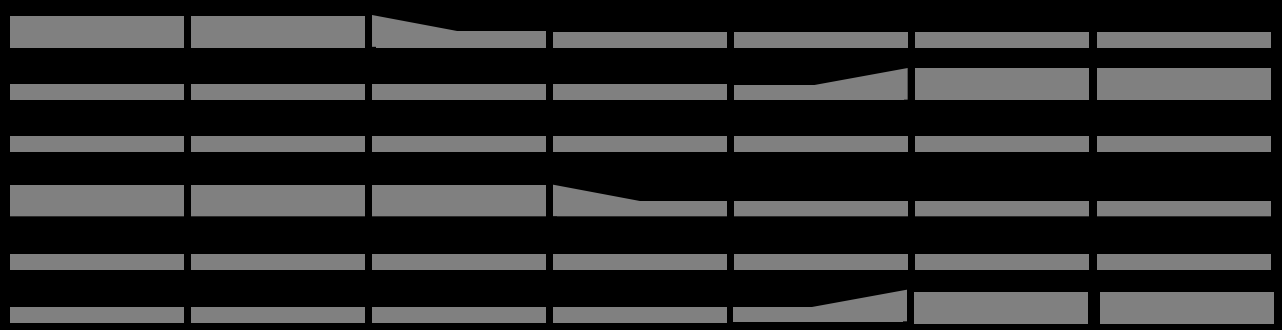

|-> Perkin Elmer Spinning Disk

Austrolebias Nigripinnis, Microinyección mRNA para la expresión de LifeAct-GFP (actina). migración de Deep Cells (DC) a través del Enveolpping Layer (EVL). (G.Reig)

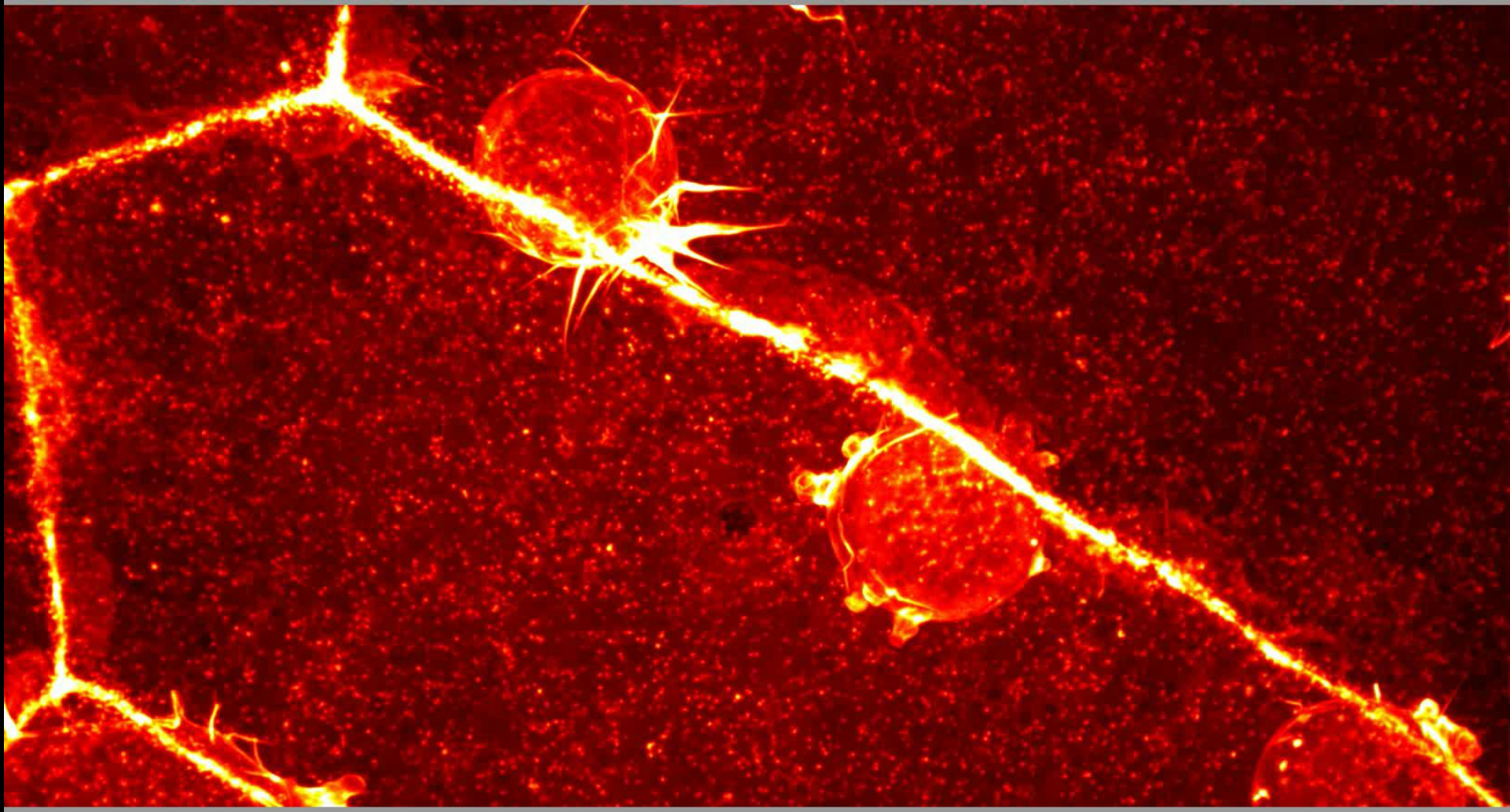

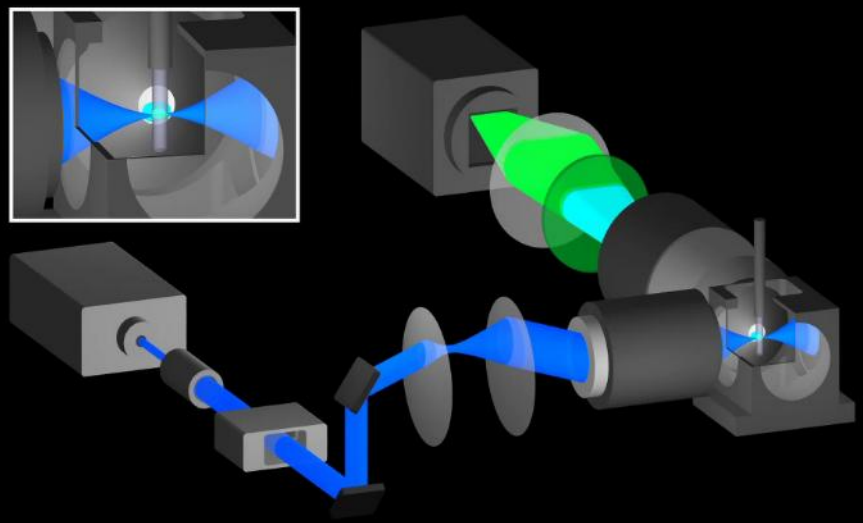

Ulrich Kubitscheck
Bonn

Pulgar, Keller, Concha, unpublished

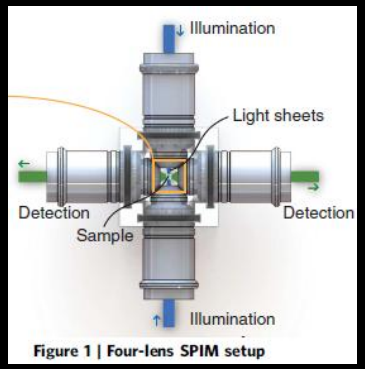

Figure 1 | Four-lens SPIM setup

Jan Huisken
Dresden

Pulgar, Keller, Concha, unpublished

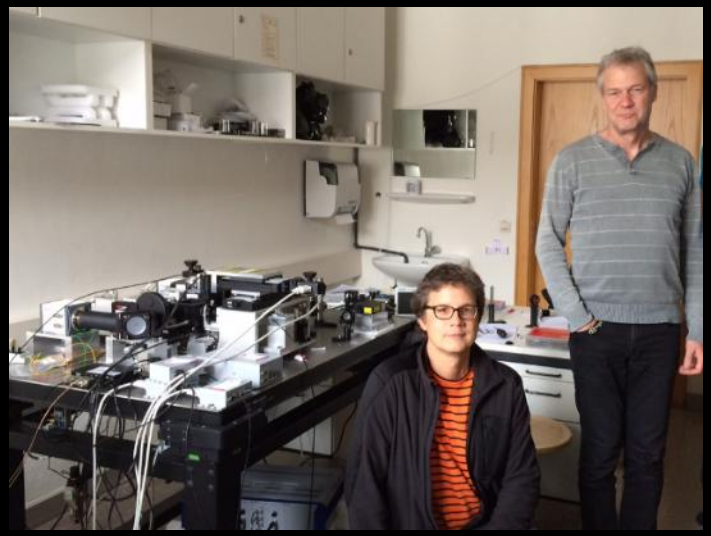

|-> Microscopy

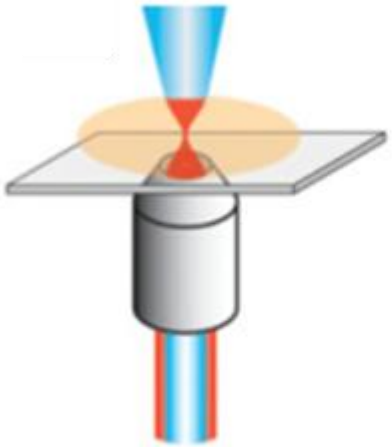

Laser scanning confocal

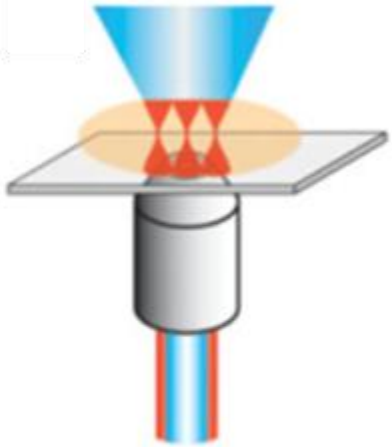

Spinning disk confocal

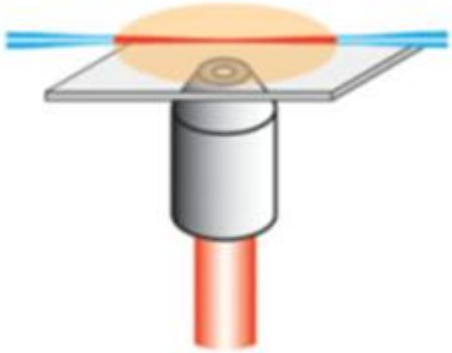

Light sheet

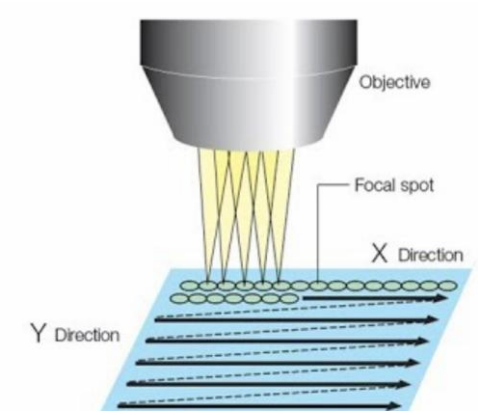

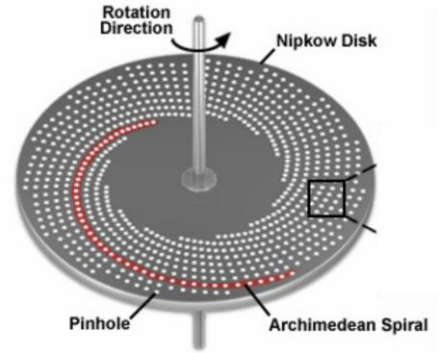

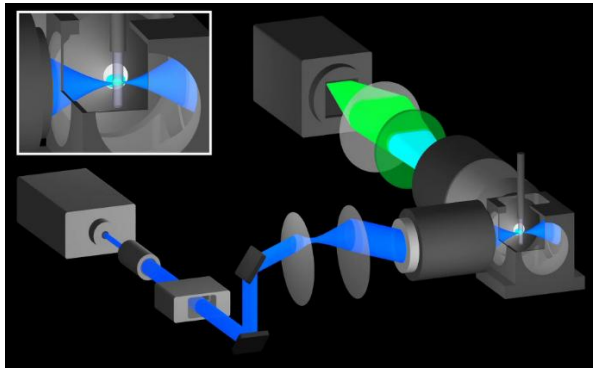

|-> Microscopy

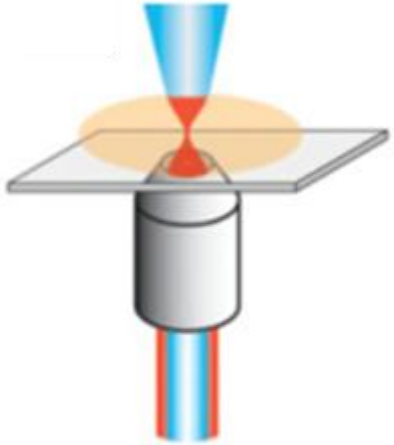

Laser scanning confocal

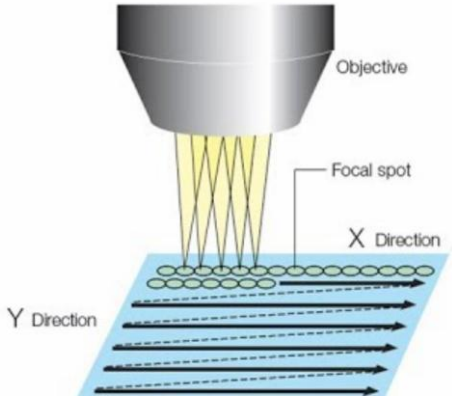

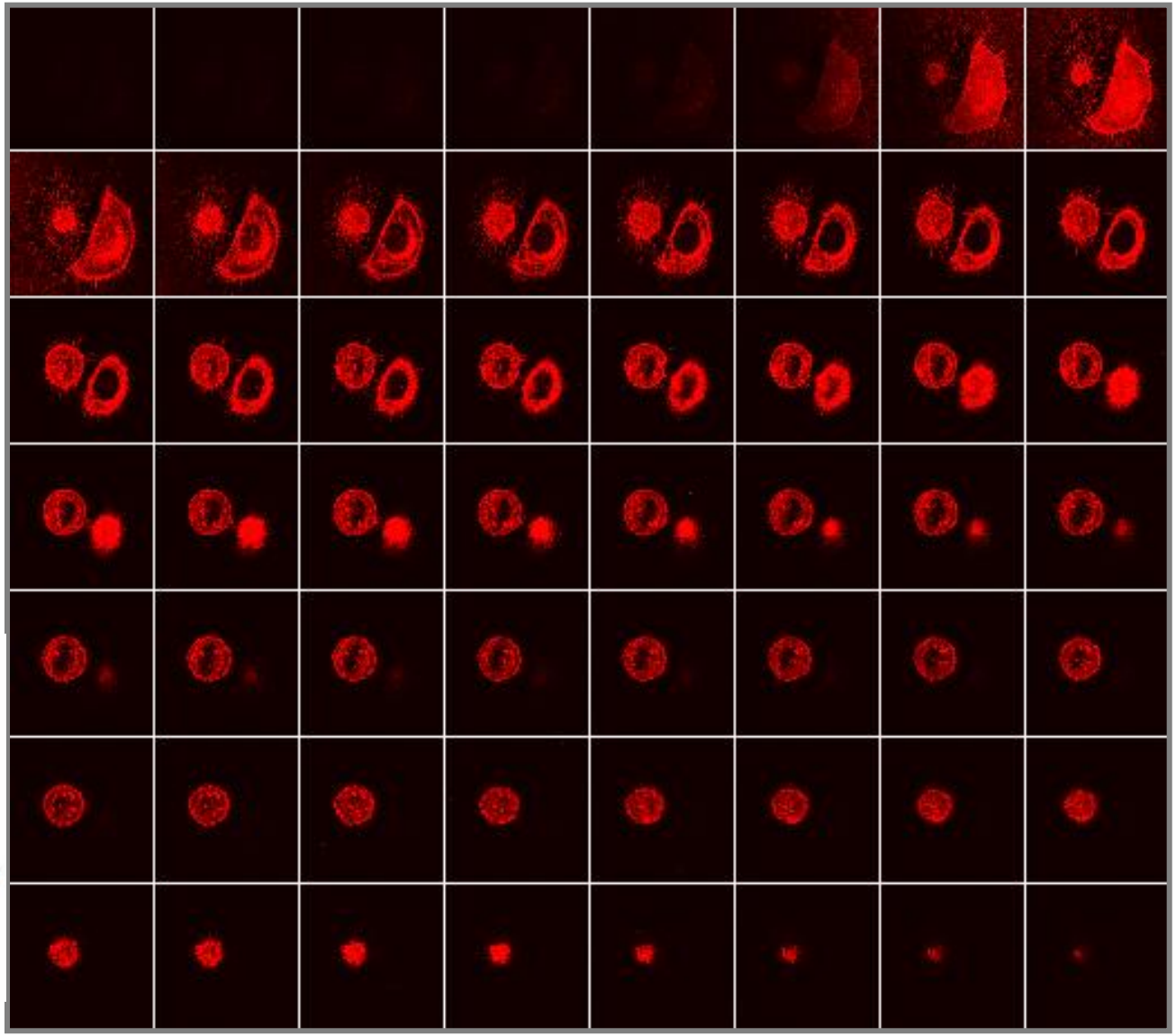

|-> Microscopy

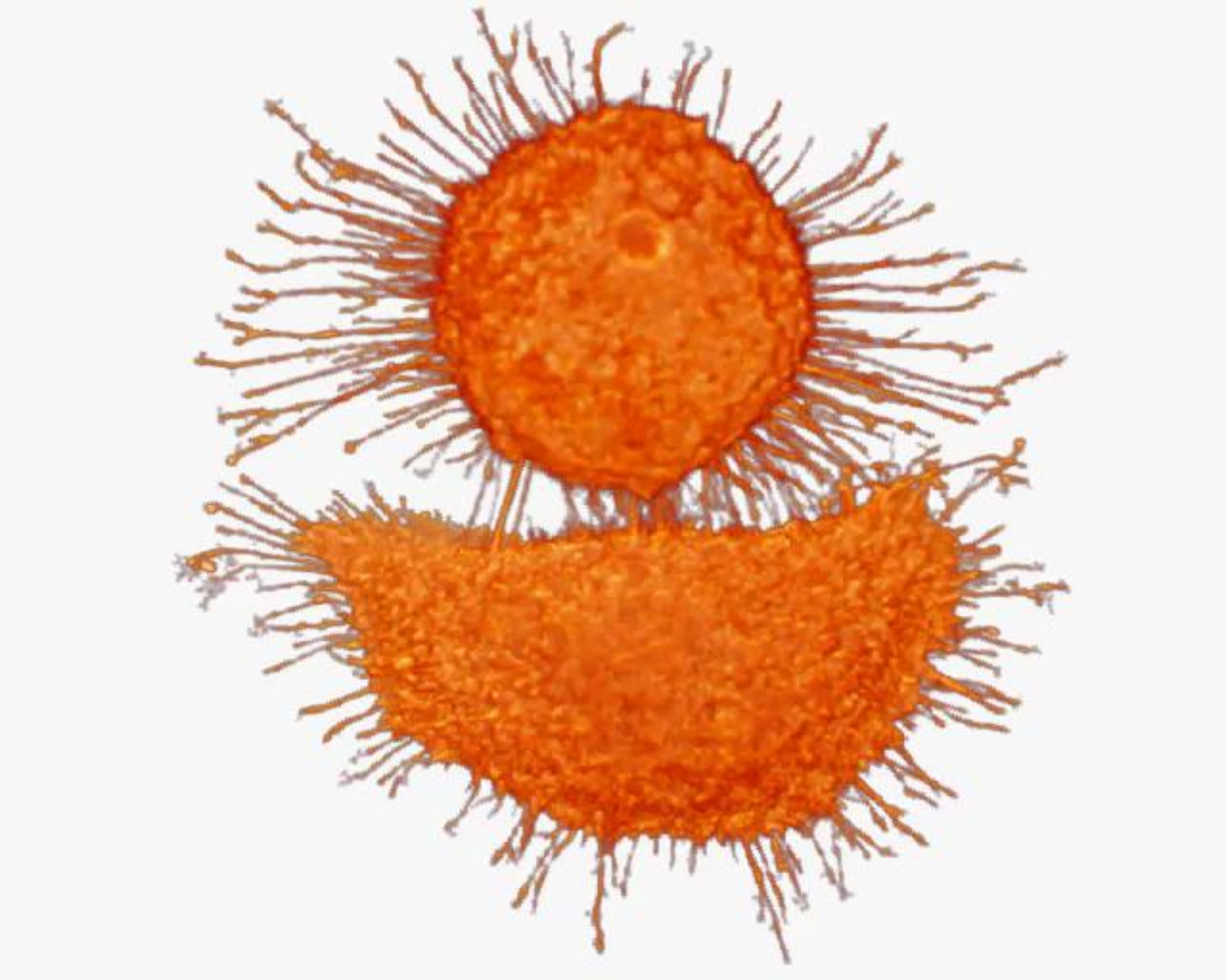

|-> Electron Microscopy

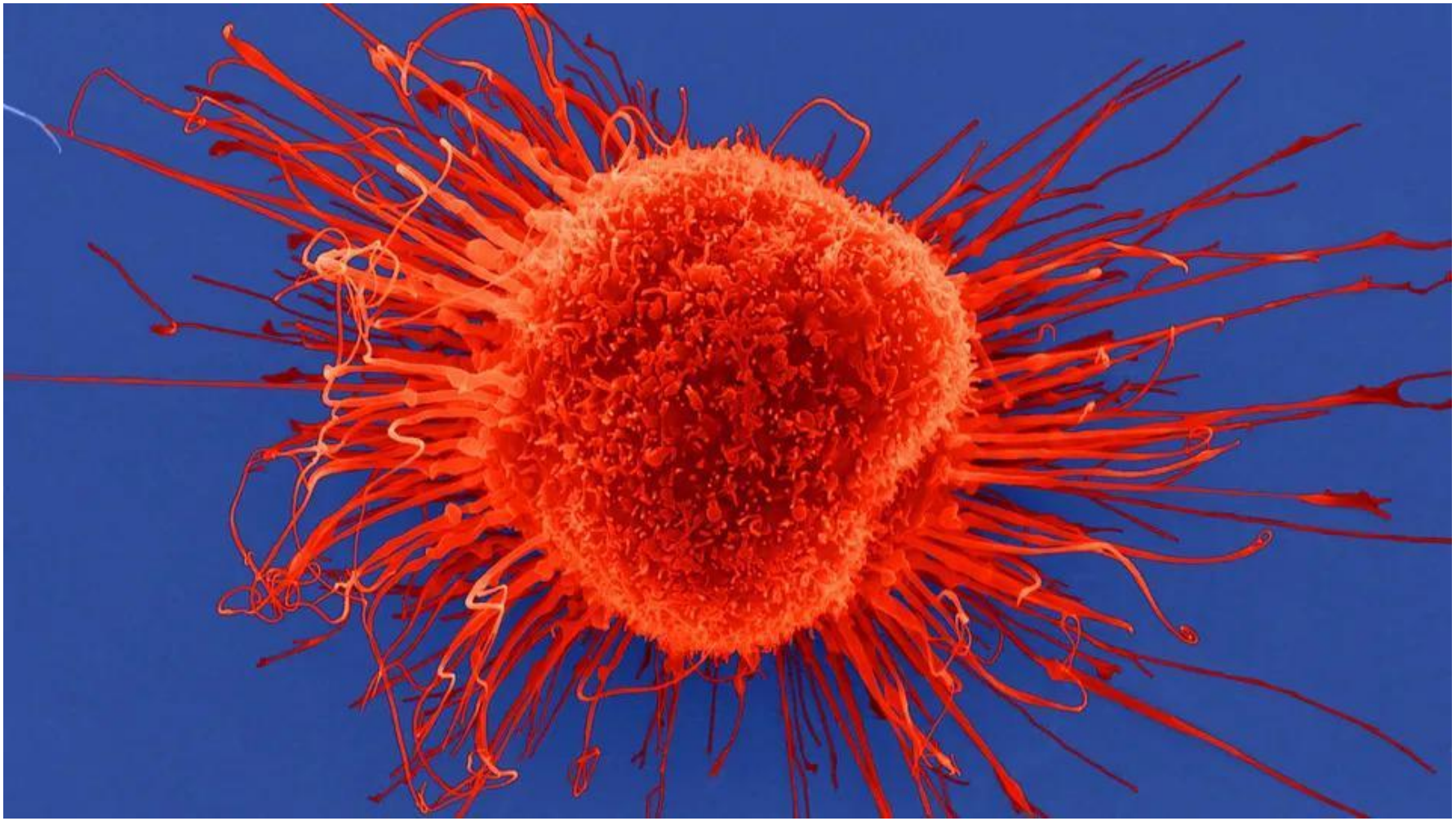

Laboratory for SCIAN Scientific Image Analysis

Light Sheet vs Spinning Disk

Biomedical Neuroscience Institute

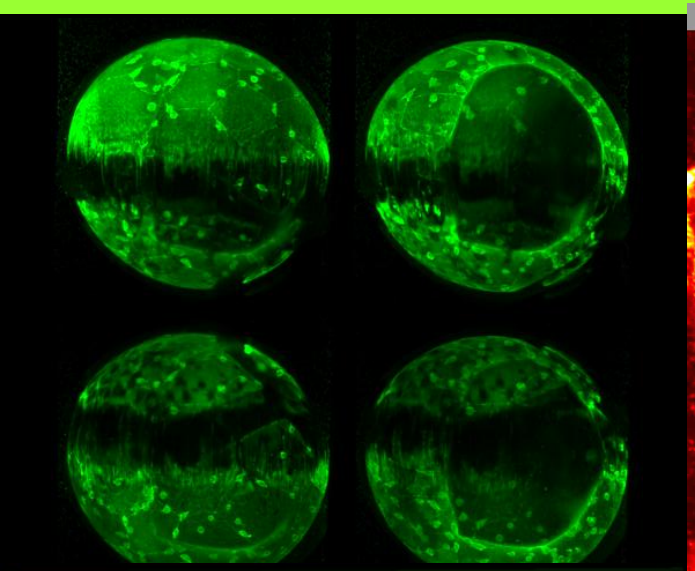

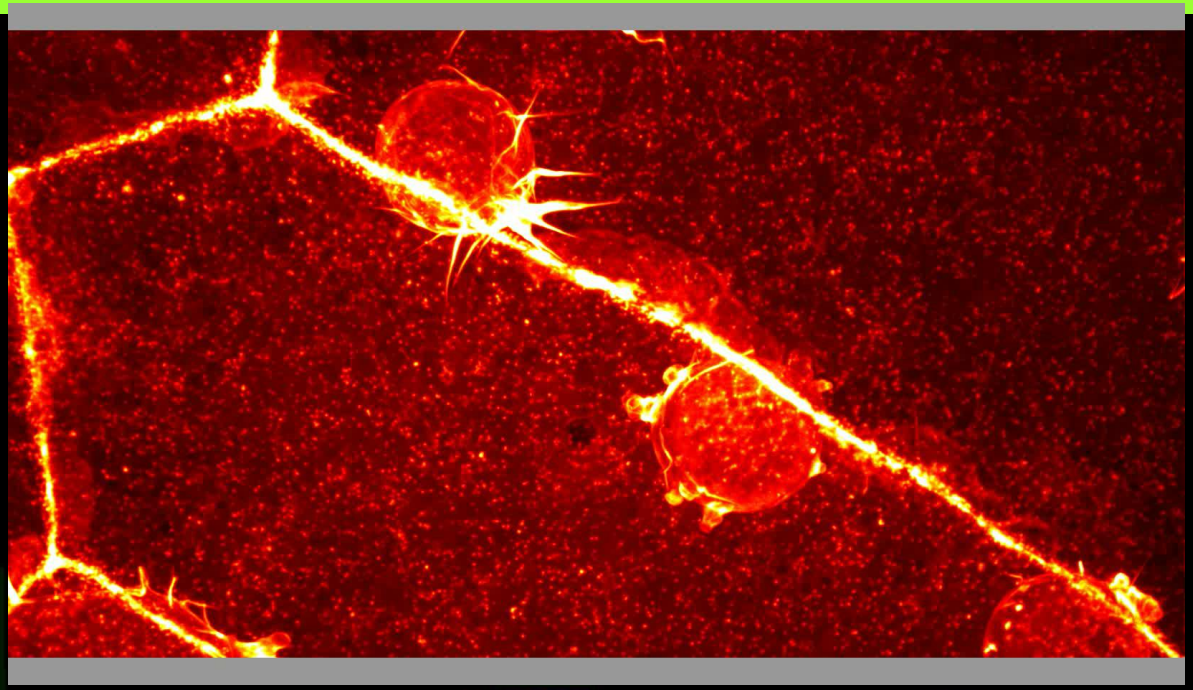

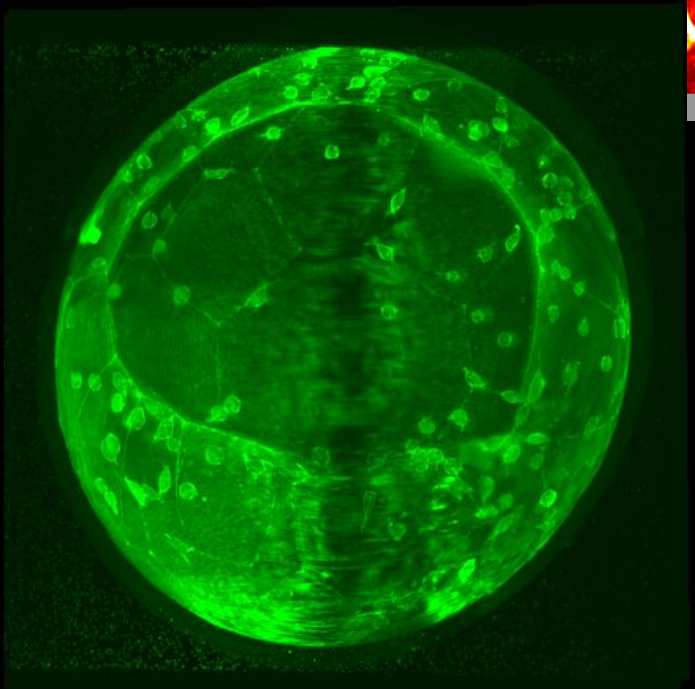

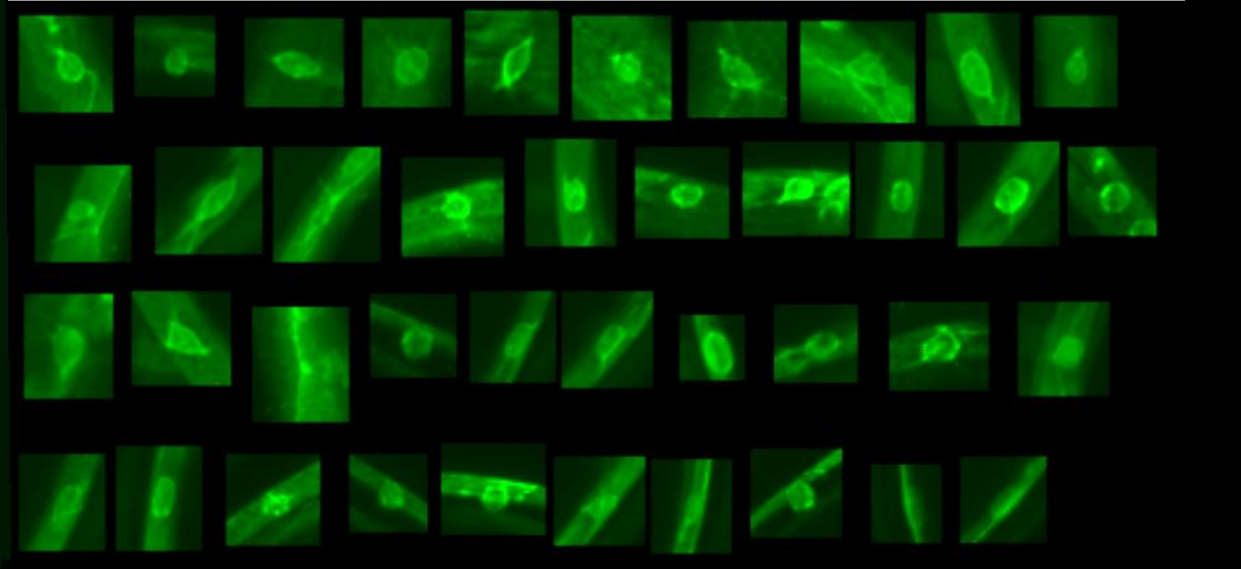

Light Sheet vs Spinning Disk

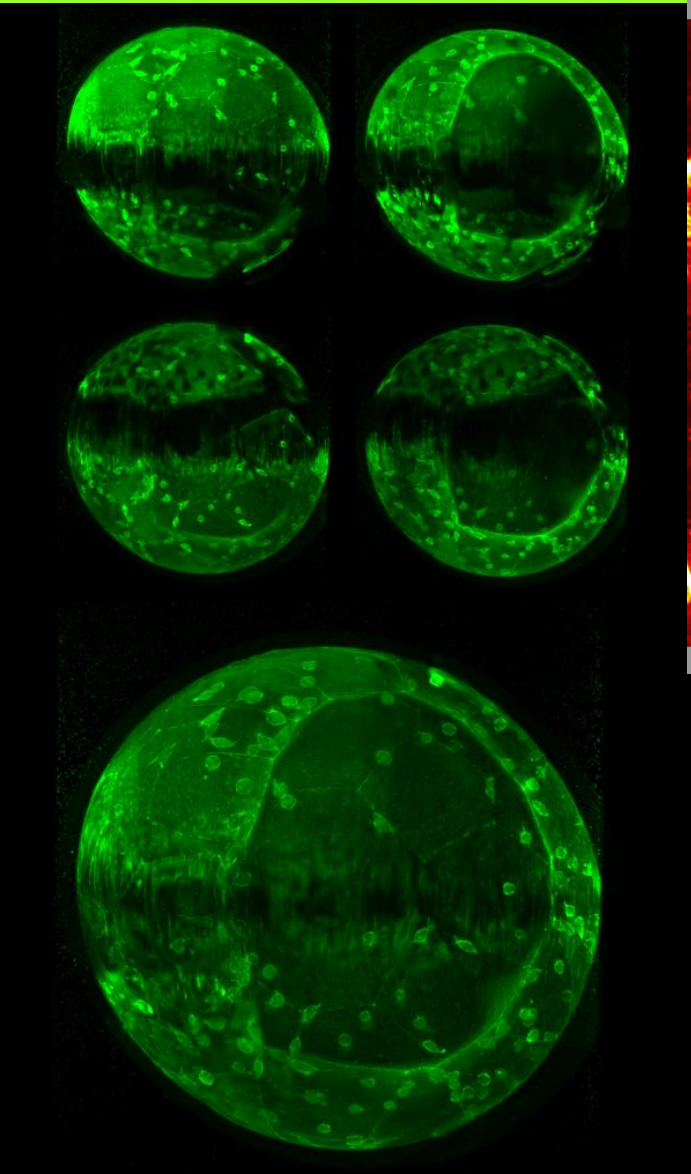

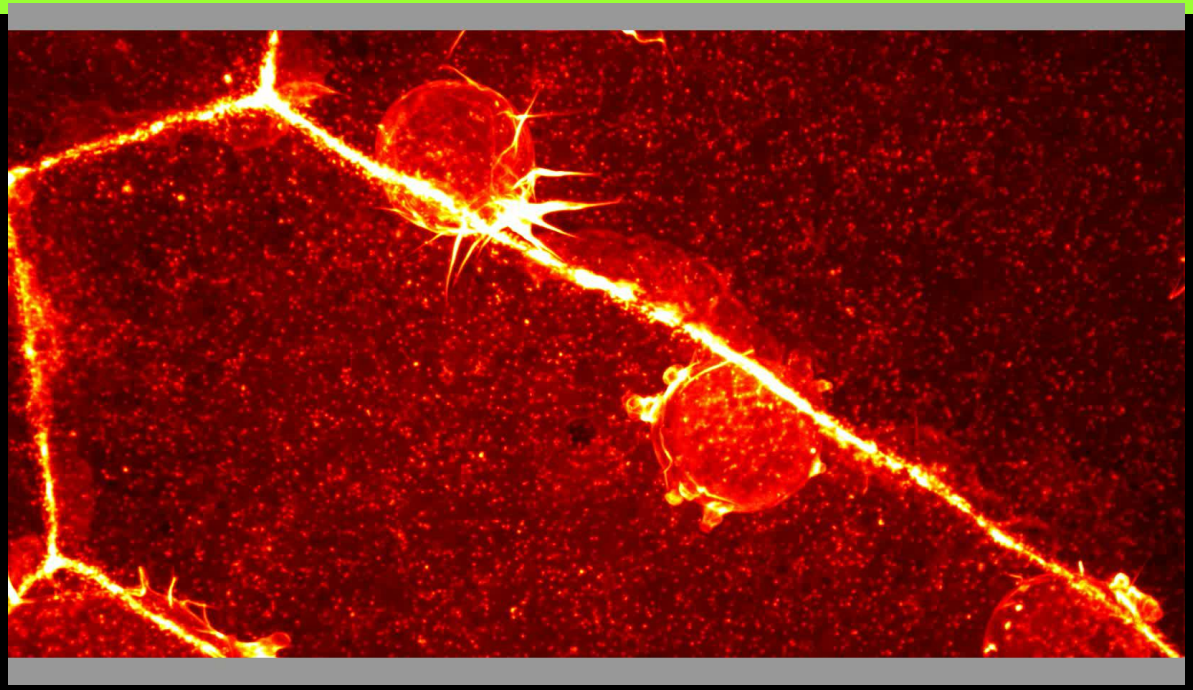

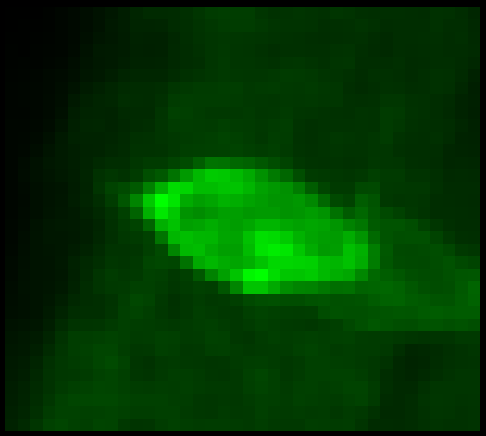

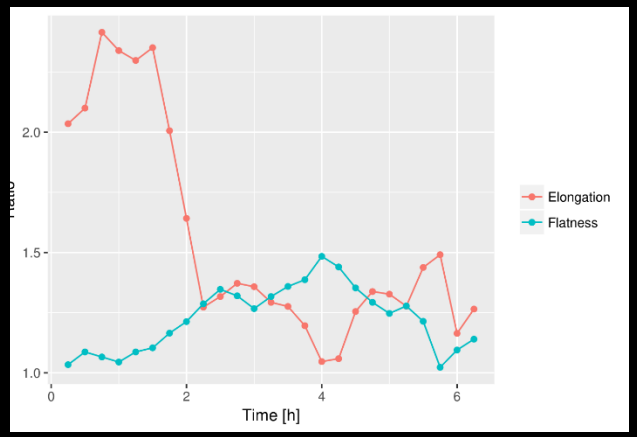

Microscopía Optica

Light–photon–matter interaction:
Intensity I, Color λ(RGB),
Absorption, Scattering, Fluorescence,
Diffraction-limited I(x,y,z,λ).
Resolution ~ 250 nm.

Image reflects optical sample properties

Confocal Microscopy

Laser–photon–matter interaction:
Intensity I, Wavelength λ, Absorption, Scattering, Fluorescence, Optical sectioning via pinhole, Diffraction-limited I(xyzλ).
Point illumination + spatial pinhole rejects out-of-focus light.
Resolution: xy ~ 200 nm, z ~ 600 nm.

Image reflects fluorescence distribution with enhanced axial resolution and contrast; true optical sections enabling 3D reconstruction.

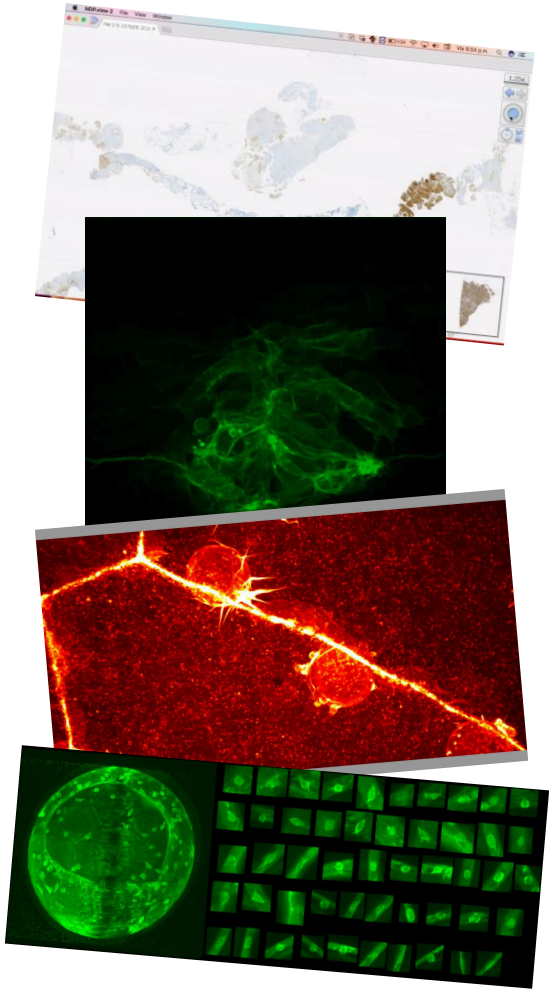

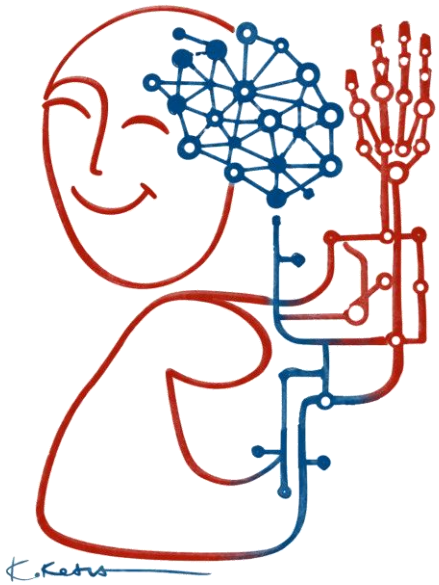

Quantitative Computational Methods

They interpret images as **high-dimensional numerical data**

... extracting explicit, reproducible, and measurable statistical and geometric patterns, without intrinsic semantic understanding.

Spinning Disk Confocal Microscopy

Parallelized pinhole illumination, Reduced photobleaching, Diffraction-limited I(x,y,z,λ).
Multiple pinholes on a rotating disk enable simultaneous confocal imaging.
Resolution: xy ~ 200 nm, z ~ 600 nm.

Image reflects fast 3D fluorescence dynamics with low phototoxicity; suitable for live-cell and time-resolved imaging.

Light Sheet Microscopy (LSM)

Intensity I, Wavelength λ, Fluorescence, Selective plane illumination, Orthogonal excitation/detection, Diffraction-limited I(x,y,z,λ).
Thin sheet of light illuminates only the focal plane; detection is orthogonal to illumination.
Resolution xy ~ 200–300 nm, z ~ 300–600 nm.

Image reflects: High-contrast volumetric fluorescence with minimal photodamage; ideal for large specimens and long-term live imaging.

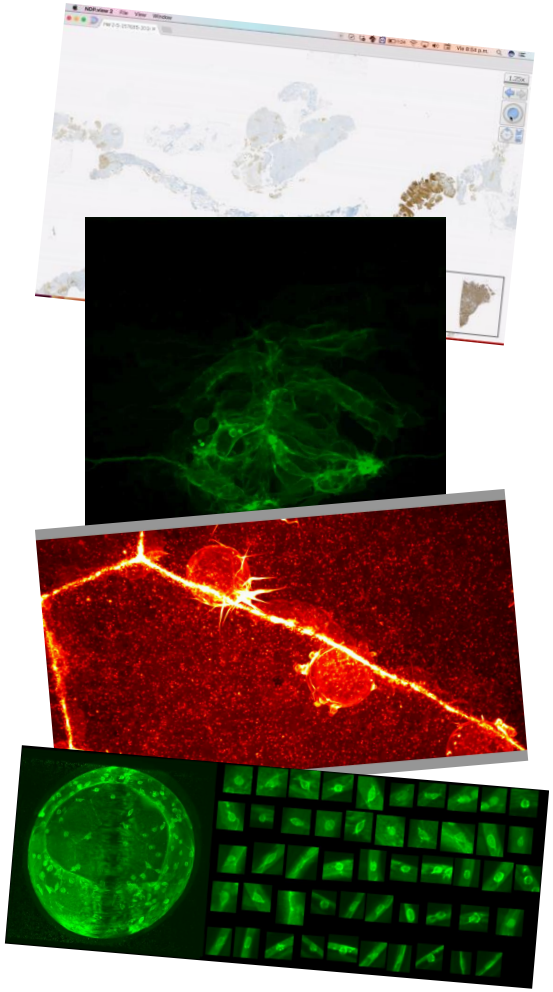

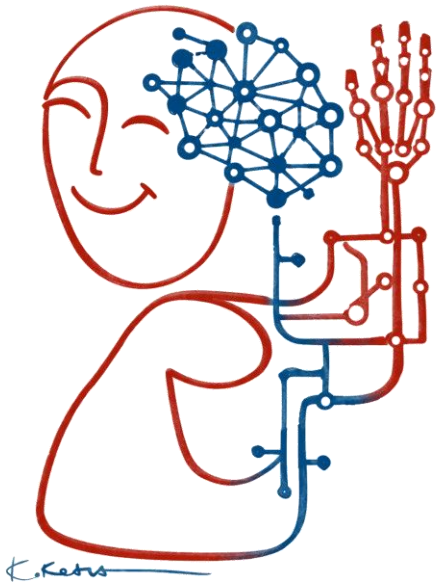

Quantitative Computational Methods

They interpret images as **high-dimensional numerical data**

... extracting explicit, reproducible, and measurable statistical and geometric patterns, without intrinsic semantic understanding.

Modality	Illumination	Optical sectioning	Speed	Phototoxicity
Confocal	Point scanning	Flexible Pinhole	Medium	Medium – High
Spinning Disk	Multi-point	Pinhole array	High	Medium – Low
Light Sheet	Planar sheet	Selective sheet illumination	Very high	Very low

Confocal *Rejects out-of-focus light*

Spinning Disk *Rejects out-of-focus faster*

Light Sheet *Avoids generating it*

Deconvolution

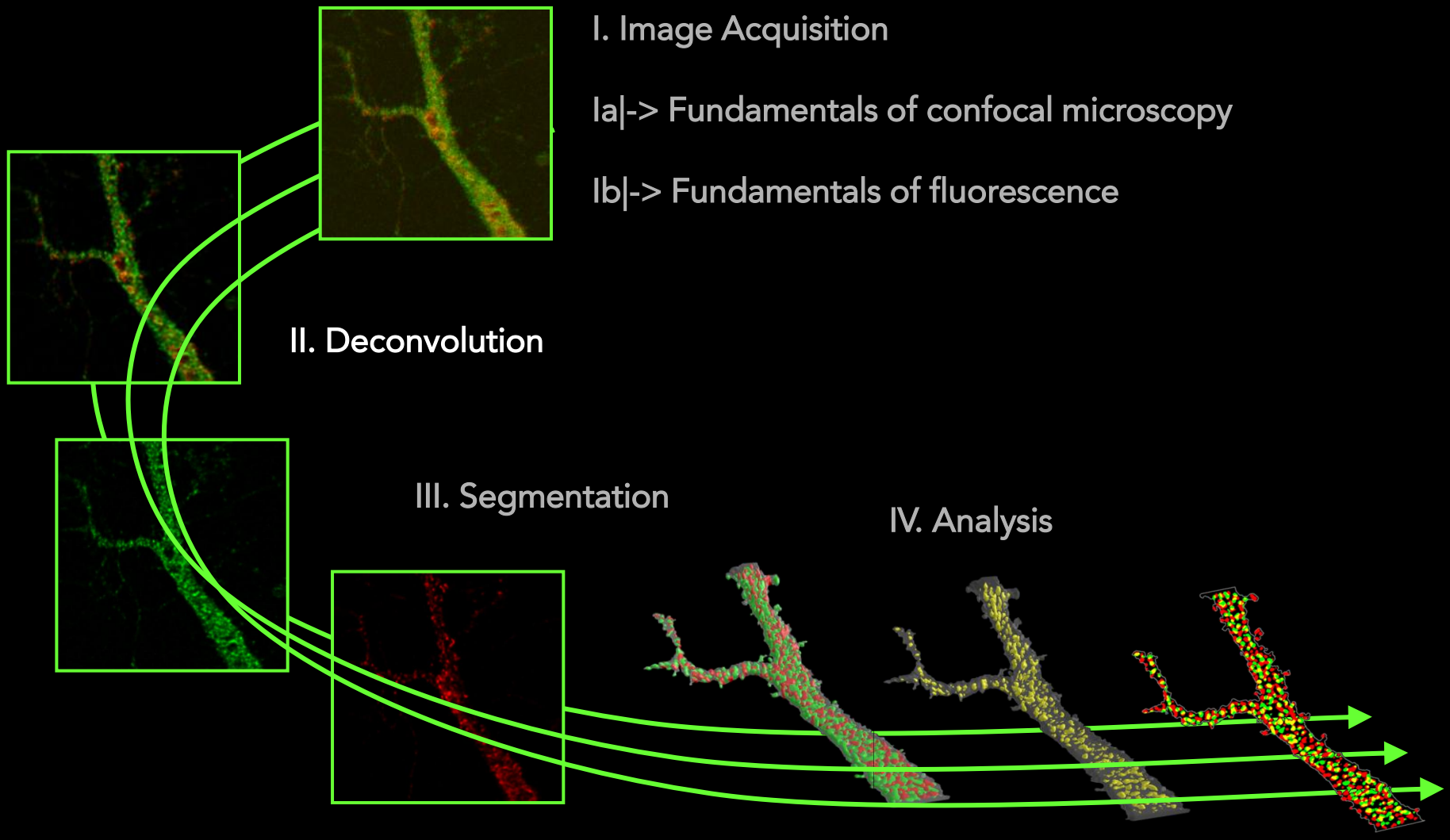

|-> Diffraction limited Microscopy

| Diffraction limited microscopy

E. Abbe († 1905)

$\lambda / 2 \cdot NA \sim \lambda / 2$ Resolution (Full Width at Halft Maximum, FWHM)

$FWHM / N^{1/2}$ Localization, N number of photons

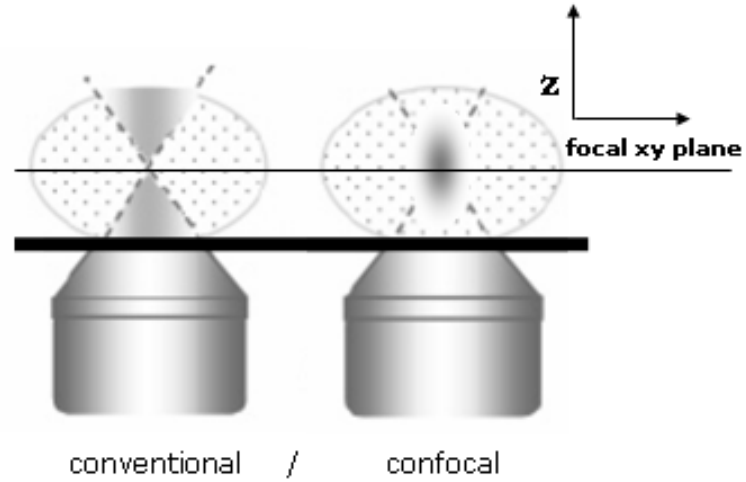

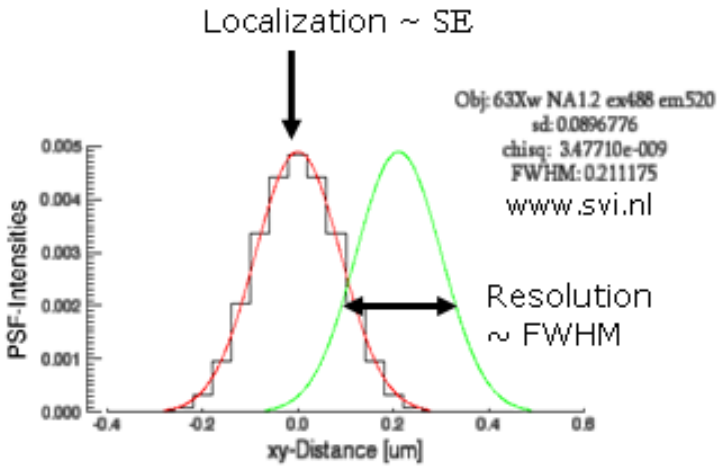

|-> PSF

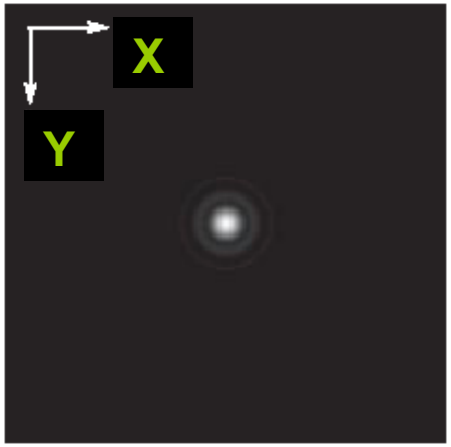
X
Y

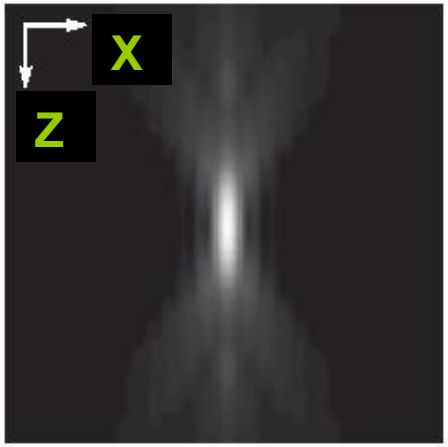
X
Z

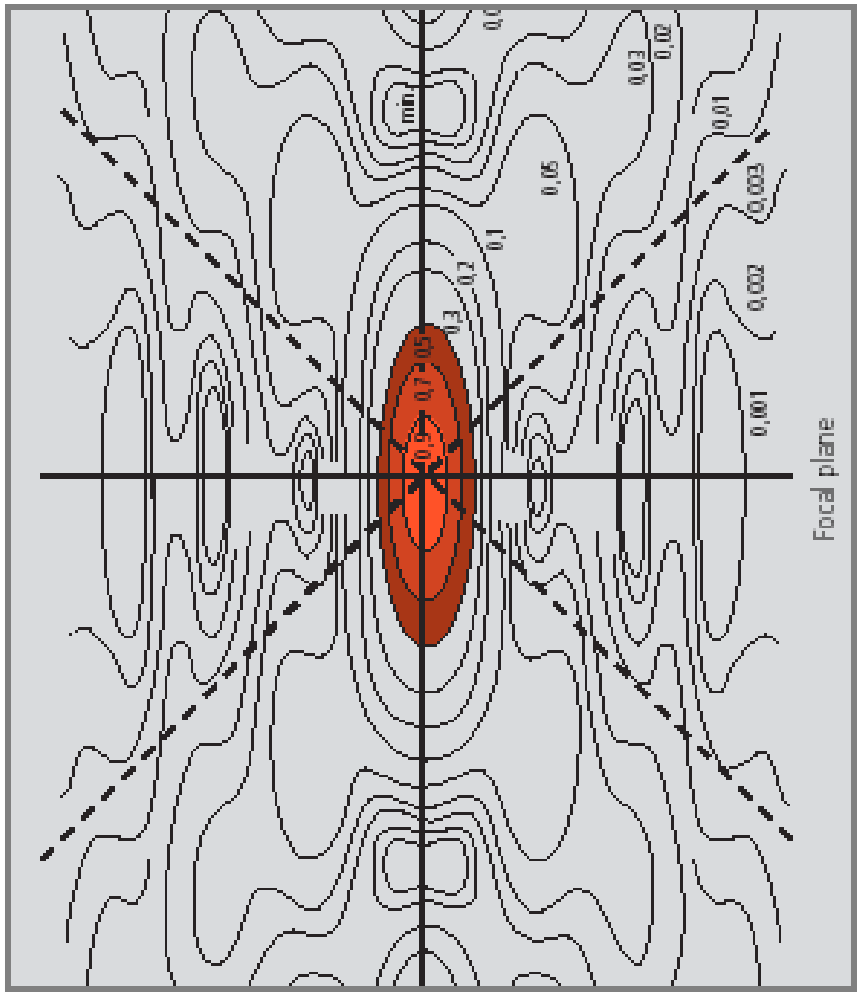
min
0,01
0,001
0,0001
0,00001
0,1
0,05
0,2
0,3
0,4
0,5
0,6
0,7
0,8
0,9
Focal plane

|-> Convolution

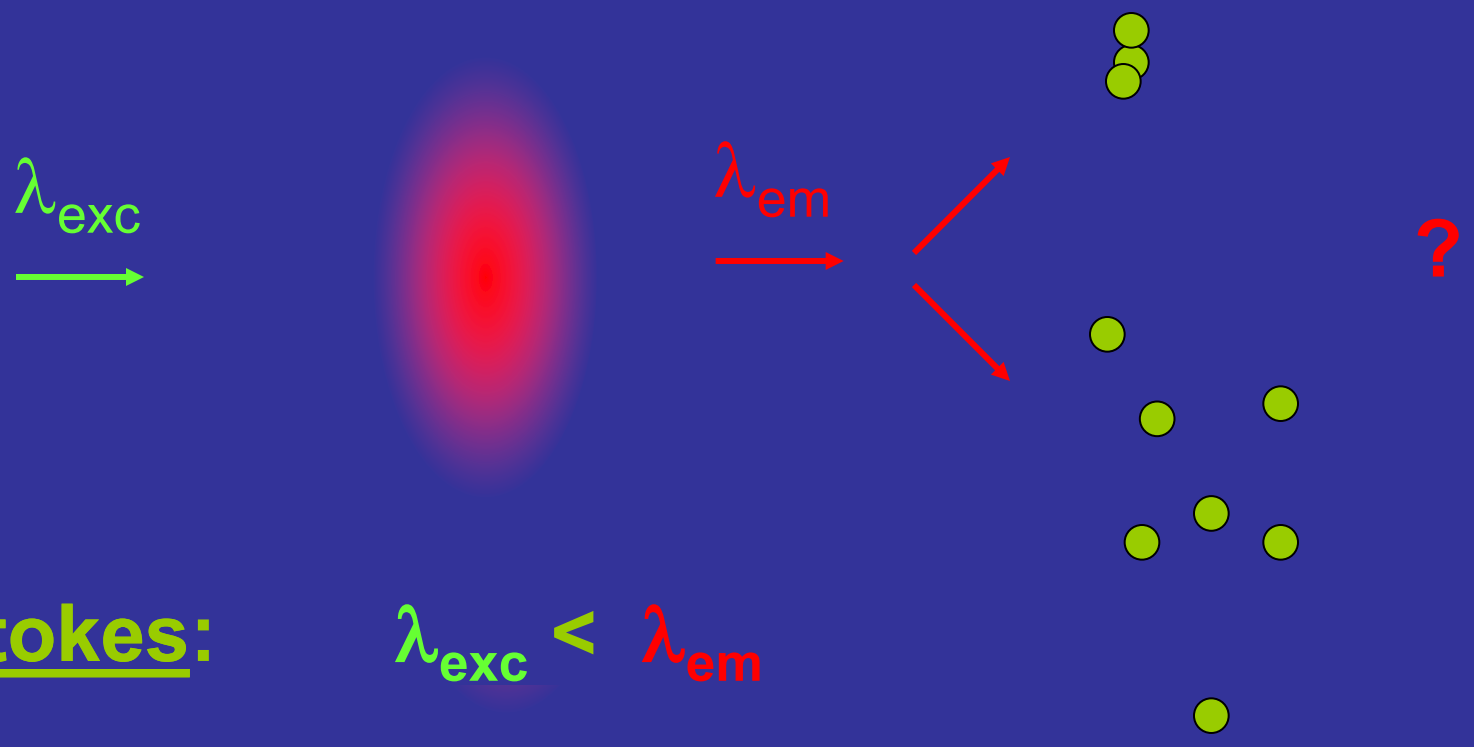

Stokes: $\lambda_{exc} < \lambda_{em}$

|-> Convolution

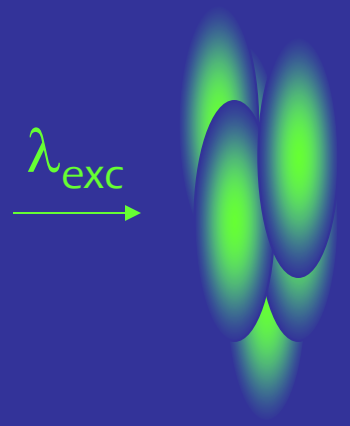

Stokes: $\lambda_{exc} < \lambda_{em}$

$n(\lambda_{exc}) > n(\lambda_{em})$

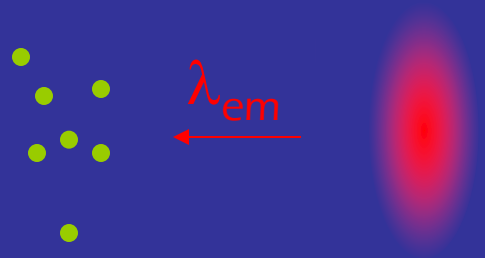

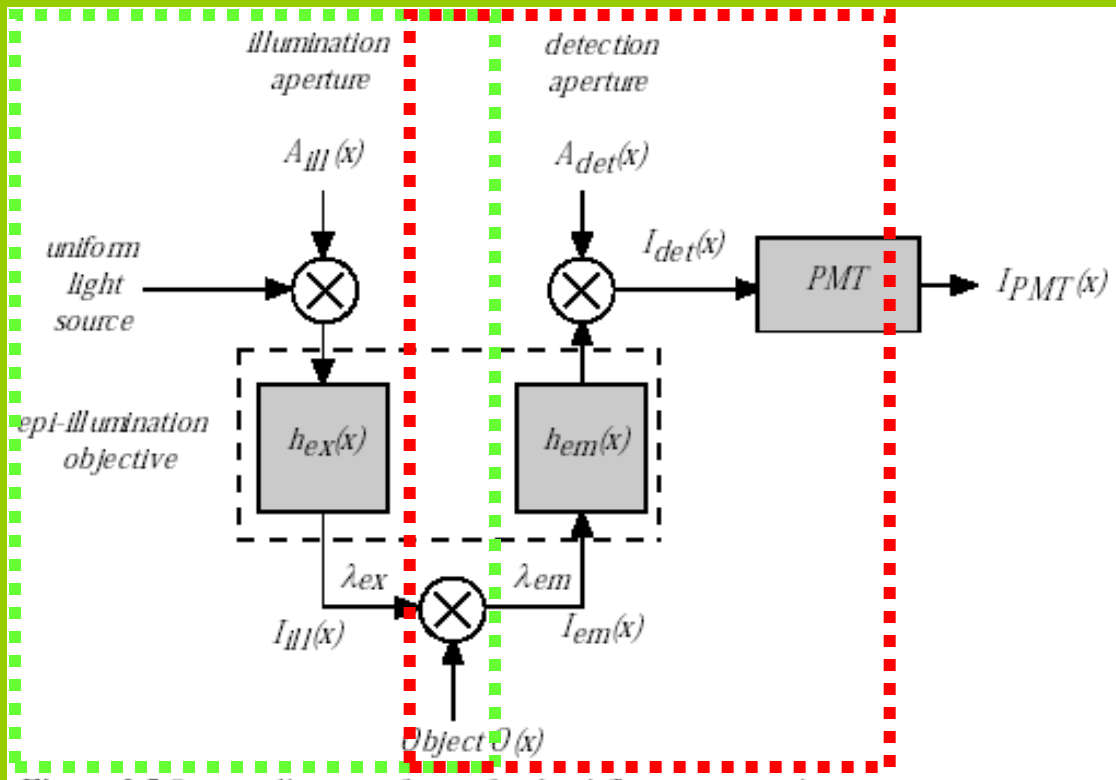

Figure 2.5 System diagram of a confocal epi-fluorescence microscope.

|-> Convolution

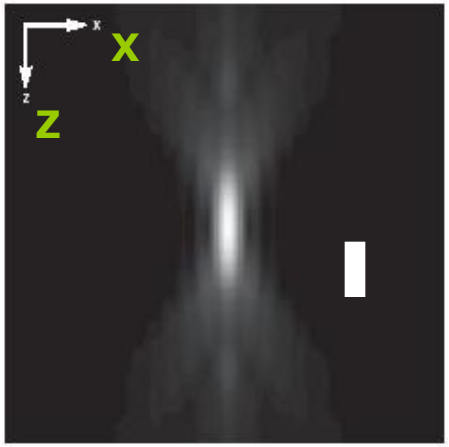

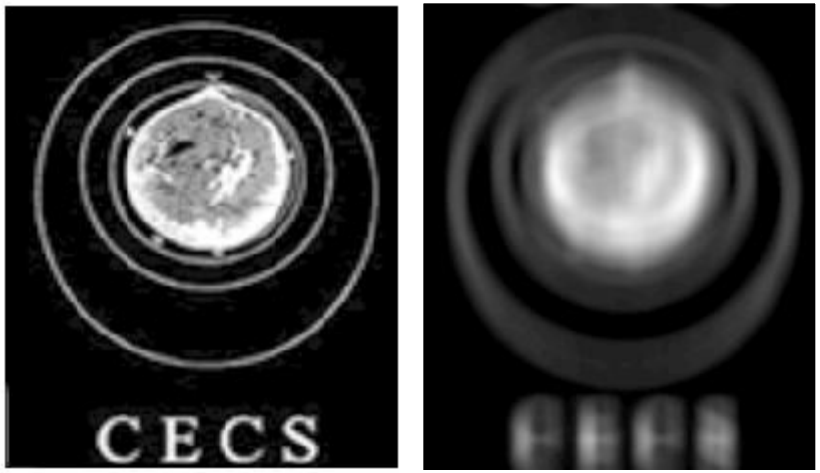

PSF:

Δxy ~ 500 nm | Δz ~ 1500 nm

|-> Deconvolution

PSF: Point Spread Function

f: Object Function

b: Offset Function

I: Image Matrix

N: Noise Function

$$N(PSF(x, y, z) \otimes f(x, y, z) + b(x, y, z)) = I(x, y, z)$$

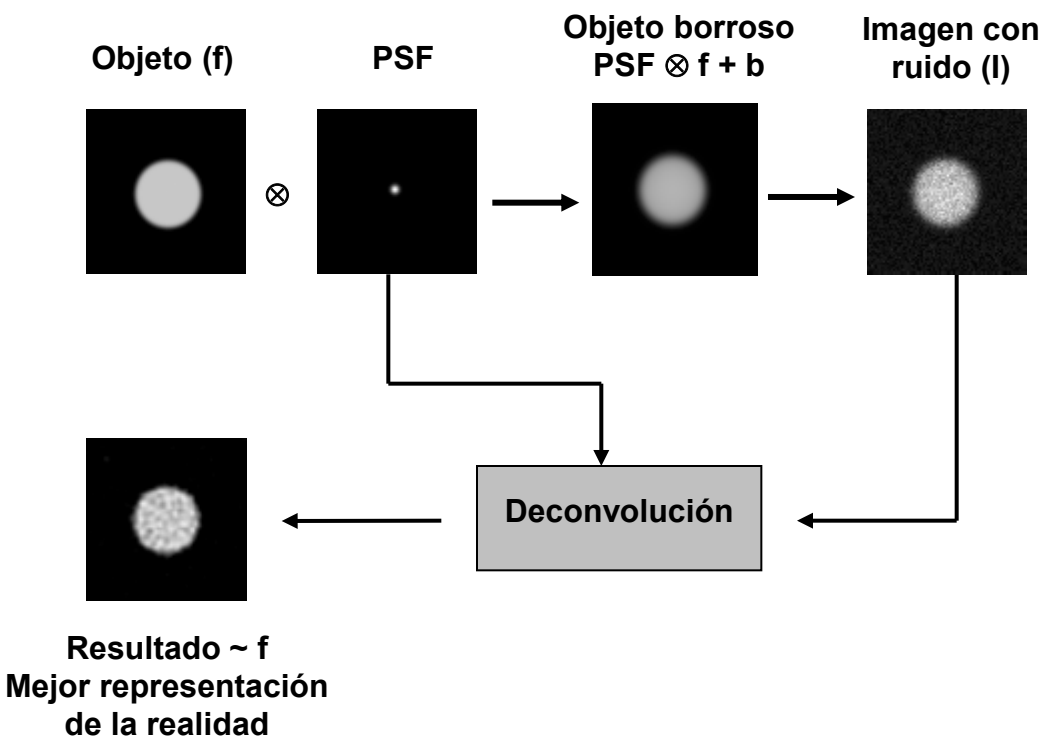

OTF: Object/Optical Transfer Function
Myoglobin in Action |Picosecond Laue Crystallography Diffraction Data
Schotte et al (2003) Science

Object → **OTF** → **O**bject**I**mage → **OTF**$^{-1}$ → **O**bject**M**odel

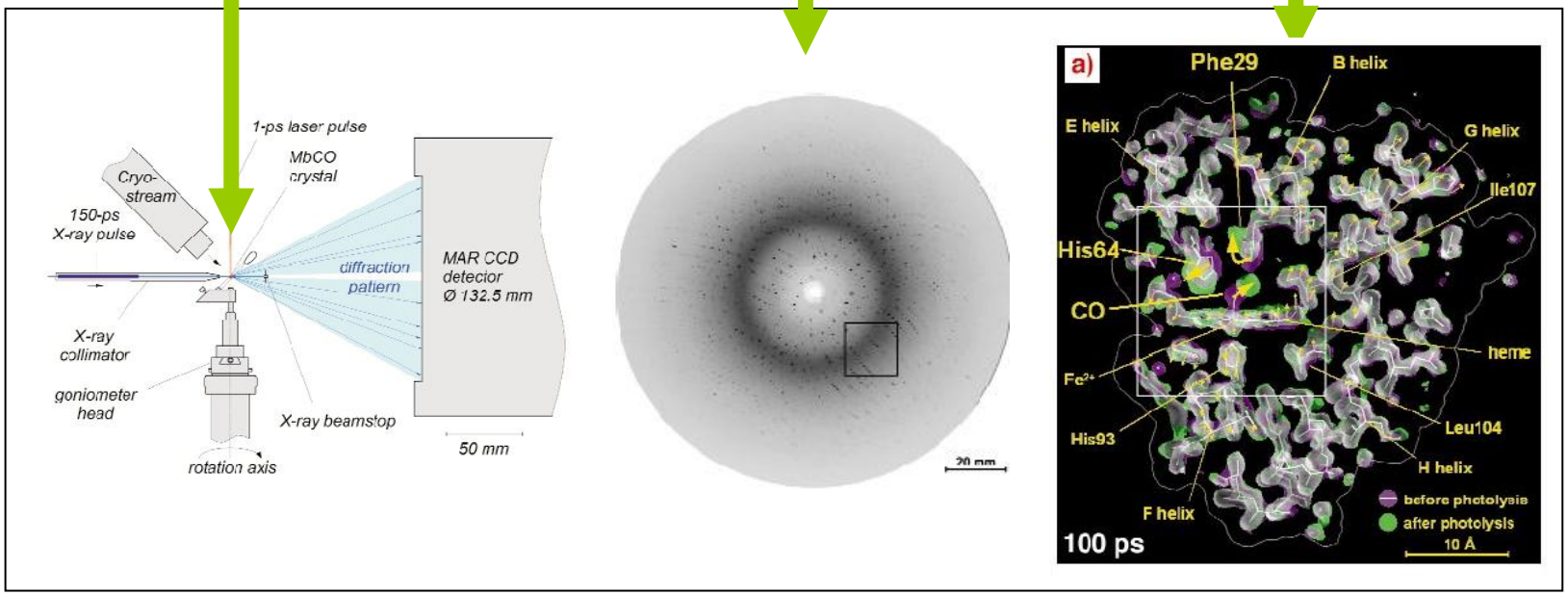

http://www.youtube.com/watch?v=lnKIBZYarzM

Diffraction Limited Resulution for a 10m telescope ~ λ/D ~ 0.01 arcsec is limited to ~ 0.5 arcsec by the turbulent atmosphere.
NAOS creates an artificial star at 90 km altitude in the Earth´s mesosphere.
The Laser Guide Star is used to correct atmospheric effects

Object → **OTF** → **O**bject**I**mage → **OTF**$^{-1}$ → **O**bject**M**odel

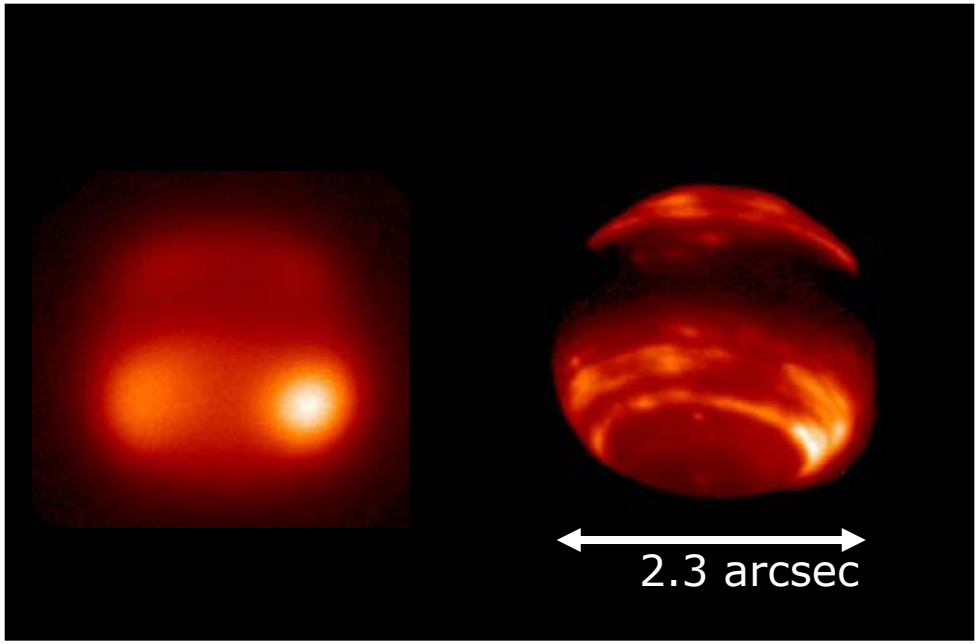

Confocal Microscopy | From Geometric Optics to Diffraction Theory

Diffraction: The deviation of an electromagnetic wavefront from the path predicted by geometric optics when the wavefront interacts with a physical object such as an opening or an edge.

Object → **OTF** → **O**bject**I**mage → **OTF**$^{-1}$ → **O**bject**M**odel

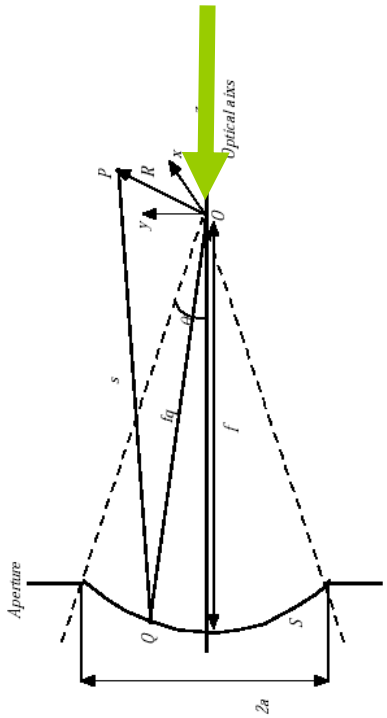

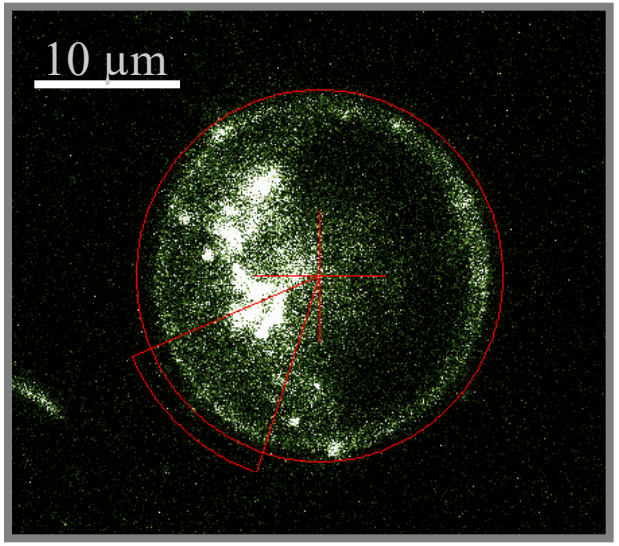

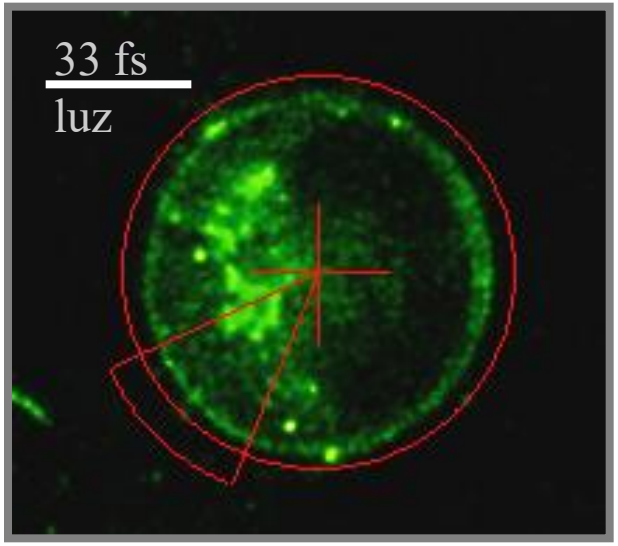

|-> Deconvolution

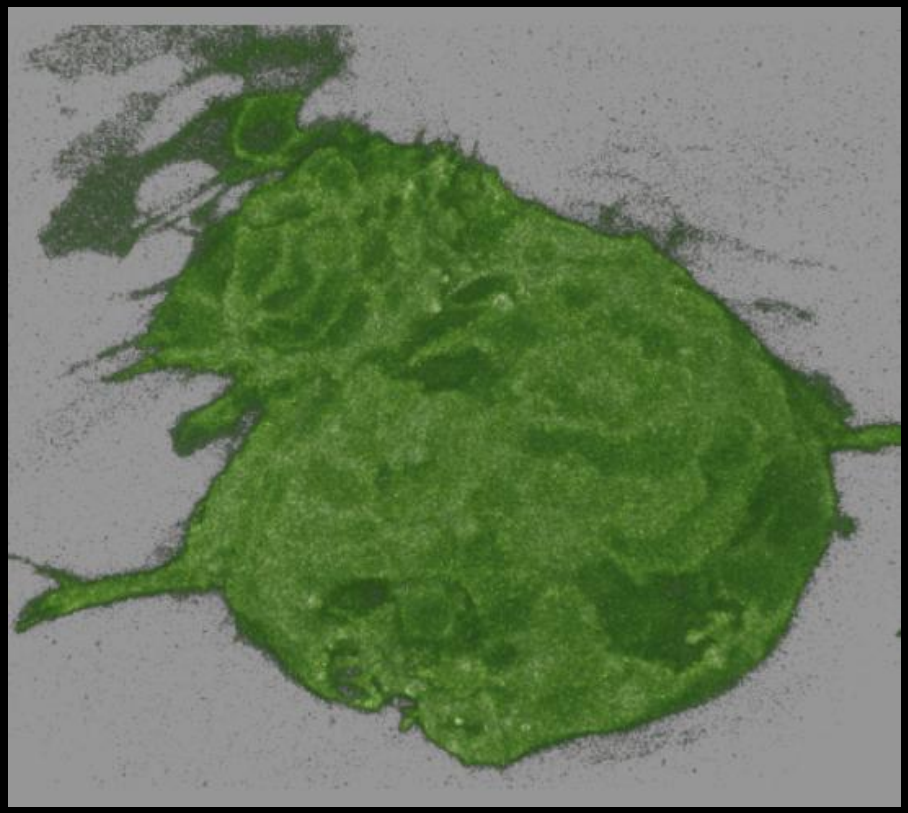

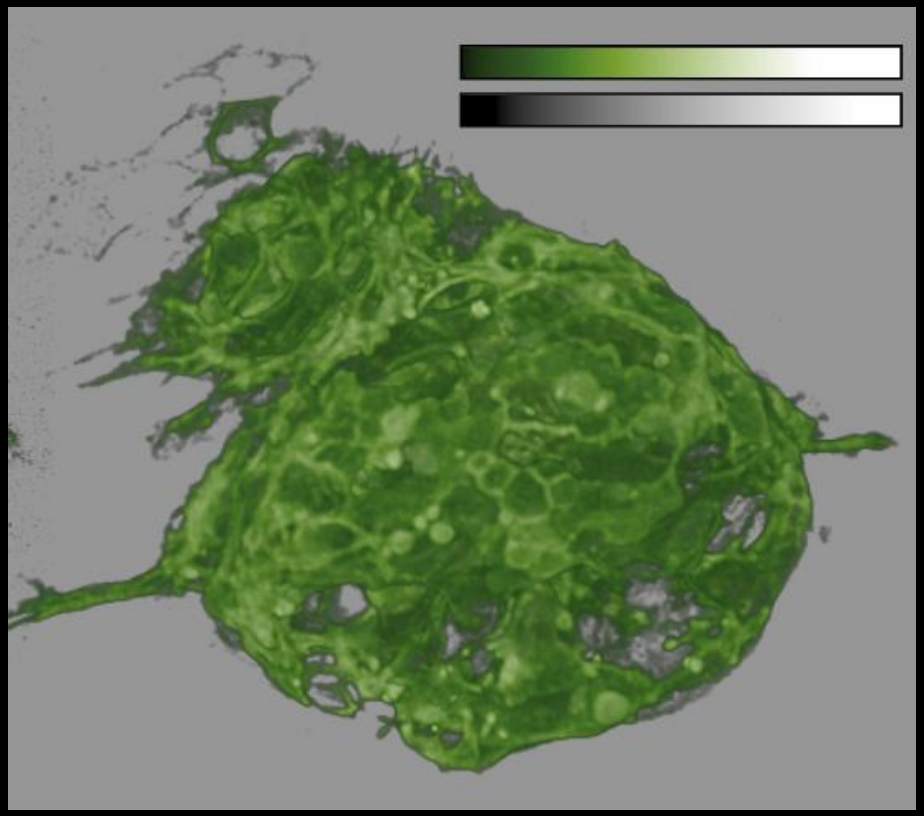

|-> Deconvolution

PSF: Point Spread Function

f: Object Function

b: Offset Function

I: Image Matrix

N: Noise Function

$$N(PSF(x, y, z) \otimes f(x, y, z) + b(x, y, z)) = I(x, y, z)$$

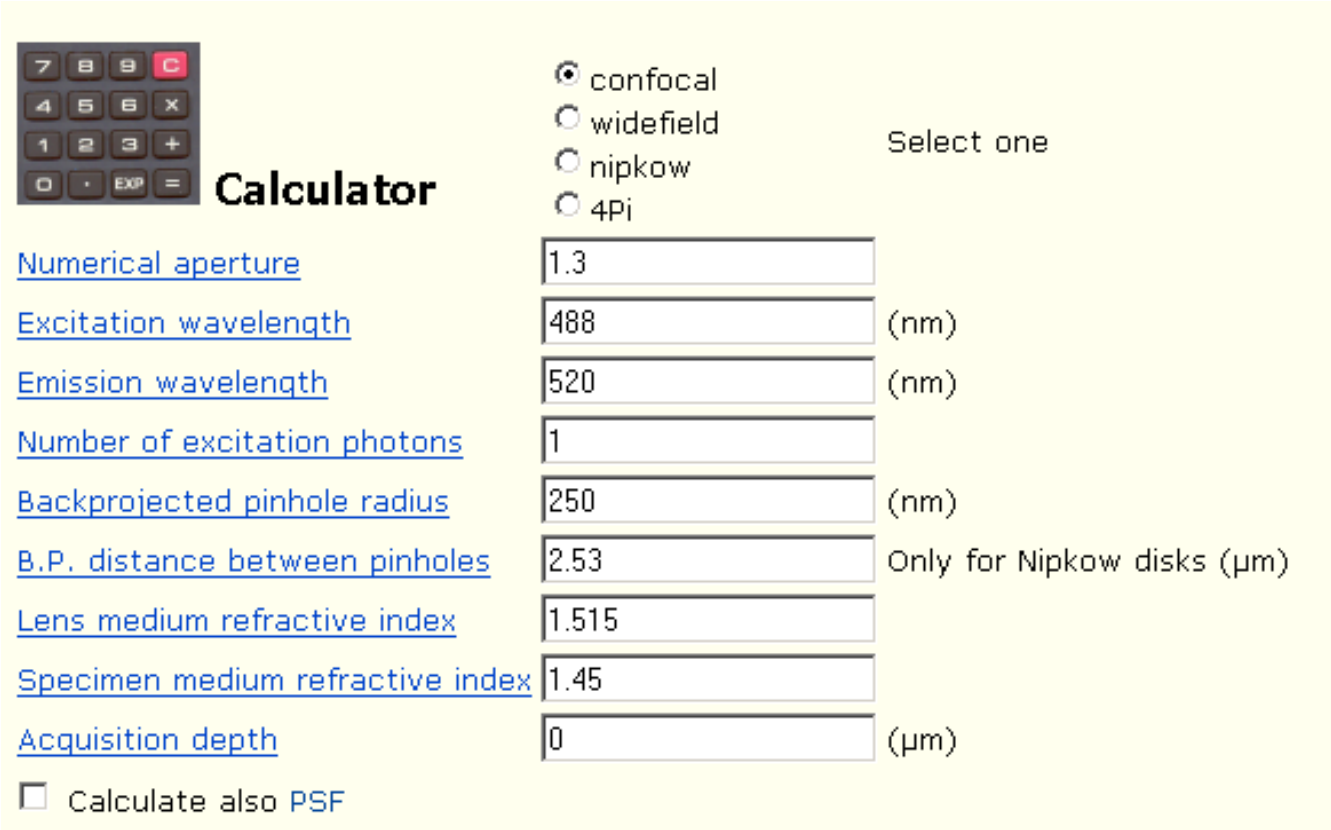

https://svi.nl/Nyquist-Calculator

|-> Pinhole

PSF: Point Spread Function

f: Object Function

b: Offset Function

I: Image Matrix

N: Noise Function

$$N(PSF(x, y, z) \otimes f(x, y, z) + b(x, y, z)) = I(x, y, z)$$

Backprojected confocal pinhole

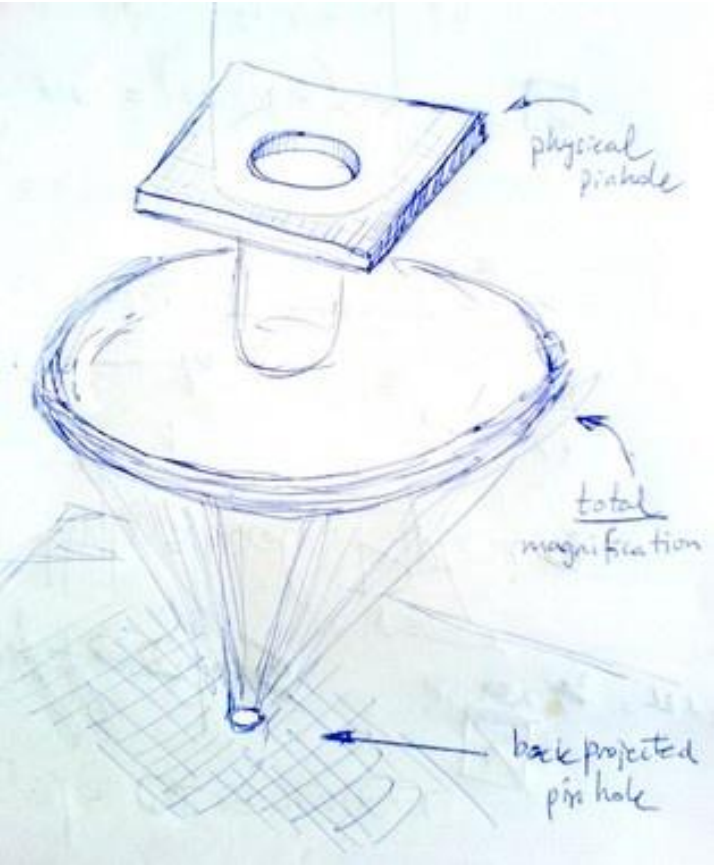

https://svi.nl/Nyquist-Calculator

|-> Pinhole

PSF: Point Spread Function

f: Object Function

b: Offset Function

I: Image Matrix

N: Noise Function

$$N(PSF(x, y, z) \otimes f(x, y, z) + b(x, y, z)) = I(x, y, z)$$

Biorad

- Biorad MRC 500, 600 and 1024
- Biorad Radiance

Leica

- Leica confocals TCS 4d, SP1 and NT
- Leica confocal SP2
- Leica confocal SP5

Nikon

- TE2000-E with the C1 scanning head

Olympus

- Olympus FV300
- Olympus FV500
- Olympus FV1000

Zeiss

- Zeiss LSM410 inverted
- Zeiss LSM510

https://svi.nl/Nyquist-Calculator

|-> Noise

Literature: eg. Noise Theory and Application to Physics: Philippe Réfrégier, Springer

|-> Noise

PSF: Point Spread Function

f: Object Function

b: Offset Function

I: Image Matrix

N: Noise Function

- *Black Body Irrdiation (Poisson)*
- *Detector Noise (Gauss)*

$$N(PSF(x, y, z) \otimes f(x, y, z) + b(x, y, z)) = I(x, y, z)$$

$$P(p, \mu) = \frac{\mu^p}{p!} \cdot e^{-\mu}$$

$$1.\ \bar{p} = \mu = \sigma^2,\ sd = \sigma = \sqrt{\bar{p}} = \sqrt{\mu}$$

$$2.\ counting:\ \bar{p} \pm \sqrt{\bar{p}}$$

$$3.\ Poisson(discrete) \rightarrow Gauss(continuous) : \mu \rightarrow \infty$$

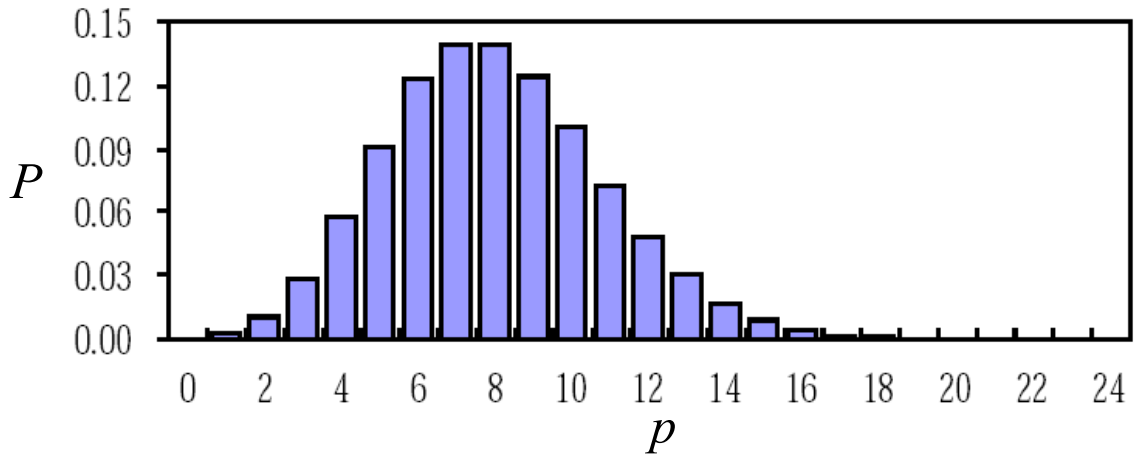

|-> Noise

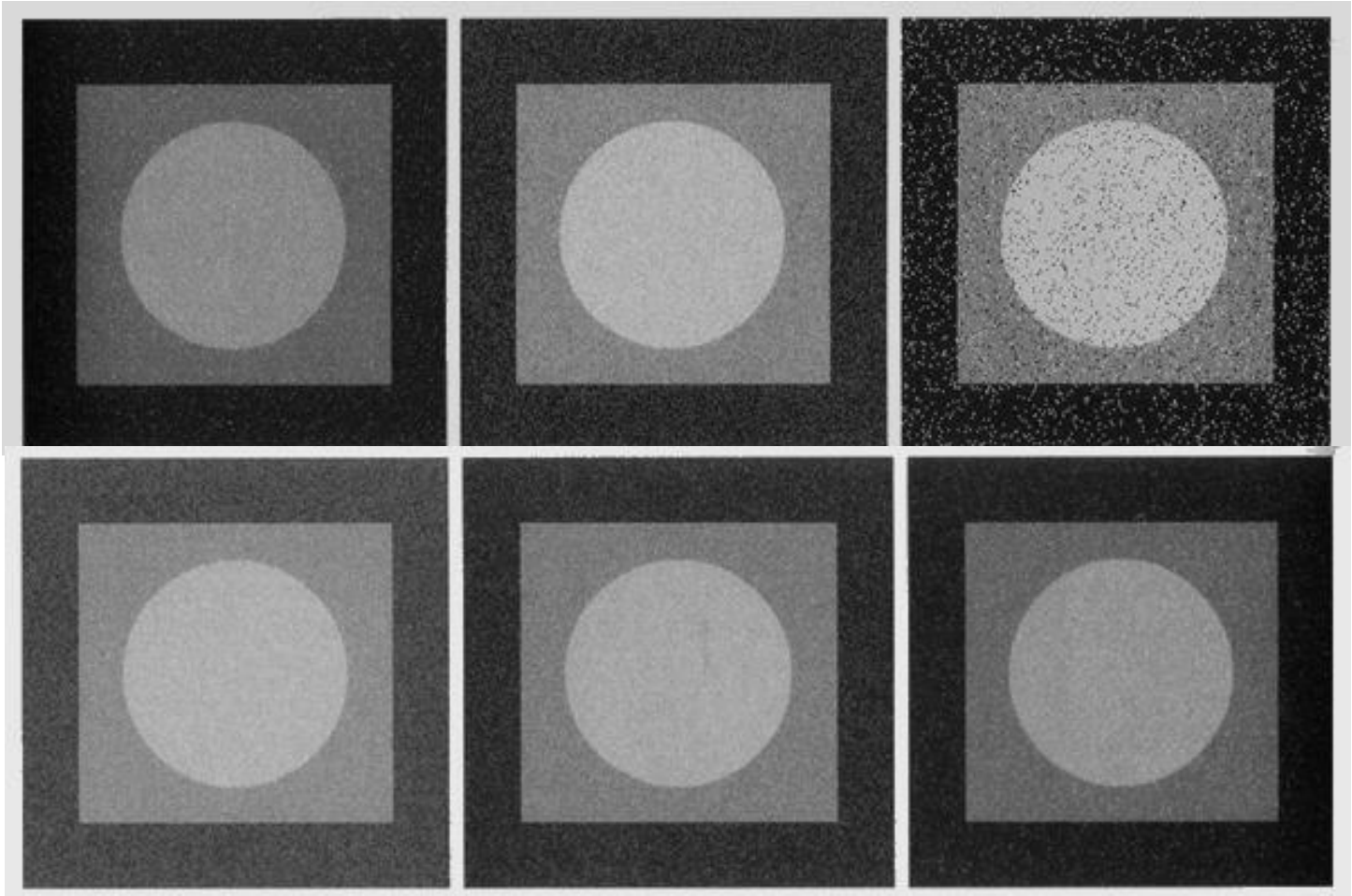

|-> Noise

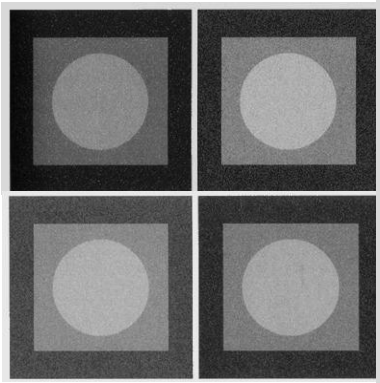

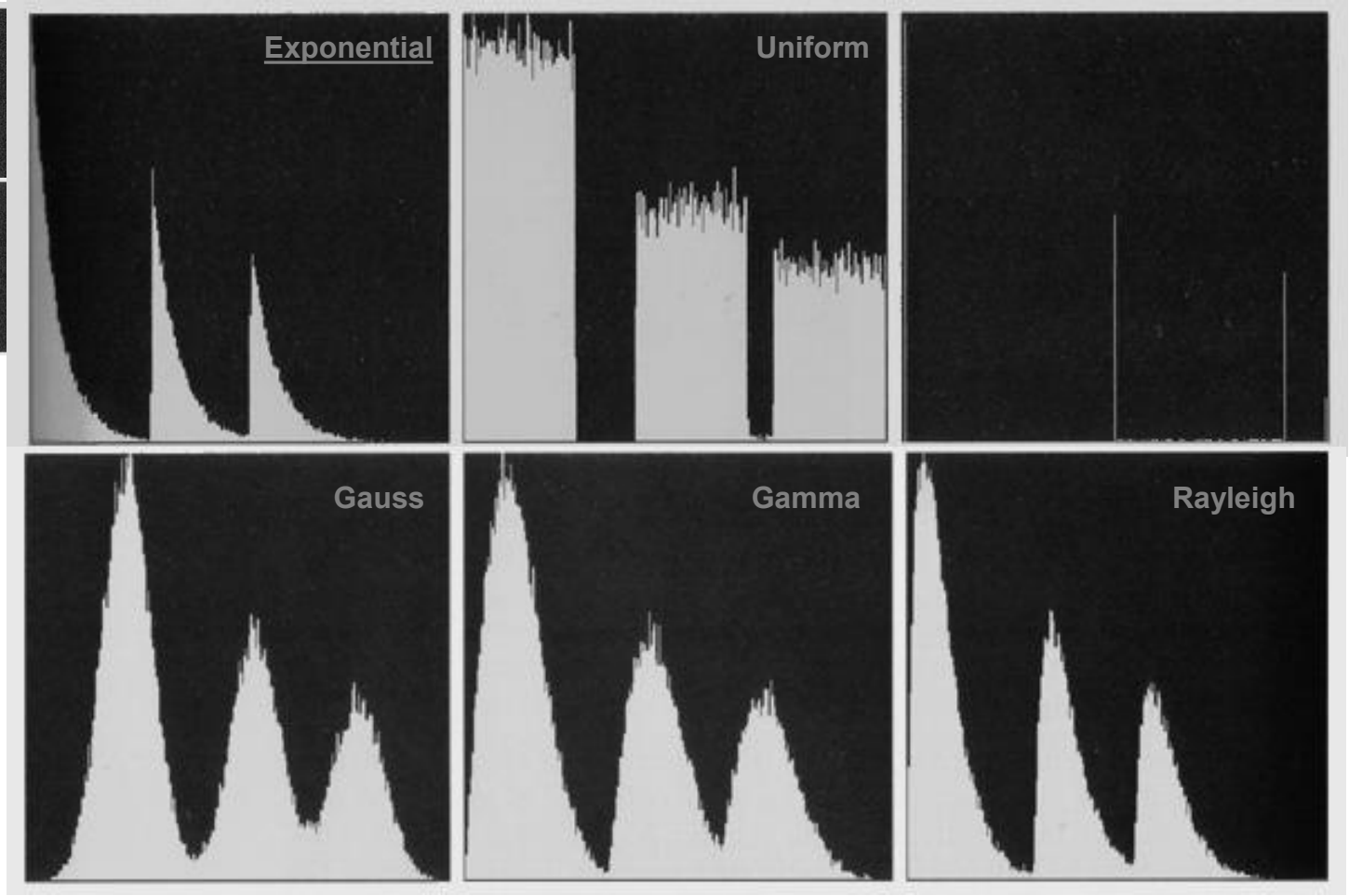

|-> Noise

The Signal to Noise ratio (SN) is a number not always easy to estimate. The easiest way to obtain some figures to look at the textures of bright areas in your object image. In the figure at left you see examples of such textures obtained from originally the same object image to which various levels of poisson noise were added.

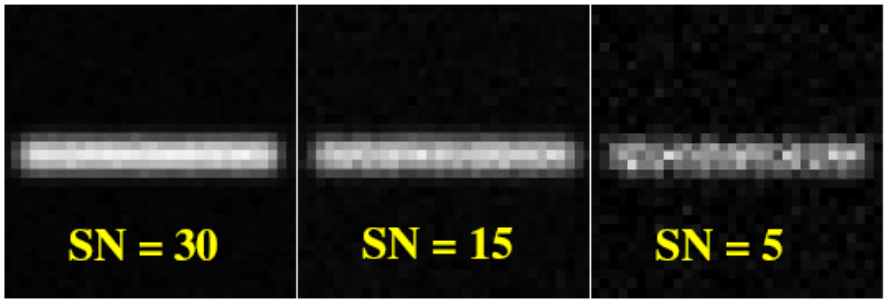

Figure 9. Images with different generated noise levels

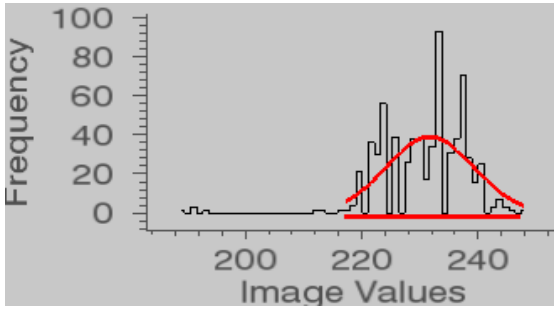

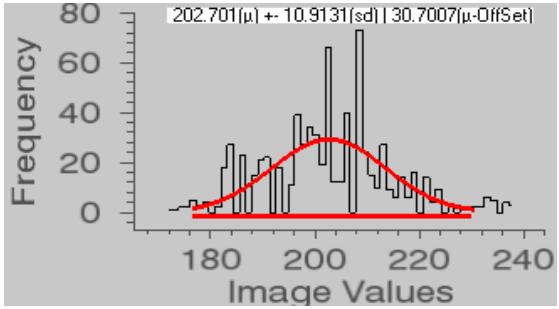

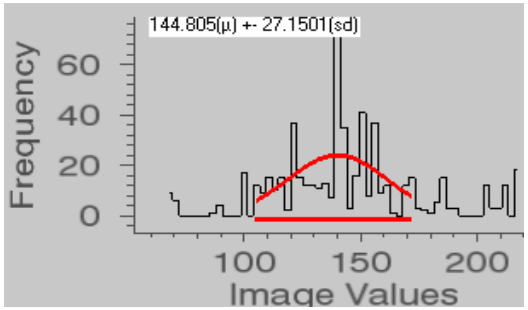

$$SNR = \frac{\bar{I}}{\sigma} = \frac{\bar{I}}{\sqrt{\sigma^2}} = \frac{229}{7.5}$$

$$SNR = \frac{\bar{I}}{\sigma} = \frac{\bar{I}}{\sqrt{\sigma^2}} = \frac{200}{10}$$

$$SNR = \frac{\bar{I}}{\sigma} = \frac{\bar{I}}{\sqrt{\sigma^2}} = \frac{139}{27}$$

|-> Nyquist /Shannon Theorem

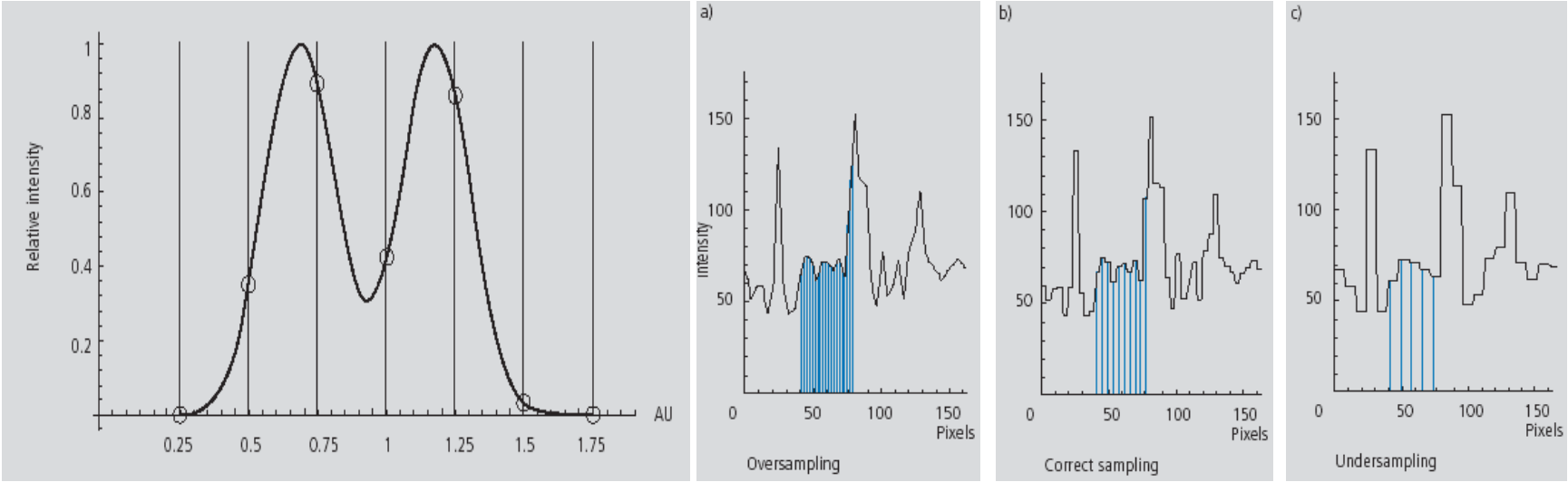

- Undersampling looses structures.
- Oversampling waists memory/computation time.

The 'Nyquist /Shannon Theorem' or 'Sampling Theorem' for the digital sampling of analogue signals suggests a Nyquist rate NR $\geq 2\nu$?

! Diffraction theory calculates lateral NR ~ 20 pixel/µm(~50 nm/pixel) !
... laxial NR ~ (~150 nm/pixel)

|-> PSF calculator

PSF: Point Spread Function

f: Object Function

b: Offset Function

I: Image Matrix

N: Noise Function

$$N(PSF(x, y, z) \otimes f(x, y, z) + b(x, y, z)) = I(x, y, z)$$

Calculator

- confocal
- widefield
- nipkow
- 4Pi

Select one

Numerical aperture	1.3	
Excitation wavelength	488	(nm)
Emission wavelength	520	(nm)
Number of excitation photons	1	
Backprojected pinhole radius	250	(nm)
B.P. distance between pinholes	2.53	Only for Nipkow disks (µm)
Lens medium refractive index	1.515	
Specimen medium refractive index	1.45	
Acquisition depth	0	(µm)

☐ Calculate also PSF

https://svi.nl/Nyquist-Calculator

|-> Snell's Law

Index of refraction: $n = (\varepsilon \cdot \mu)^{1/2} = c/v$,

ε electric permittivity and μ magnetic permeability.

<u>Snell's Law:</u>

$\sin\Theta_1 \, n_1 = \sin \Theta_2 \, n_2$

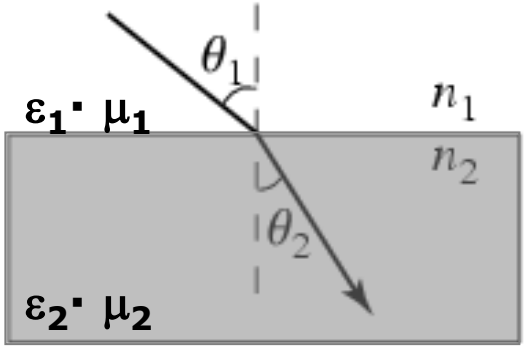

- **1.518 [Zeiss Oil]**
- **1.33 [Water]**
- **1.0008 [Air]**

|-> Refractive index

Refractive Index:

$RI = n_1/n_2 = v_2/v_1$

Snell's Law:

$\sin\Theta_1 \, n_1 = \sin \Theta_2 \, n_2$

$n = n(\lambda)$!

- **1.518 [Zeiss]**
- **1.33 [Water]**
- **1.0008 [Air]**

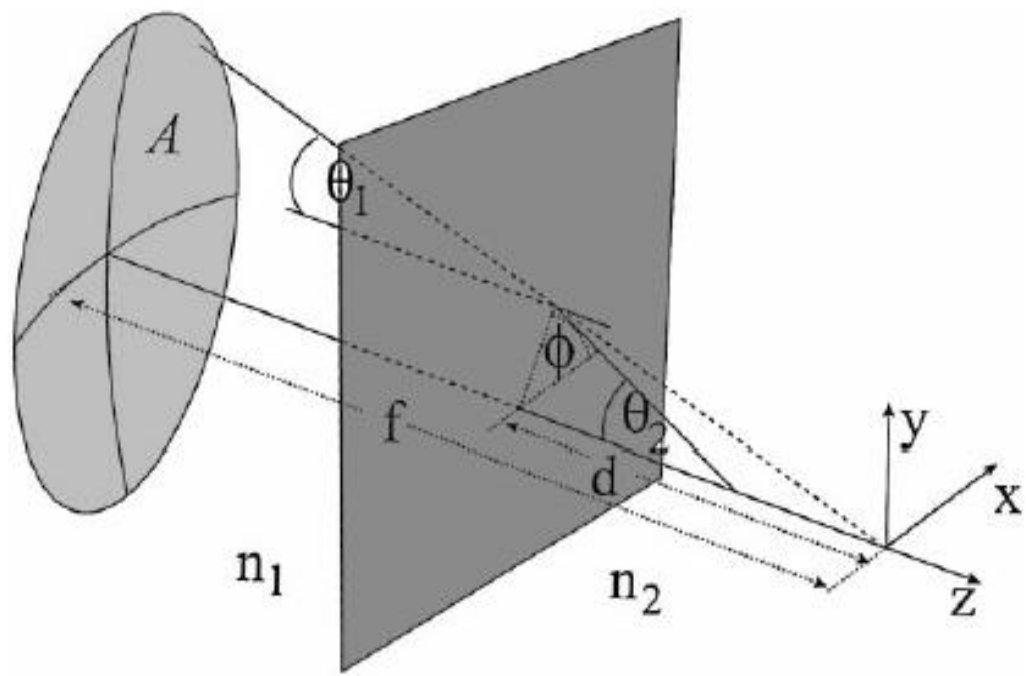

Fig. 1. Geometry when focusing with refractive index mismatch.

(Egner et al 1998)

|-> Refractive index

- **Micro-esfera:** ∅ = 6 µm

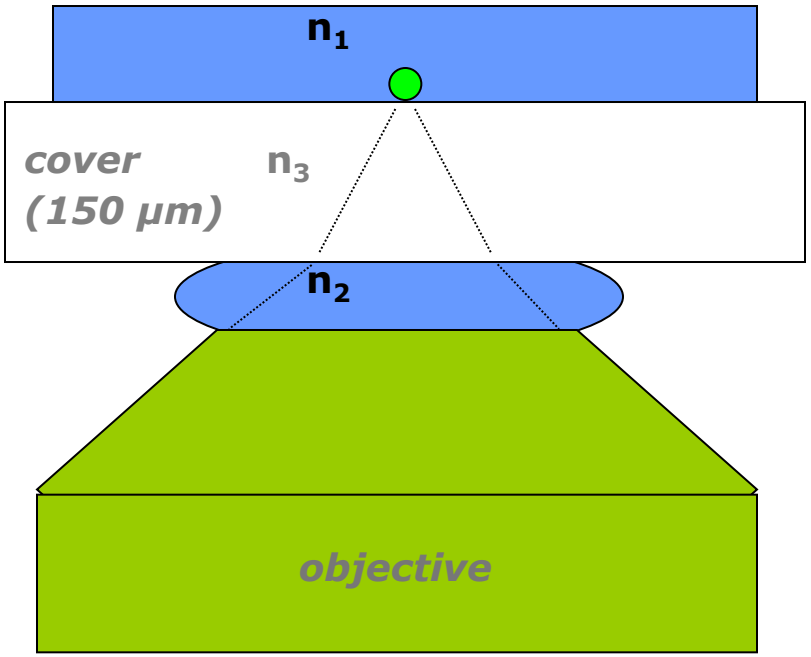

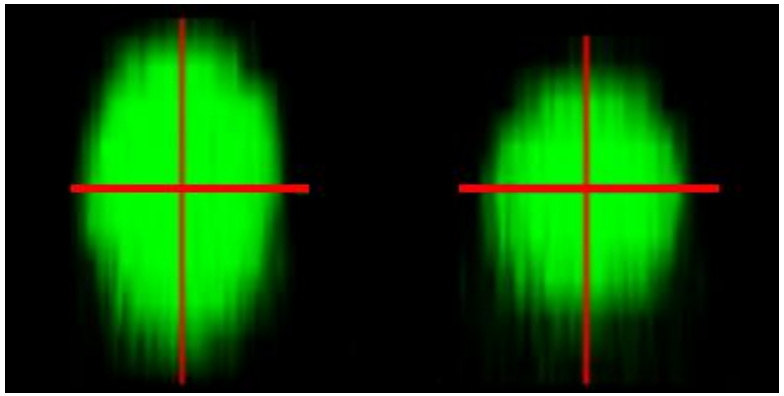

agua/aceite -- *aceite/aceite*

$n_1 \neq n_2$ $\quad$ $n_1 = n_2$

Ley de Snell: $n_i \cdot \sin\Theta_i = n_k \cdot \sin\Theta_k$

$n = n(\lambda)$!

|-> Summary I

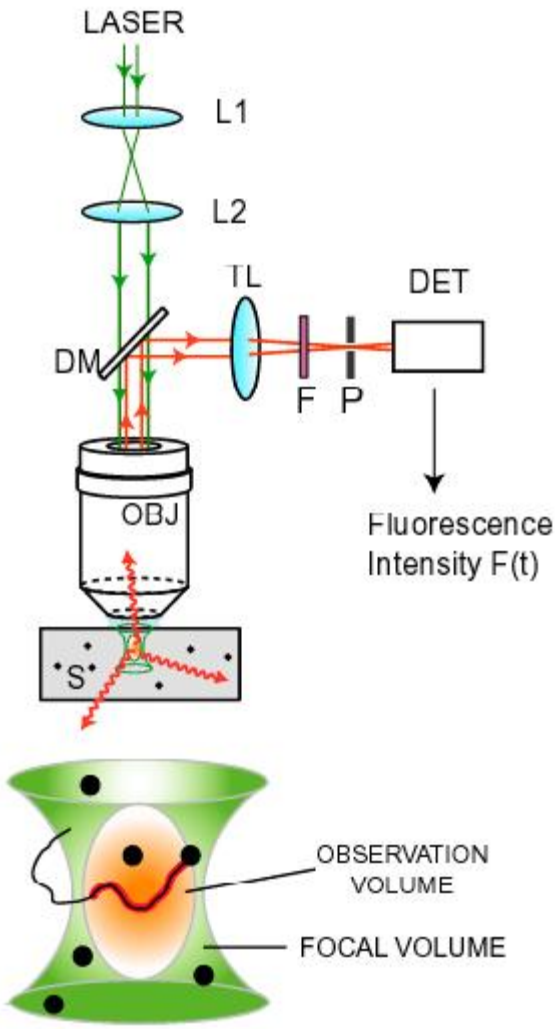

The observation volume (femtoliter) defined by the Point Spread Function must be considered as a <u>mini-sprectrofluorimeter</u>.

1. You need to consider the Offset I(0) in order to calibrate your signal $I(0) \geq 0$!
2. Never saturate the signal: $I \leq I_{max}$ (255 for 8 bit) !

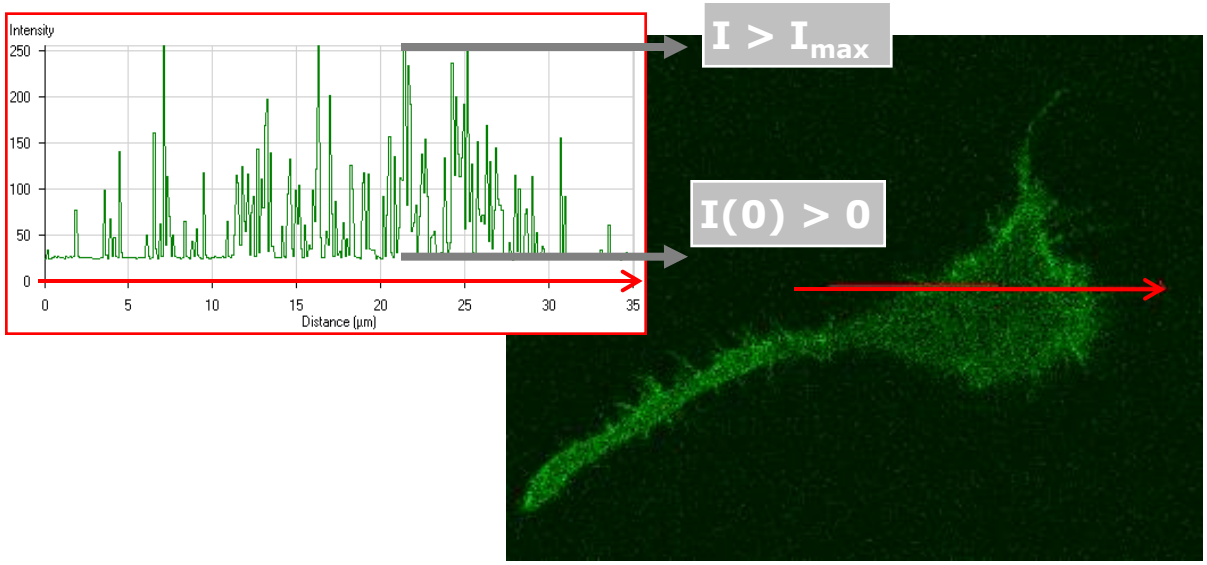

|-> Summary II

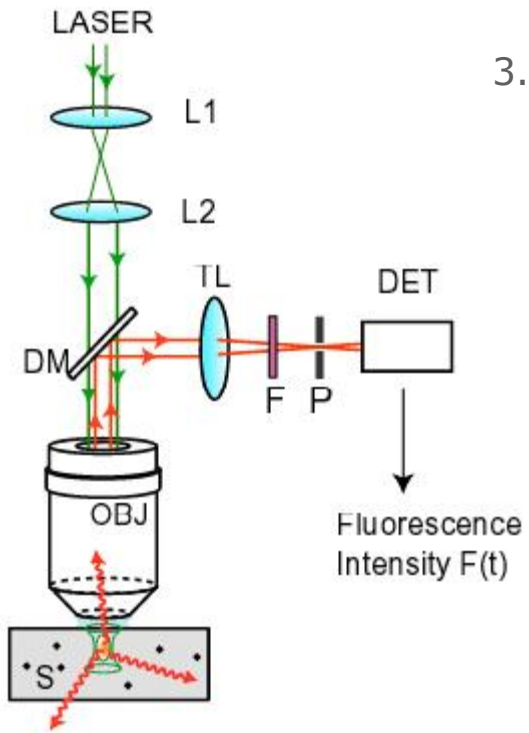

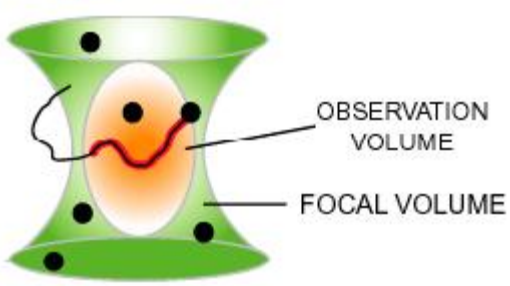

3. You need to consider sampling distances in Δx and $\Delta y \approx 50$ nm and $\Delta z \approx 150$-300 nm for later deconvolution, or calculate the explicit sample distances @ http://support.svi.nl/wiki/NyquistCalculator

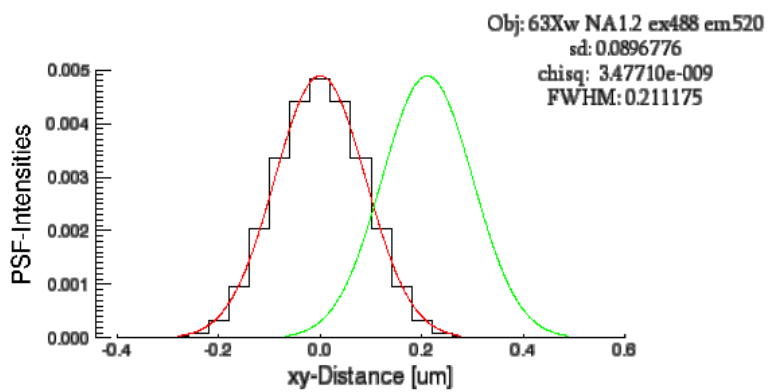

|-> Summary III

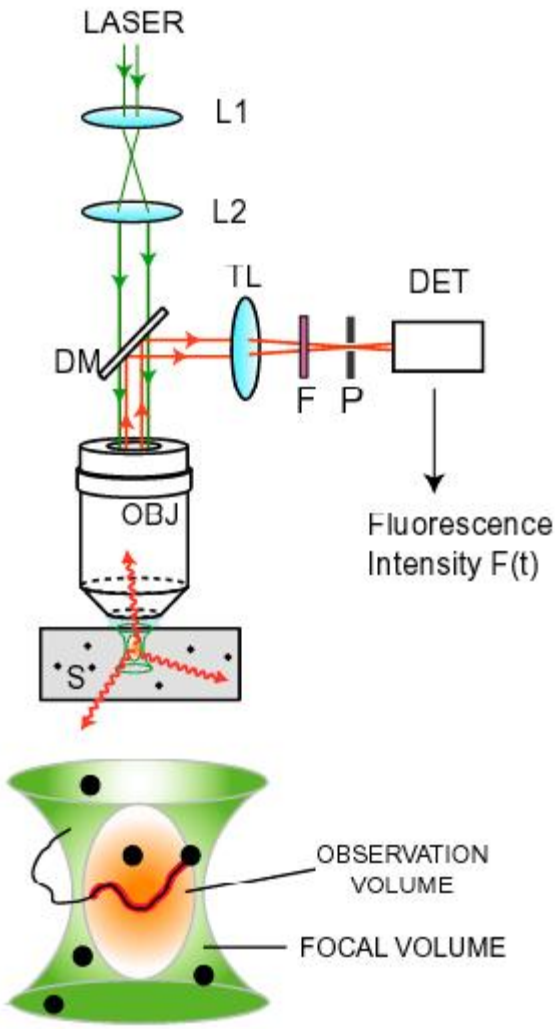

4. Use the right inmersion setup !

   n1 = n2 !

   Keep refractive index / index of refraction constant !

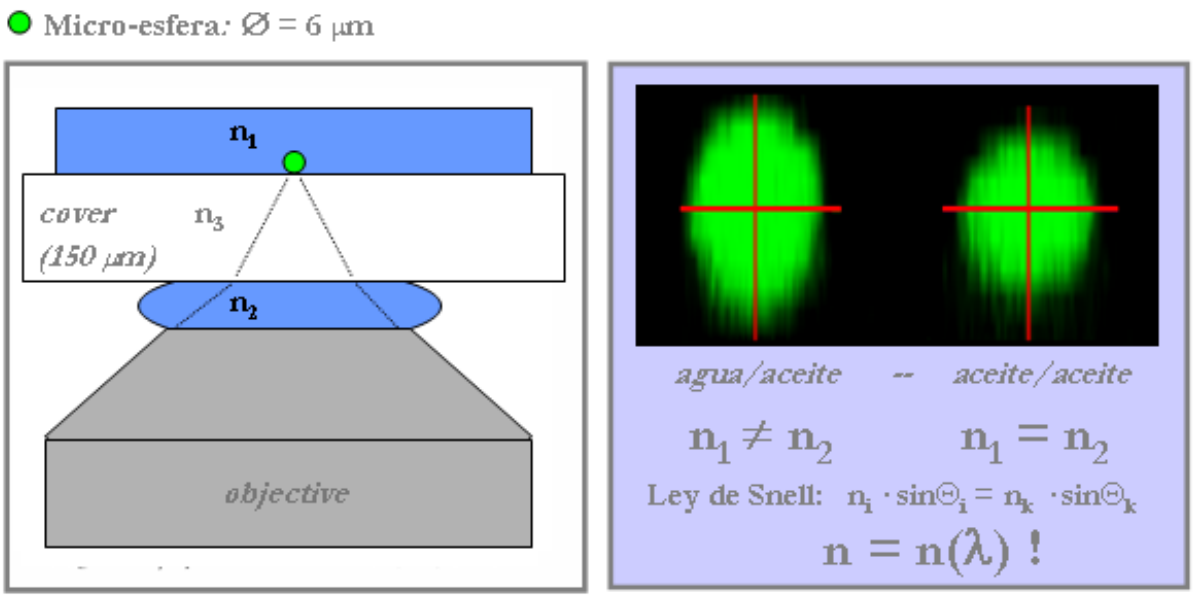

|-> Microscopy & Tools

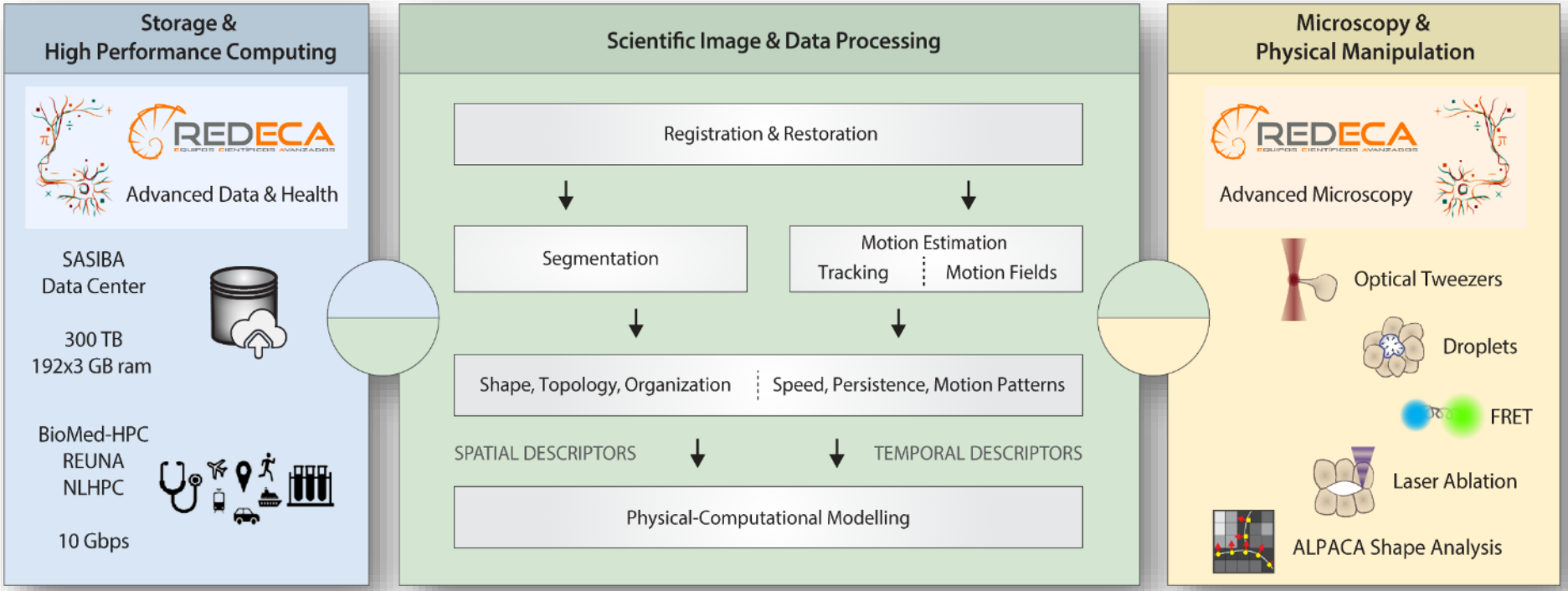

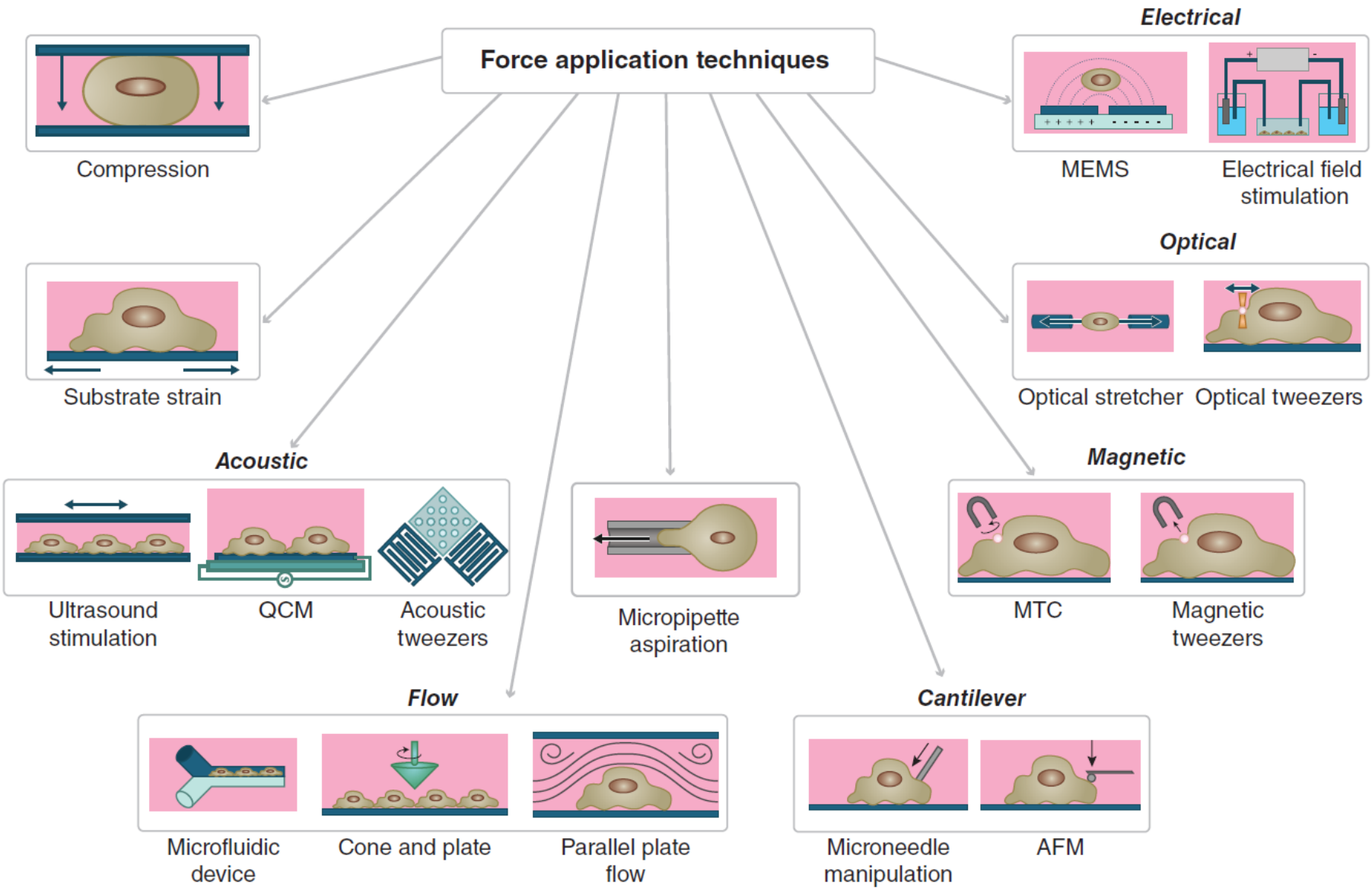

Rodriguez et al (2013) Review on Cell Mechanics: Experimental and Modeling Approaches, 65(6):60801, DOI:10.1115/1.4025355

Dr Jorge Jara: User-driven Trainable Model Refinement with Geometric Features of Cellular Aggregates in Biomedical Microscopy Images.

ALPACA: ALgorithm for Piecewise Adjacent Contour Adjustment

Optimizing adjacent membrane segmentation and parameterization in multi-cellular aggregates by piecewise active contours.

Jara-Wilde J, Castro I, Lemus CG, Palma K, Valdés F, Castañeda V., ... & Härtel S (2020). Journal of Microscopy, 278(2), 59-75.

Zebrafish *D. rerio*
Spinning-disk

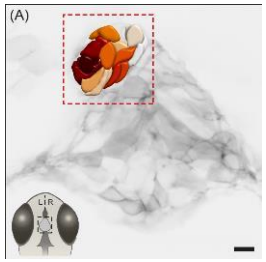

166x166x500nm xyz
1344 x 1024 x 70
24hrs/5 min intervals
8-16 bits/pixel
~20 GB raw data

Contour Sections

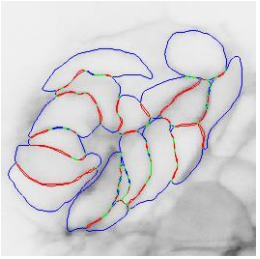

Overlapping

Non-adjacent

Piecewise Contour Sections

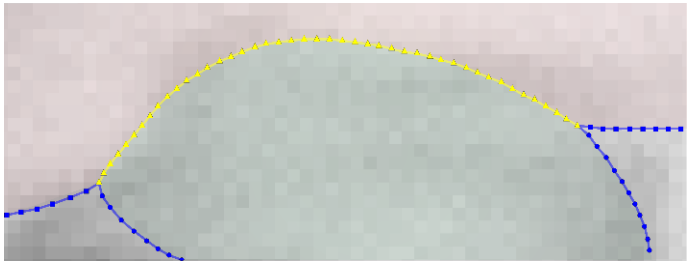

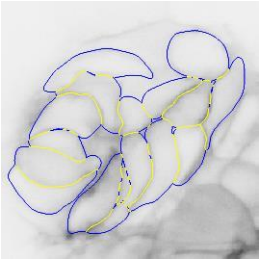

Shared, Adjacent Contours

Shape conservation

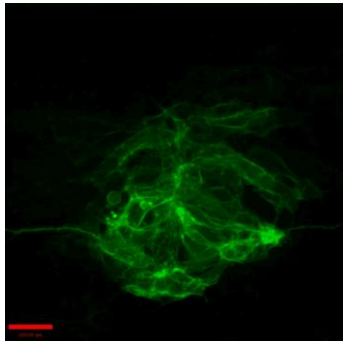

Parametric contour algorithms (geometry-based) use single-to-multi core computing

Trainable ALPACA requires GPU architecture

Dr Jorge Jara: User-driven Trainable Model Refinement with Geometric Features of Cellular Aggregates in Biomedical Microscopy Images.

ALPACA: ALgorithm for Piecewise Adjacent Contour Adjustment

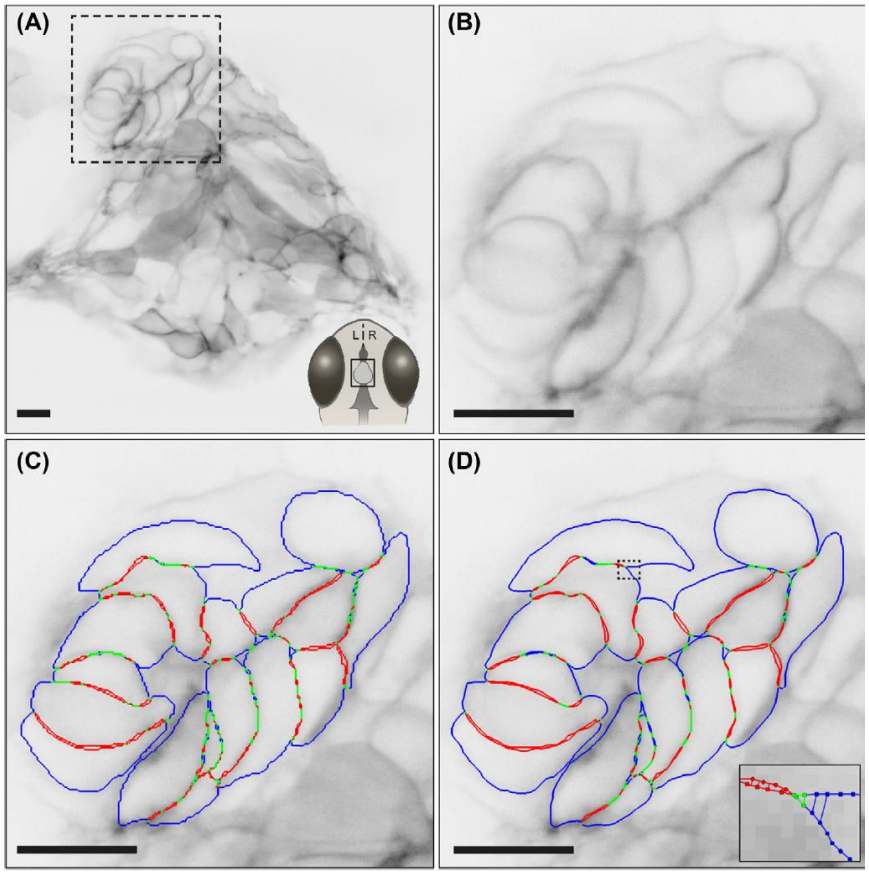

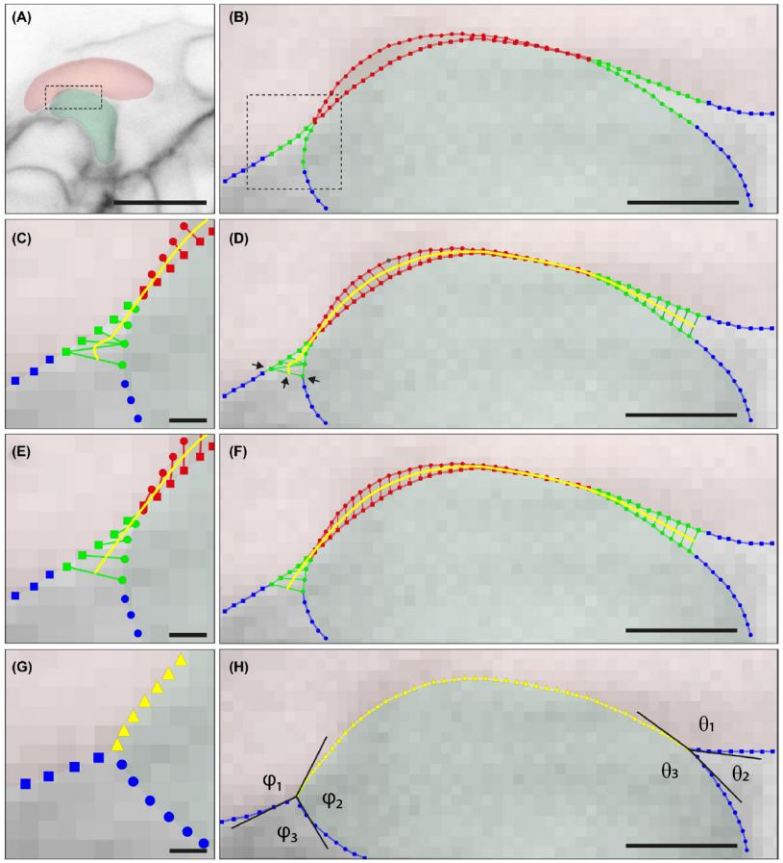

Dra Karina Palma: Droplets as Force Sensors in Cell Migration with Live Fluorescence Microscopy Imaging.

DROPLET & TRANSWELL MIGRATION ASSAY SET UP

Background

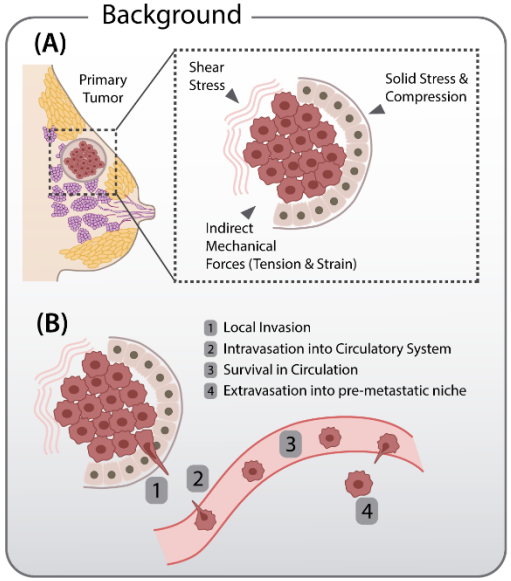

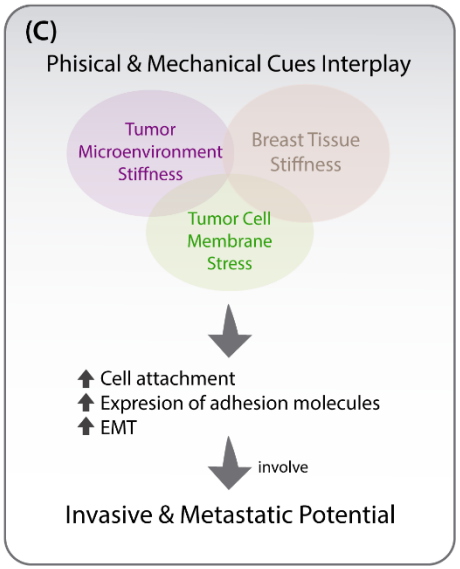

Specific Objectives Methodology

SO1

3D Invasion Assay

3D printable setup for live imaging of a Novel 3D Invasion Assay

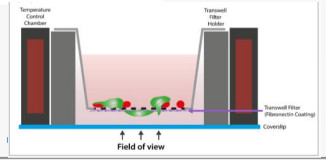

1 Temperature Control Chamber
2 Microscopy Transwell Filter Holder
3 Transwell Insert (on focus distance)
4 Coverslip

SO2

BMD & Geltrex Matrix Calibration

(A)

Pendant Drop Method & Software Calibration Analysis for BMD *Interfacial Tension* (γ)

$$\gamma = \frac{\Delta\rho g R_0^2}{\beta}$$

(B)

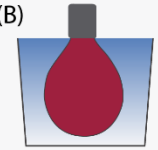

Pendant Drop Method & Software Calibration Analysis for Geltrex® and BMD Intefacial Tension

SO3

Fluorescent Labeling of Breast Cancer Cells

(A)

GAP43-eGFP membrane

Transfection of Constructs with Fluorescent Protein to access cell Morphplogy and Cytoskeleton

(B)

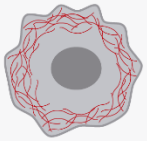

Lifeactin-Ruby

SO4

3D Invasion Assay Testing

Geltrex® & BMD combination:

(A)

(B)

(C)

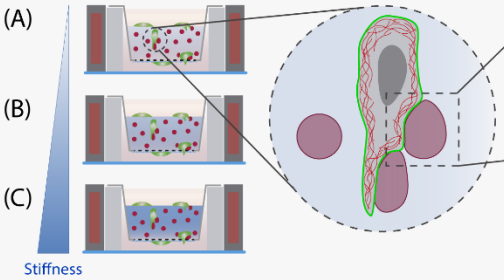

Dra Karina Palma: Droplets as Force Sensors in Cell Migration with Live Fluorescence Microscopy Imaging.

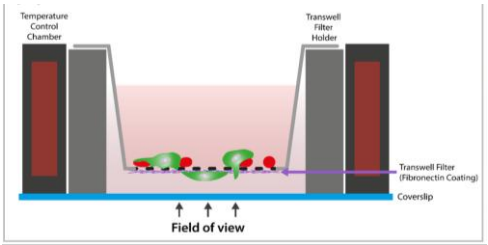

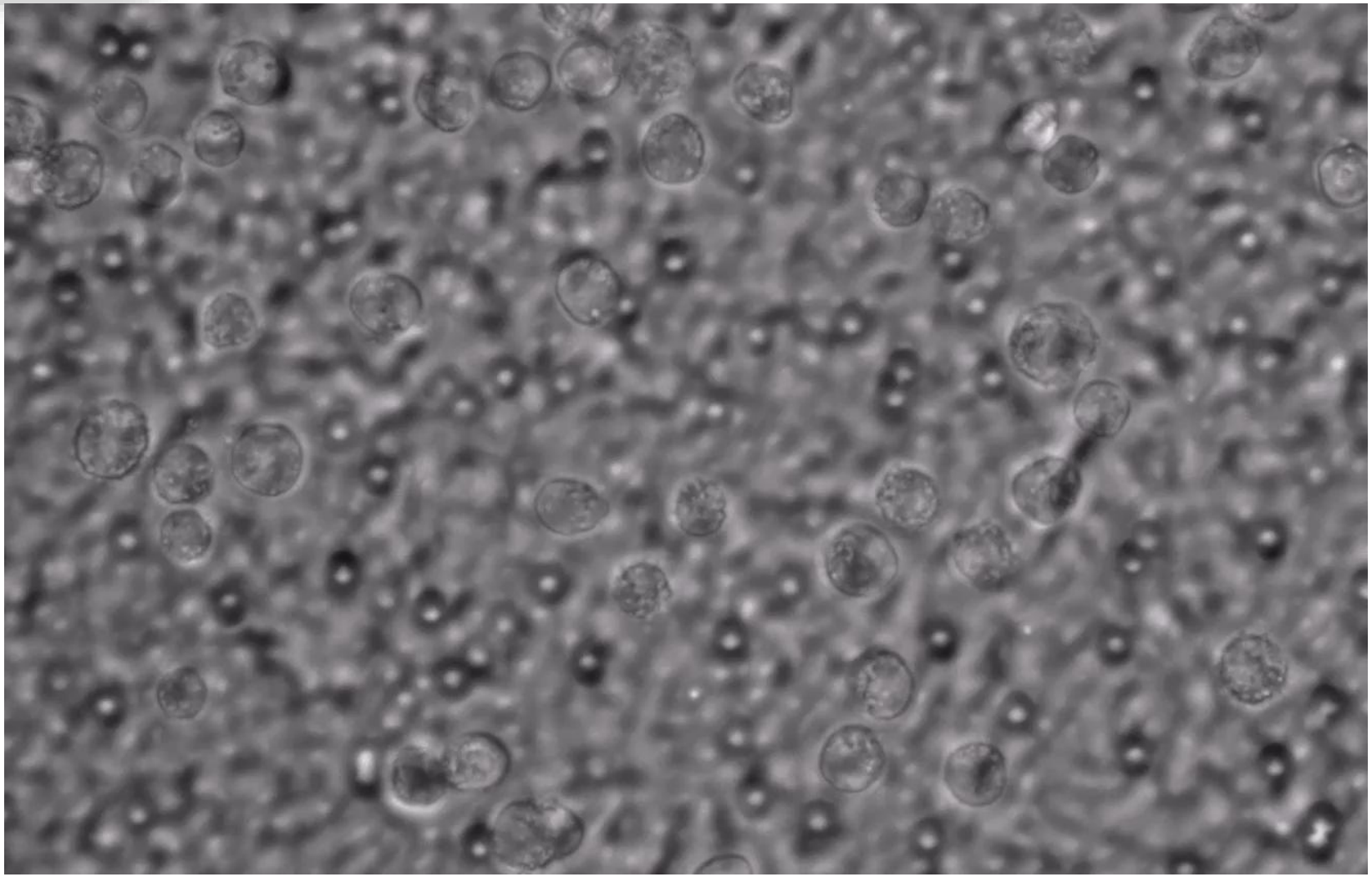

Dra Karina Palma: Droplets as Force Sensors in Cell Migration with Live Fluorescence Microscopy Imaging.

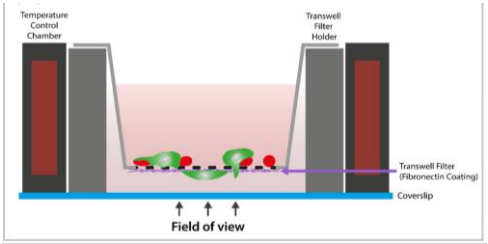

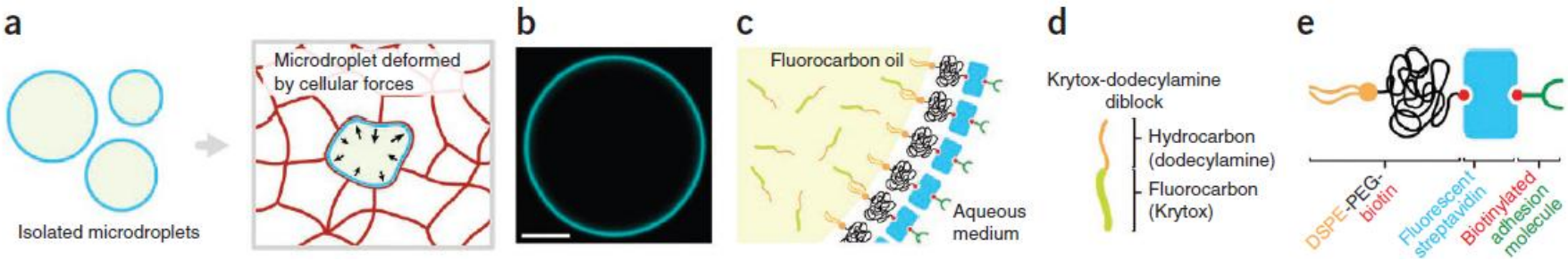

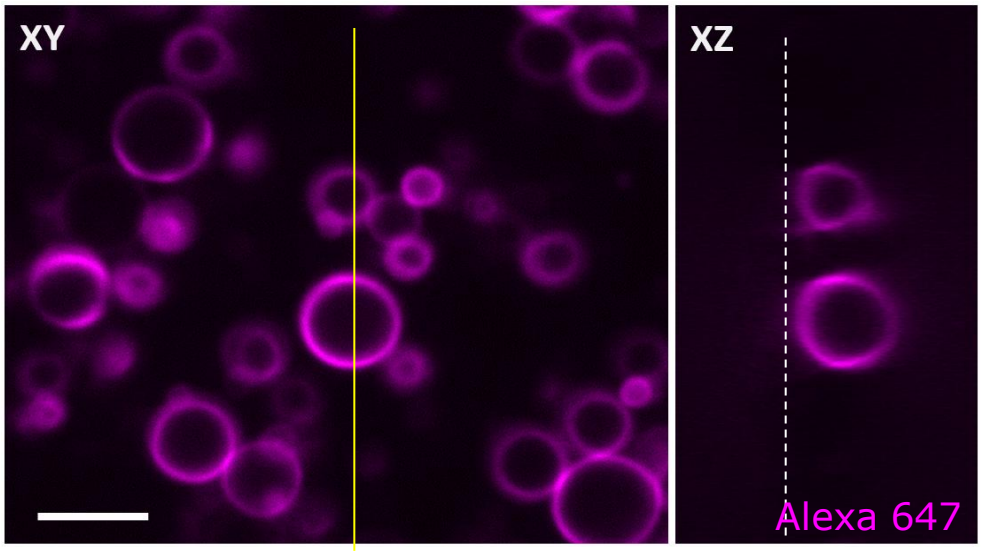

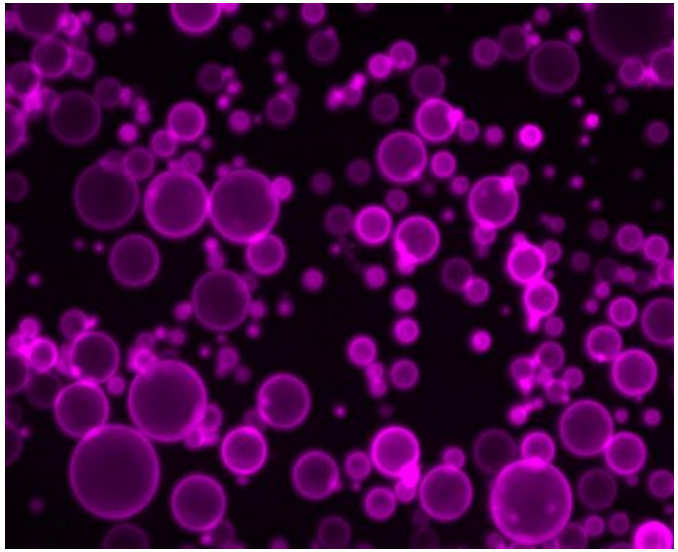

Fluorescent Fluorocarbon Droplets. Droplets present a uniform, circular shape in the XY plane. In the XZ (yellow line in XY), the surface in contact with the cell membrane (white segmented line) flattens. Most droplets have diameter under 10 µm. Scale bar: 10 µm.

Dra Karina Palma: Droplets as Force Sensors in Cell Migration with Live Fluorescence Microscopy Imaging.

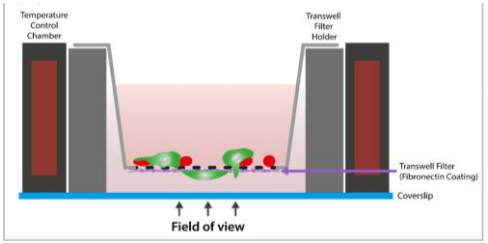

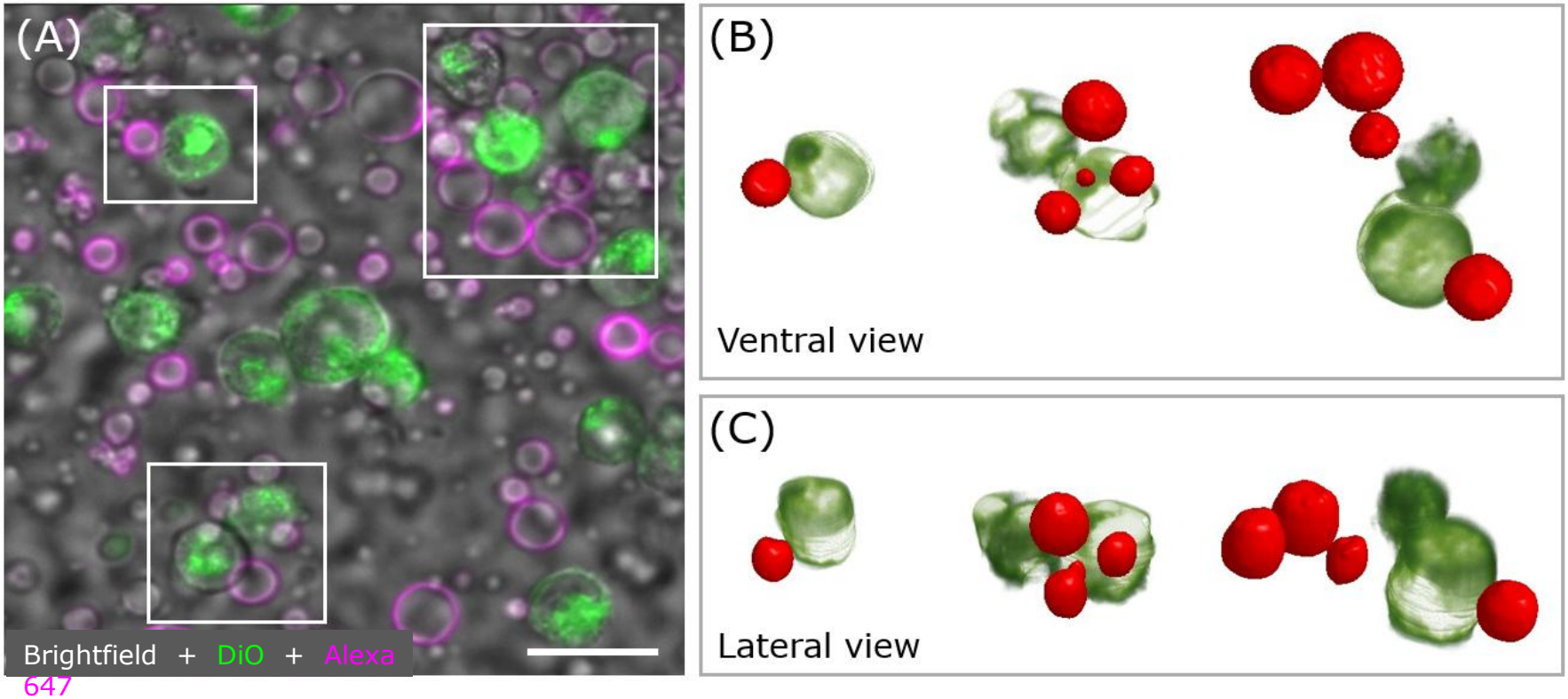

2D/3D visualization of the Droplet-Cell Interaction. (A) Merge image of brightfield (cells and transwell membrane) and cell-droplet fluorescence. Cells in close contact with droplets of different sizes were selected for semi-automatic segmentation (white rectangles). **(B)** Ventral view of 3D intensity (green) and active contour (red) models, representing the cells and droplets clusters selected (white rectangles in A). The leftmost cluster corresponds to the smaller rectangle; the mid cluster, to the lower rectangle; and the rightmost cluster, to the right corner rectangle. **(C)** Lateral view of the 3D reconstructions in (B). Scale bar in (A): 20 µm.

2D Calibration: Interfacial Tension γ by Bond Number β

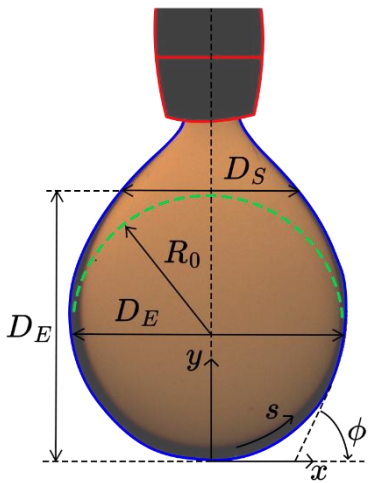

$$\gamma = \frac{\Delta\rho g R_0^2}{\beta}$$

$$\beta = \beta(\sigma)$$

$$\sigma = DS/DE$$

3D Measurement: Normal Anisotropic Stress $\delta\sigma$

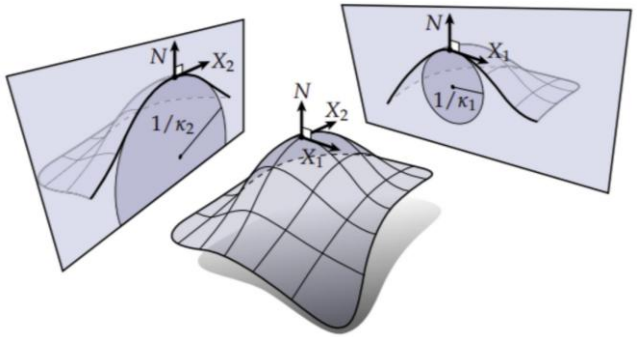

$$H = \frac{\kappa_1 + \kappa_2}{2}$$

$$\delta\sigma(q) = 2\gamma\left(H(q) - \frac{1}{R}\right)$$

$$R = \sqrt[3]{\frac{3}{4\pi}V}$$

Hansen F. K. y Rodsrud G. (1991), Surface tension by pendant drop.

Campàs O. et al. (2015), Quantifying cell-generated mechanical forces within living embryonic tissues.

PENDANT DROP METHOD FOR INTERFACIAL TENSION ADQUISITION

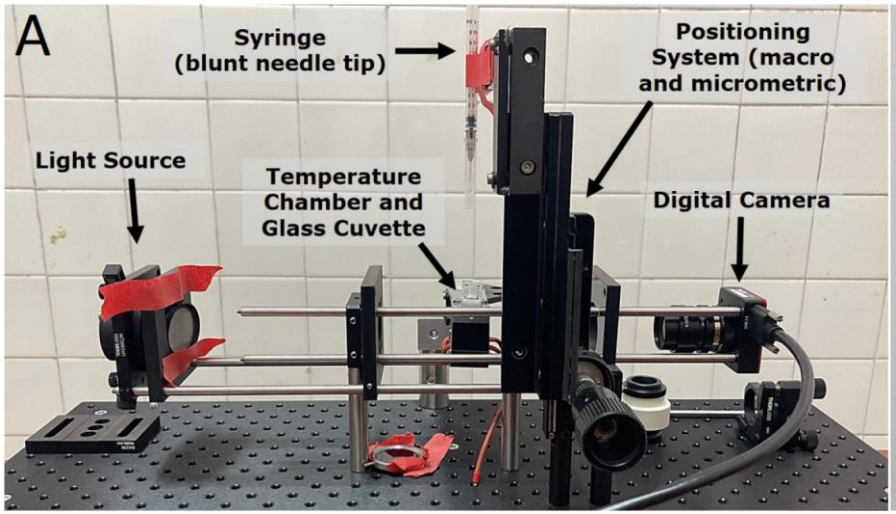

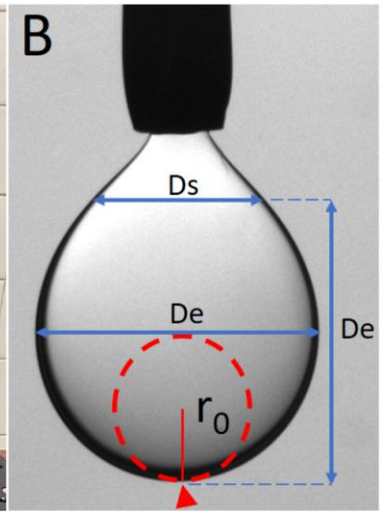

Pendant Drop Setup. **(A)** Custom Made Pendant Drop Calibration Setup, including a DCC1545M - USB 2.0 CMOS Camera, 1280x1024 pixel size image (Thorlabs©). A system that allows positioning of the drop in the camera field of view and focus, a led light source, and a couvette holder with temperature control for the drop external medium (37°C), simulating experimental conditions. **(B)** Calibration of surface tension of fluorocarbon pendant drop by two different approaches. Image of a fluorocarbon (fluorinert fc-70) pendant drop immersed in distilled water. **(B)** Optimization routine based on Young-Laplace differential equation by OpenDrop [2] adjusts the initial, rough drop profile to a more accurate profile (green and red dashed lines), to calculate the Bond Number and droplet surface tension. **(C/D)** Alternate approach to calculate surface tension based on a geometric factor. **(C)** Surface curvature $K_0 = 1/R_0$ can be determined at the Apex. **(D)** *De* is the maximal width of the pendant droplet. *Ds* is the width at a distance *De* measured from the Apex. The Bond number is given by $Bo = 0.12836 - 0.7577\left(\frac{Ds}{De}\right) + 1.7713\left(\frac{Ds}{De}\right)^2 - 0.5426\left(\frac{Ds}{De}\right)^3$. Finally, the drop surface tension was obtained with the equation in **(E)**. Scale bar: 0.8 mm.

$$\gamma \equiv \frac{\Delta\rho g R_0^2}{\mathrm{Bo}}$$

γ: tensión superficial [N/m]
Δρ: diferencia de densidad [Kg/m^3]
g: aceleración de gravedad [9.8 m/s^2]
R_0: radio de la gota [m]
Bo: número de Bond

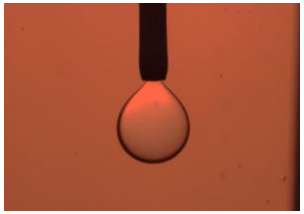

Inputs:

- Experiment image
- Δρ density difference
- Needle gauge

SCIAN-Drop
measures
Bond Number β
interfacial tension γ

SCIAN-Force
calculates stress
$\delta\sigma(q)$ on the droplet
surface

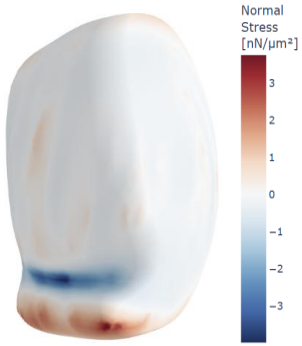

Output: 3D
Droplet surface &
deformation
model

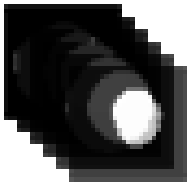

Input: Image stack

**SCIAN-Soft / Python /
FIJI**
reconstruct 3D mesh

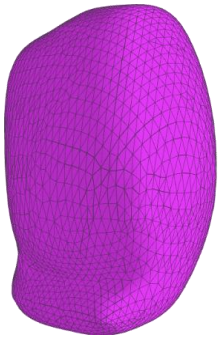

Github Repositories

SCIAN-Drop / SCIAN-Force (software)

Hanging drop method: shape parameters Ro and β are determined from the drop profile, after which the surface tension γ is calculated as

$$\gamma = \frac{\Delta\rho \; g \; R_0}{\beta}$$

de Gennes, P-G (2003)
Capillarity and Wetting Phenomena

β is approximated by least-squares from the ratio Ds/De.

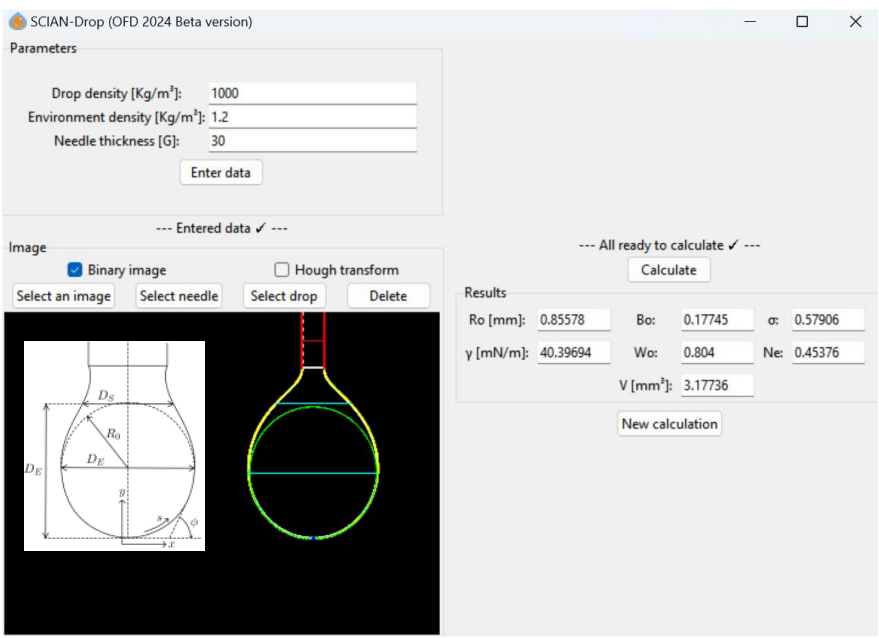

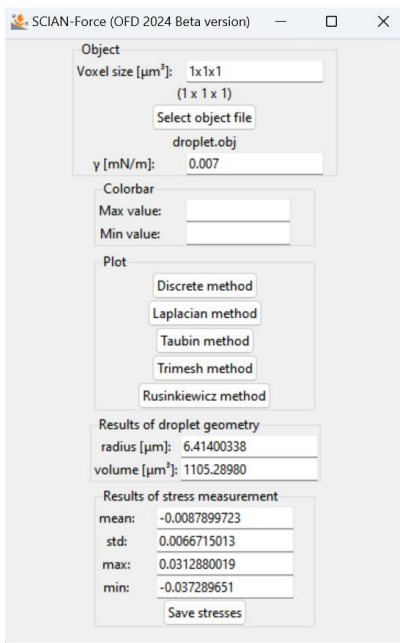
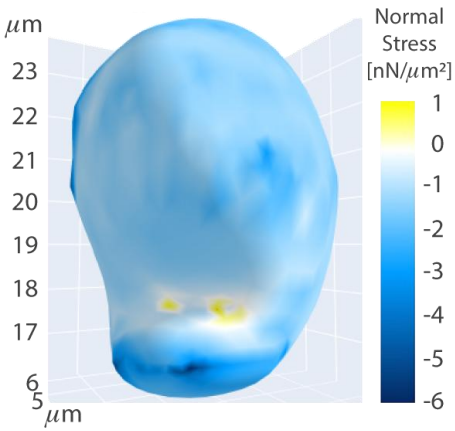
Normal Stress δσ on the surface.